Fakultät für Medizin

Epigenetik der Hautalterung

Implication of Nucleophagy during Cellular Aging

Xiang Lu

Vollständiger Abdruck der von der Fakultät für Medizin der Technische Universität München zur Erlangung des akademischen Grades eines

Doktors der Naturwissenschaften (Dr. rer. nat.)

genehmigten Dissertation.

Vorsitzender: Prof. Dr. Carsten Schmidt-Weber

Prüfer der Dissertation:

1. Prof. Dr. Karima Djabali
2. Prof. Dr. Thomas Brück

Die Dissertation wurde am 08.01.2019 bei der Technische Universität München

eingereicht und durch die Fakultät für Medizin am 15.05.2019 angenommen.

Introduction

1. Aging Theory

Aging is not a brand-new aspect of human biology yet less understood mystery that people have been striving for elixirs. It was documented that 2,200 years ago, the first emperor of China, Qin Shi Huang, gave an order to hunt for a potion that would grant him immortality. Obviously, the emperor couldn't live forever but the journey of searching for that magic "potion" never stopped. Nowadays, lots of researchers tend to regard aging as a programmed process, however, there is scarce evidence for such a program. It is a significant challenge as to why aging occurs, how it is caused, and whether it can be reversed. Accordingly, various aging theories have been proposed, thus improving our understanding of the mystery of aging.

1.1.Somatic Mutation Theory

Accumulations of somatic mutations, DNA damage, and copy number variation (CNV) were found within aged human cells and model organisms, such as mouse, *C. elegans* and *Drosophila* (Faggioli, Wang et al. 2012, Forsberg, Rasi et al. 2012, Moskalev, Shaposhnikov et al. 2013). These DNA alterations may lead to cellular dysfunctions by affecting essential genes and transcriptional signaling pathways and subsequently result in homeostasis collapse within the cell. Under normal conditions, DNA damage or malfunctions could be corrected. However, deficiencies in DNA repair machinery cause accelerated aging in mice and several human progeroid syndromes, such as Werner syndrome, Bloom syndrome, and Hutchinson-Gilford Progeria Syndrome (HGPS) (Best

2009, Hoeijmakers 2009, Murga, Bunting et al. 2009, Gregg, Gutierrez et al. 2012). In mouse studies, senescence-accelerated mice were found to have increased accumulation of somatic mutations on HLA-A gene. In comparison, mice have longer lifespan showed a lower ratio of mutant accumulation (Morley 1998). Besides, the general relationship between longevity and DNA repair has been well studied on the enzyme poly (ADP-ribose) polymerase-1 (PARP-1). PARP-1, a rapid DNA damage response protein which guards the genomic stabilities, is positively correlated with the lifespan of mammalian species (Burkle 2001). These findings suggest that somatic mutation contributes to the aging process and the functionality of DNA repair machinery plays a significant role in regulating the progression of aging.

1.2.Telomere Loss Theory

Somatic cells in most human tissues can only duplicate for a limited cycles, suggesting that the capability of cell division declines with age (Hayflick 1965). This process has been linked to the exhaustion of telomeres, regions at the end of linear chromosomes that stabilize DNA (Greider and Blackburn 1985). It has been proposed that telomeres act as an intrinsic “division counter” in somatic cells. Erosion of telomeres is considered as a protective trade-off between infinite cell dividing towards cancer development and end replication towards cell senescence (Campisi 2005). Normal aging is accompanied by telomere shortening in mammals. Based on this, pathologically accelerated telomere attrition in premature mice and humans provide evidence that maintaining the functionalities of telomere may delay the progress of aging (Ouellette, McDaniel et al. 2000, Decker, Chavez et al. 2009, Benson, Lee et al. 2010).

1.3.Free Radical Theory of Aging

ROS, reactive oxygen species, is the by-product of respiration by OXPHOS (oxidative phosphorylation) in mammalian cells. The vast majority of ROS generation can be traced to mitochondria, which are the principal generator of cellular ATP (adenosine triphosphate). Studies have reported that functions of mitochondria decline with age, due to the increased sensitivity of mitochondria to the ROS induced oxidative stress (Shigenaga, Hagen et al. 1994). Mitochondrial dysfunction has a profound impact on accelerating the aging process in mammals (Trifunovic, Wredenberg et al. 2004, Kujoth, Hiona et al. 2005, Vermulst, Wanagat et al. 2008). Increased mitochondrial DNA (mtDNA) damages are thought to be age dependent, which have been observed in a number of post-mitotic tissues such as the brain tissues (Richter, Park et al. 1988). In aged brain tissues, the levels of 8-oxo-2'-deoxyguanosine (oxo8dG), a biomarker of DNA damage, are significantly higher in the mtDNA compared to the nuclear DNA (Richter, Park et al. 1988). Moreover, impairments of mitochondria that are induced by ROS lead to increased free radical generation. This is so-called "vicious cycle" that results in further damages to mitochondria.

2. Hutchison-Gilford Progeria Syndrome (HGPS)

Aging and its related diseases are complex. Extreme cases can be used as models to study unusual aging process in order to reflect normal physiological aging. Hutchinson-Gilford Progeria Syndrome (HGPS) is a rare premature aging syndrome that consists of various symptoms of physiological aging. Cells derived from HGPS patients are good models to characterize molecular mechanisms of cell aging in humans.

2.1.Cause of HGPS

HGPS is an extremely rare disease that involves accelerated aging. Children affected with HGPS generally appear normal at birth but fail to thrive and start to exhibit prominent eyes, lipodystrophy, alopecia, abnormal distal-joint, sclerotic skin, and reduced vascular function from 10 months onwards (Merideth, Gordon et al. 2008). Most children live to their teenage and die from heart failure or stroke at an average age of 14 years old.

In 2003, a genomic and transcriptional study of reported that 90% of the children with HGPS contain a *de novo* mutation of G608G (GGC > GGT) in exon 11 of LMNA gene (De Sandre-Giovannoli, Bernard et al. 2003). This dominant mutation makes no change in coding the amino acid (a.a.), but generates an alternative splicing donor site resulting in a mRNA missing 150 nucleotides. This in-frame deletion leads to a truncated form of lamin A protein termed progerin, which lacks 50 a.a. within its C-terminus. This finding has drawn great attention to the importance of the LMNA gene and its products nuclear lamina proteins in cell aging process.

2.2.The nuclear lamin protein

The nuclear lamina is a complex network composed of multiple lamin proteins, including lamins A, C, B1, and B2, which are members of the intermediate filament proteins family (Stuurman, Heins et al. 1998). The nuclear lamina proteins have multiple roles in maintaining the nuclear integrity and homeostasis of the nuclear matrix. The nuclear lamina proteins localize beneath the inner nuclear membrane to support the structure of

the nucleus. Moreover, the nuclear lamina proteins are also thought to be involved in binding to chromatin, a class of NE proteins, and various transcriptional factors, which are all essential for nuclear integrity and genome stability (Gruenbaum, Margalit et al. 2005).

Mammalian cells express A- and B-type lamins, which are encoded by *LMNA*, *LMNB1*, and *LMNB2* genes, respectively (Gerace, Blum et al. 1978, Gerace and Blobel 1980). In particular, *LMNA* encodes two major proteins of lamin A and C by alternative splicing (Lin and Worman 1993, Wydner, McNeil et al. 1996). Like other cytoplasmic intermediate filament proteins, A- and B-type lamins share a similar structure that comprises an N-terminal head domain (NT), a central a rod domain, and a C-terminal tail domain (CT) (Fisher, Chaudhary et al. 1986). Distinct from the other intermediate filament proteins, most nuclear lamins harbor a NLS sequence and a C-terminal CaaX motif, which is essential for their post-translational modifications (PTM) (Beck, Hosick et al. 1990). The CaaX motif (C, cysteine; a, aliphatic amino acid; X, any amino acid) with an exact sequence of CSIM is present at the C-terminus of all B-type lamins and the lamin A precursor, known as prelamin A (Vorburger, Kitten et al. 1989). Prelamin A undergoes multiple steps of PTM at its C-terminus. Firstly, the CaaX motif gets prenylated, which recruits a farnesyl group to its cysteine residue and becomes farnesylated (Casey and Seabra 1996, Fu and Casey 1999). Following farnesylation, the removal of the aaX residues of CaaX motif by the Rec 1 or Zmpste 24 endoprotease induces protein carboxymethylation (Sinensky, McLain T. et al. 1994). Then, the last 15 amino acids from the C-terminus are removed by Zmpste 24 and finally the mature

lamin A protein is released and integreated into the nuclear lamina (Sinensky, McLain T. et al. 1994, Barrowman, Hamblet et al. 2008).

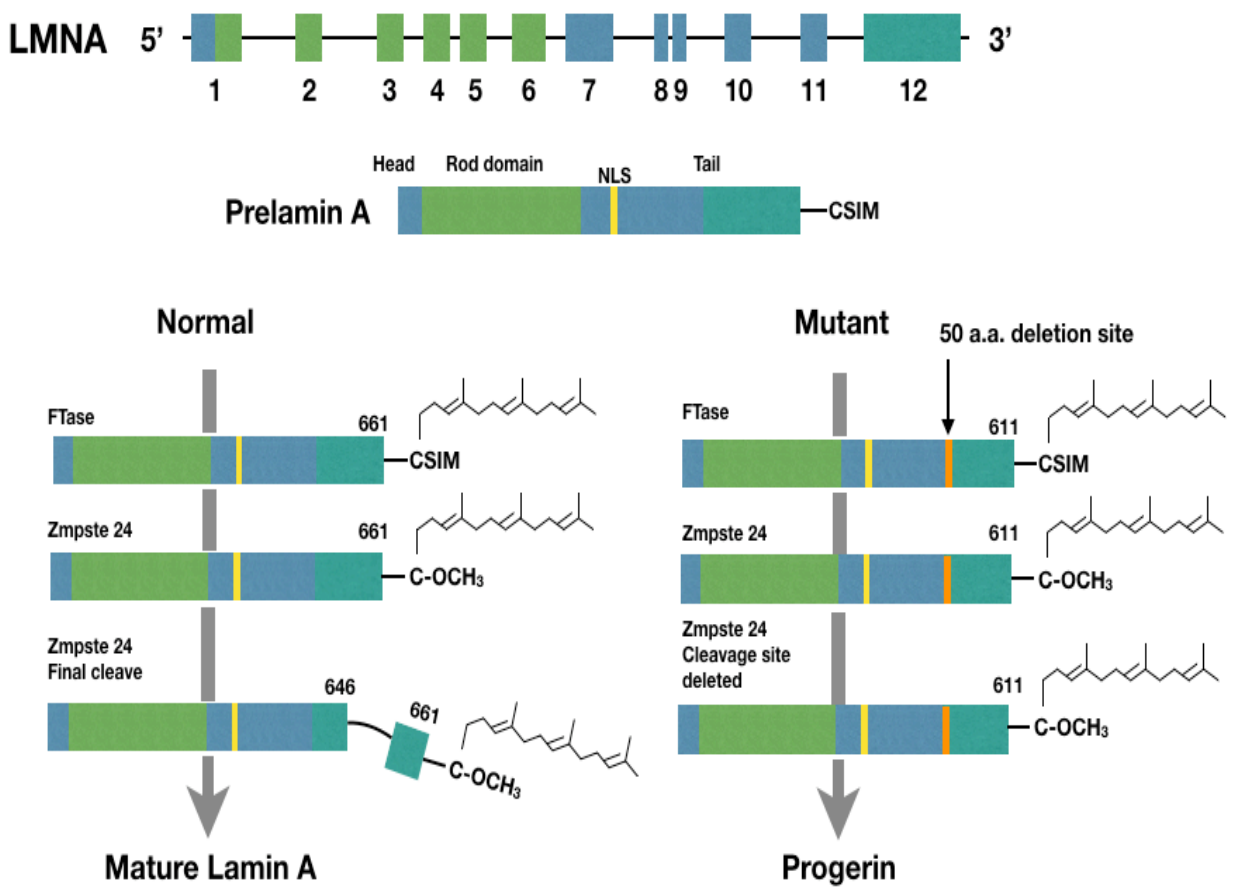

Figure 1. Lamin A maturation with normal and mutant splicing. A-type lamins are encoded by the LMNA gene, which comprises 12 exons. Common structure shared between A-type lamins contains a head, rod, and tail domain. At normal stage, prelamin A undergoes a series post-translational modification, including farnesylation, carboxymethylation, first and final cleavage by the enzyme Zmpste 24, and final release of mature lamin A. At mutant stage, due to lacking the cleavage site for Zmpste 24, a truncated form of prelamin A is released maintaining the farnesyl group at its C-terminal end.

In HGPS cells, the mutation of G608G in *LMNA* gene causes the absence of the second Zmpste 24 cleavage site of prelamin A (Figure 1) leading to permanent farnesylation and carboxymethylation at the C-terminus of progerin (Capell, Erdos et al. 2005, Yang,

Bergo et al. 2005). Emerging evidence suggested that farnesylated progerin is insoluble and permanently anchoring beneath the inner nuclear membrane, thus becoming toxic to cells. Furthermore, this irreversible dominant negative nuclear localization of progerin disrupts the functions of the normal nuclear lamina and leads to downstream nuclear defects that are characteristic of HGPS cells, such as nuclear blebbing, heterochromatin disorganization, mislocalization of NE proteins, and disrupted gene transcription (Dechat, Pfleghaar et al. 2008).

3. The nuclear envelope proteins

The NE is a continuous extension of the endoplasmic reticulum (ER) double membrane, which contains an outer nuclear membrane (ONM) facing the cytoplasm, a perinuclear space, and an inner nuclear membrane (INM) facing the nucleoplasm (Hetzer 2010). The NE is highly organized that separates the components of the nucleus from the cytoplasmic compartments. The ONM and INM only meet at the joint site where the nuclear pore complex is located. Underlying the INM is the nuclear lamina, which directly or indirectly binds to various NE proteins and chromatins.

Although a large amount of NE proteins remain uncharacterized, it has been shown that nuclear lamina proteins and chromatin directly interact with some of the NE proteins such as lamina-associated polypeptide (LAP) proteins, emerin, and SUN (Akhtar and Gasser 2007, Dorner, Gotzmann et al. 2007). The NE proteins are associated with various diseases exhibiting multiple dysfunctions in chromatin organization, transcription, and DNA metabolism (Mattout, Dechat et al. 2006, Heessen and Fornerod 2007, Reddy, Zullo et al. 2008).

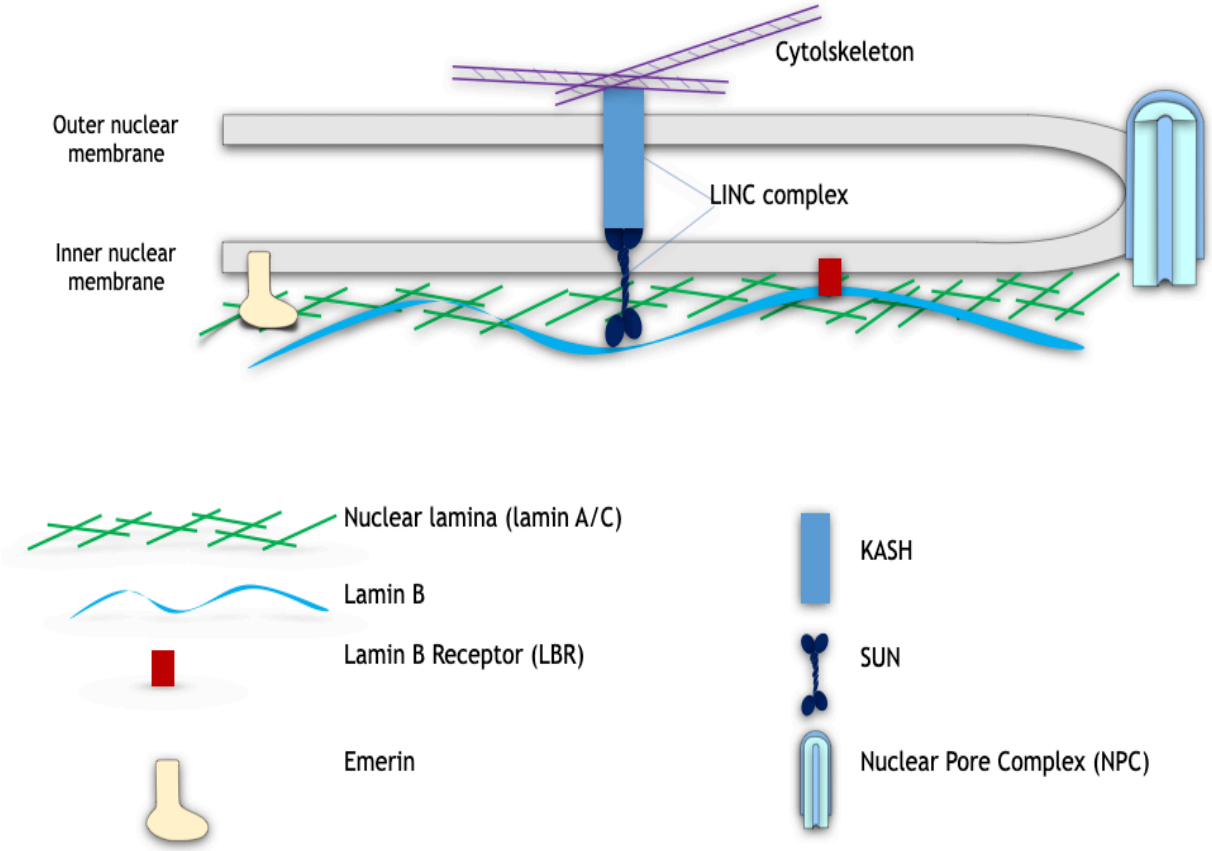

Figure 2. Schematic illustration of the nuclear envelope. Outer nuclear membrane and inner nuclear membrane are fused at the site of the nuclear pore complex. Emerin locates at the INM, interacting with the nuclear lamina. Nuclear lamina proteins form a meshwork underlying the INM. Lamin B receptor (LBR) resides at the INM and binds to lamin B protein. SUN protein dimer and KASH protein form LINC complex that connects nucleoskeleton and cytoskeleton.

3.1.Emerin regulates gene expression via interacting with nuclear lamina

Emerin is a conserved LEM-domain protein, which shares a common LEM-domain with several proteins such as LAP2 and MAN1 (Cai, Huang et al. 2001). LEM (LAP2, Emerin, MAN) is a motif that comprises about 45 residues that fold as two α-helices (Laguri, Gilquin et al. 2001). The LEM-domain proteins are known to directly bind Barrier to Autointegration Factor (BAF), a conserved chromatin protein (Furukawa 1999; Cai 2001, Lee 2001, Shumaker 2001, Shimi 2004, Cai 2007). Emerin was found to be a direct binding partner for numerous transcriptional regulators, suggesting multiple roles for emerin in regulating gene expression and genomic organization (Holaska, Lee et al. 2003, Haraguchi, Holaska et al. 2004, Markiewicz, Tilgner et al. 2006, Holaska 2008). For example, Demmerle et al. reported that emerin could directly bind to the histone deacetylase 3 (HDAC3), which is believed to regulate gene transcription by catalyzing deacetylation reaction, as well as recruit HDAC3 to the nuclear periphery (Demmerle, Koch et al. 2012). This could facilitate the activity of HDAC3 in repressing certain gene expression (Demmerle, Koch et al. 2012). However, HDAC3 depletion mice appeared to have increased expression of lipogenic genes causing severe hepatosteatosis (Sun, Feng et al. 2013).

Emerin and other LEM proteins are integral membrane proteins that localize predominantly at the INM and bind directly to the nuclear lamins, forming a major component of the nuclear lamina. It is becoming clear that the nuclear lamina not only provides a structural support for the nucleus but also a transcriptionally repressive

environment by tethering of genomic regions and leads to gene repressions (Finlan, Sproul et al. 2008, Reddy, Zullo et al. 2008).

Importantly, mutations in the genes that encode emerin and lamin A proteins cause diseases with a wide spectrum of both overlapping and distinct phenotypes, including progressive skeletal muscle wasting, lipodystrophy, and premature aging (Vlcek and Foisner 2007). It has been shown that lamin mutant cells have disrupted nuclear targeting and distribution of emerin (Wu, Flannery et al. 2014). The dynamics study of emerin distribution through the cell cycle suggested that in normal cells, emerin temporally correlates with lamin A when reforming the NE (Eisch, Lu et al. 2016). In HGPS cells, however, emerin and progerin form aggregates from metaphase to cytokinesis indicating that distribution and organization of emerin are dependent on lamin A protein (Eisch, Lu et al. 2016).

3.2.SUN may contribute to HGPS pathology

SUN proteins are integral components of the INM. The carboxy-terminal domains of SUN proteins localize to the perinuclear space, which directly interacts with nucleoskeleton, such as the nuclear lamina. Besides, SUN proteins also contain a transmembrane domain that physically interacts with KASH proteins (Klarsicht, ANC-1, Syne homology), which span the outer nuclear membrane and perinuclear space (Tapley and Starr 2013). SUN and KASH proteins build a bridge across the nuclear envelope, termed as LINC (linker of nucleoskeleton and cytoskeleton) complex. The LINC complex functions to connect the nuclear components to the cytoskeleton. Such a

connection facilitates nuclei movement and nuclear responses to mechanical stimuli that are transmitted to the cell through the cytoskeleton (Tapley and Starr 2013).

Mutations in SUN and KASH proteins are related to many diseases, including HGPS (Chen, Chi et al. 2012, Chen, Wang et al. 2014). The mechanism by which progerin directly contributes to the pathology of HGPS is not completely understood. However, the tight connection between progerin and SUN1 might contribute to the structural changes in the NE and the ER in HGPS cells (Chen, Wang et al. 2014). Moreover, concomitant with the accumulation of progerin in HGPS cells, SUN1 levels are also increased (Chen, Chi et al. 2012, Chen, Wang et al. 2014). The SUN1-progerin interaction appears to depend on the permanent farnesylation of progerin causing both proteins to remain associated within the ER during mitosis (Chen, Wang et al. 2014, Eisch, Lu et al. 2016). Farnesylation of progerin enhances its interaction with SUN1 and reduces SUN1 mobility, thereby promoting the aberrant recruitment of progerin to the ER membrane during postmitotic assembly of the NE and subsequently resulting in the accumulation of SUN1 over consecutive cell divisions (Chen, Wang et al. 2014, Eisch, Lu et al. 2016).

3.3. Nuclear Pore Complex and its role in nuclear morphology

Membrane-enclosed organelles within eukaryotic cells exchange molecules extensively with each other. Various compartments or organelles including the Golgi apparatus and ER communicate in multiple ways such as transporters and vesicle trafficking. Whereas mutual transport of molecules between cytoplasm and nucleus requires a distinct channel - the nuclear pore complex proteins (NPCs), which are located in the fusion loci

of inner and outer nuclear membranes (Bilokapic and Schwartz 2012, Grossman, Medalia et al. 2012)

Given the enormous size and unique position of the NPCs, their structure can be visualized by electron microscopy (EM). The NPC is evolutionary conserved and modular assembled, which comprises dynamic and stable components including ~30 nucleoporins and ~50 fiber-like dispersed repeats (Allen, Huang et al. 2001, Terry and Wente 2009). The complex structure of NPCs requires both stability and flexibility to keep molecule transport function efficiently, including RNA and protein exchange between cytoplasm and nucleus. Disruption of the NPCs causes fundamental alterations of nucleo-cytoplasmic communication, which may lead to cancer and autoimmune diseases (Cronshaw and Matunis 2004). Ultrastructural studies of the nuclei in progeria cells showed an increased number of nuclear envelope invaginations with clustering of the NPCs (Goldman, Shumaker et al. 2004, Paradisi, McClintock et al. 2005, McClintock, Gordon et al. 2006). Importantly, NPCs are shown to anchor into the nuclear lamina with B-type lamins concentrating in the pore-rich region and A-type lamins in the pore-free loci (Hutchison 2002, Maeshima, Yahata et al. 2006, Guo, Kim et al. 2014). Accordingly, aberrant distribution of NPCs is also associated with a reorganization of the nuclear lamina (Fiserova and Goldberg 2010, Maeshima, Iino et al. 2010).

4. Autophagy

Autophagy is typically known as a conserved intracellular components turnover process. This process involves trafficking substrates such as organelles and proteins to lysosomes via autophagosome vesicles for degradation (Cuervo 2004, Levine and Klionsky 2004, Shintani and Klionsky 2004, Klionsky 2005, Mizushima and Klionsky 2007). In comparison to the ubiquitin-proteasome system, autophagy is rather a simple process, which consists of several sequential steps including induction of autophagy, the formation of autophagosomes, degradation of substrates, and peptide generation. Each step has a great variety of functions, which allow autophagy to be multifunctional. However, the complex functions of autophagy remain elusive.

Autophagy is triggered by cellular stress such as depletion of nutrient. Under nutrient starvation conditions, the robust autophagy process is initiated. The activated autophagosomes target to the designated substrates for degradation, including mitochondria, peroxisomes, and aggregate-prone proteins. This results in amino acid generation and transportation to the cytosol for reuse in order to protect cells against starvation (Suriapranata, Epple et al. 2000, Sagne, Agulhon et al. 2001, Yang, Huang et al. 2006). Autophagy plays essential roles in multiple biological functions and defects in autophagy are associated with various diseases such as neurodegenerative diseases and cancer (Mizushima, Levine et al. 2008).

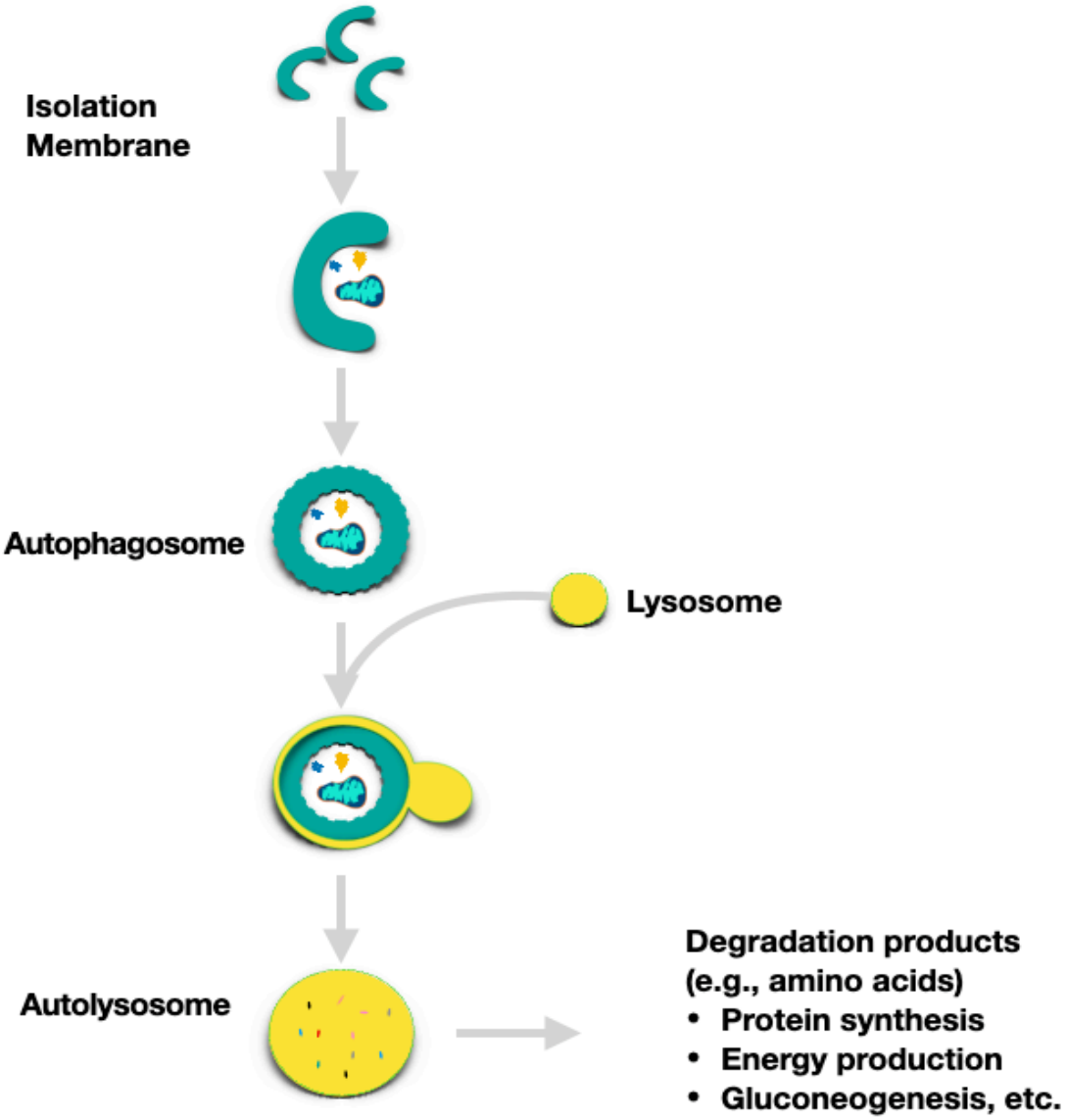

Figure 3. Autophagy. Schematic illustration of autophagy process. A portion of the cytoplasm is enclosed by an isolation membrane including organelles such as mitochondrion to form an autophagosome. The outer membrane of the autophagosome fuses with the lysosome, and the internal components are degraded in the autolysosome. After degradation by autophagy, the resultant products, such as amino acids can be used for different purposes, including new protein synthesis, energy production, and gluconeogenesis, etc.

4.1.Autophagy and Genomic Integrity

4.1.1.Autophagy regulates the cellular response to stress

The involvement of autophagy in genome maintenance was first observed in *beclin+/-* mutant mice, where autophagically compromised cells appear to have higher level of DNA damage and aneuploidy, which are hallmarks of genomic instability (Karantza-Wadsworth, Patel et al. 2007). This has been attributed to accumulation of damaged mitochondria, which then leads to abundant production of ROS (Mathew, Karp et al. 2009). Abundant ROS generation results in increased oxidative stress for both mitochondrial and nuclear DNA. Damaged mitochondria could be eliminated via autophagy, also called mitophagy. Mitophagy plays a critical role in maintaining normal function of mitochondria by reducing ROS abundance and ensuring a robust matrix for both cytoplasm and nucleoplasm (Kurihara, Kanki et al. 2012, Pickles, Vigie et al. 2018). Nrf2-Keap1 complex has been associated with the autophagy-mediated antioxidant process, which is one of the main cellular defense systems against oxidative stress (Itoh, Wakabayashi et al. 1999, Wakabayashi, Itoh et al. 2003). The Nrf2 protein (nuclear factor erythroid 2-related factor 2) regulates expressions of various antioxidant response genes to mediate cellular resistance to oxidant stress. Under the quiescent condition, Nrf2 is constitutively degraded via ubiquitin-proteasome pathway by its binding partner Keap1(Kelch-like ECH-associated protein 1), an adaptor of the ubiquitin ligase complex (Cullinan, Gordan et al. 2004, Kobayashi, Kang et al. 2004, Furukawa and Xiong 2005). Keap1 interacts with p62 and competes for its binding to Nrf2, which acts to release and stabilize Nrf2. Subsequently, it leads to transcriptional activation of

Nrf2 and its targeted genes for damage response (Komatsu, Kurokawa et al. 2010). The p62 protein is another autophagy substrate, which in turn suggests that the p62-dependent activation of Nrf2 for antioxidant stress response is regulated by autophagy.

4.1.2.Autophagy regulates the degradation of nuclear components

Since the discovery of autophagy in the 1950s, most studies have focused on the degradation of the cytoplasmic components, while the importance of nuclear materials degradation has been underrated. The nucleus plays crucial roles in maintaining genomic integrity under various physiological and pathological stresses. In order to respond to various stresses and maintain nuclear homeostasis, eliminating undesirable nuclear components are necessary. Until recently, the nuclear autophagy, also called nucleophagy, was observed in yeast cells (Roberts, Moshitch-Moshkovitz et al. 2003). This has clearly extended our understanding on the role of autophagy in regulating nuclear homeostasis.

LC3, the microtubule (MT) -associated protein 1A/1B-light chain 3, is a soluble protein distributed ubiquitously in mammalian cells. It plays critical roles in forming autophagosomal and autolysosomal membranes for autophagy (Kabeya, Mizushima et al. 2000). There are more than 500 candidate proteins potentially interacting with LC3. Strikingly, about one-third of these interacting proteins are associated with nuclear components and pathways (Behrends, Sowa et al. 2010). Most recently, Dou and colleagues have reported that LC3 is actively involved in the turnover of nuclear lamina components by directly interacting with lamin B1 (Dou, Xu et al. 2015). In this study, Dou et al. showed that lamin B1 is a selective substrate for autophagy upon RAS-

induced oncogenic stress (Dou, Xu et al. 2015). Lamin B1 and other nuclear lamina proteins are associated with transcriptionally inactive heterochromatin domains called LADs (lamin-associated domains) (Dechat, Pfleghaar et al. 2008). Depleting lamin B1 can result in destabilization of the nuclear envelope and extensive loss of nuclear integrity. Moreover, numerous studies have stated that lacking of lamin B1 leads to premature cell senescence and impaired DNA repair (Shimi, Butin-Israeli et al. 2011, Dreesen, Chojnowski et al. 2013, Shah, Donahue et al. 2013, Butin-Israeli, Adam et al. 2015). Upon abnormal cellular activities, autophagy is involved in the coordination of the compromised chromatin architecture and gene expression in lamin B1-depleted cells. This process is crucial for altering the cell fate such as arresting cell cycles via cellular senescence.

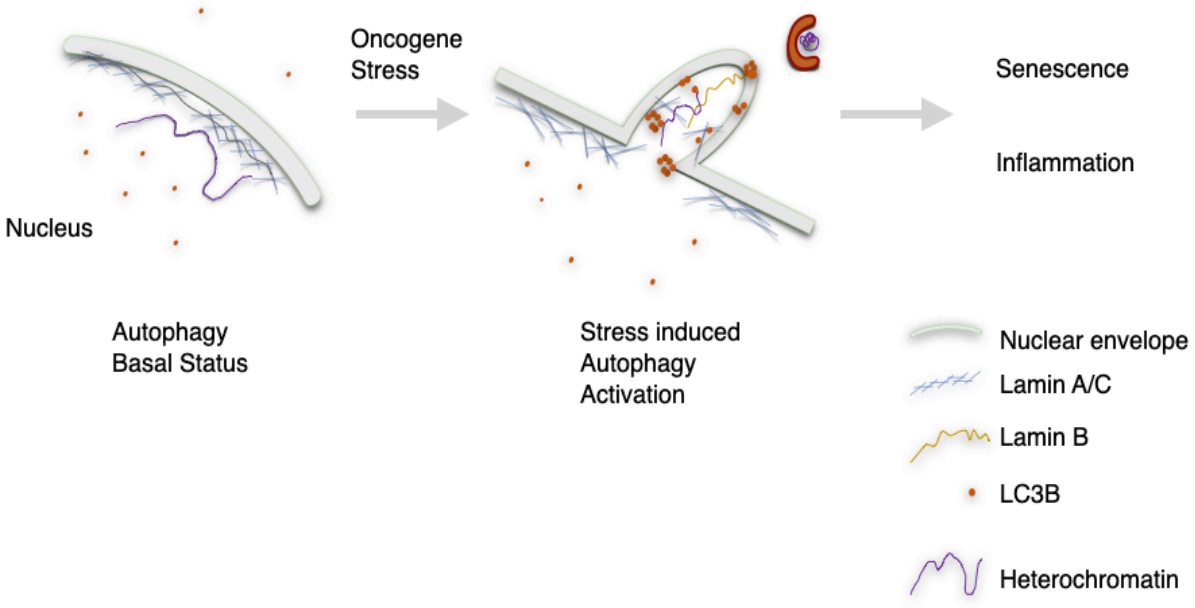

Figure 4. Oncogene-induced autophagy activation degrades nuclear components. At state, LC3B scarcely spreads in the nucleus. Under oncogene stress state, nuceloautophagy is activated, causing degradation of nuclear lamina and leaking of heterochromatin. Exposure of nuclear components to the cytoplasm leads to variable consequences, such as senescence, and inflammation.

4.2.Autophagy and Aging

Autophagy plays a critical role in recycling macromolecules as well as eliminating aggregate-prone proteins. Accumulated protein aggregation accompanied with chronically neuron loss characterizes late-onset neurodegenerative diseases. Most neurodegenerative disease-associated proteins have been shown to be substrates for autophagy, such as mutant α-synuclein (which causes Parkinson's disease), tau (implicated in Alzheimer's disease), and polyglutamine-expanded proteins like mutant huntingtin (that causes Huntington's disease) (Ravikumar, Duden et al. 2002, Webb, Ravikumar et al. 2003 , Ravikumar, Vacher et al. 2004, Rubinsztein, Codogno et al. 2012). Maintaining functional proteins in brain tissues requires high fidelity and efficiency of protein control (Forman, Trojanowski et al. 2004). Studies have shown that lacking essential autophagy genes in knock-out mouse models causes abnormal intracellular proteins accumulation, aggregation, and inclusions. Consequently, it leads to development of neurodegeneration (Hara, Nakamura et al. 2006, Komatsu, Waguri et al. 2006). Importantly, increased autophagy activity decreases the level of aggregated proteins in such models with beneficial effects.

5. The Search for Anti-aging Interventions

Over the years, aging and anti-aging researches have advanced intervention approaches against aging and aging related diseases. These approaches involve different aspects, including physiological, pharmacological, and genetic interventions.

5.1.Intervention for Physiological aging

Caloric restriction (CR) is one of the most tested anti-aging interventions, which refers to reduced food intake without malnutrition. CR has been shown to extend lifespan in many organisms, including rodents and rhesus monkeys, where CR-induced major reduction of insulin and insulin-like growth factor 1 (IGF-1) contributes to lower incidence of diabetes, cardiovascular disease, cancer, and brain atrophy (Colman, Anderson et al. 2009).

CR is the most efficient physiological inducer of autophagy through inhibiting IGF signaling, which also results in TOR suppression (Levine and Kroemer 2008, Kenyon 2010). TOR, an evolutionarily conserved protein kinase, is a major regulator of cellular metabolism by promoting cell growth in response to various environmental cues. More importantly, TOR negatively regulates autophagy. In mammalian cells, rapamycin, a lipophilic macrolide antibiotic, acts to enhance autophagy by inhibiting the activity of mTOR, the mammalian target of rapamycin (Rubinsztein, Gestwicki et al. 2007). Studies have shown that rapamycin-induced autophagy promotes clearance of undesirable protein species and organelles such as damaged mitochondria to protect cells against apoptosis (Ravikumar, Berger et al. 2006). However, it also suggests that rapamycin is not suitable for extending lifespan in humans because long-term track of rapamycin promotes insulin resistance and diabetes in mice (Lamming, Ye et al. 2012). Alternatively, intermittent rapamycin feeding has been shown to increase lifespan in mice (Anisimov, Zabezhinski et al. 2011). These studies opened new opportunities to avoid immunosuppression and its potentially detrimental effects on lifespan extension.

5.2.Finding the cure for premature aging

There is no cure for progeria to date. Interventions for physiological aging provide certain hints for finding therapeutic methods to delay the aging progress in progeria patients, but some approaches may not apply. The search for progeria treatment is still a long way ahead.

Lonafarnib, the first-ever progeria clinical trial, is a type of farnesyltransferase inhibitor (FTI), which was originally developed to treat cancer. Children receiving FTIs treatment have shown improvement in body weight, hearing, bone structure, and flexibility of blood vessels by restoring the nuclear morphology and genome integrity of cells (Gordon, Kleinman et al. 2012). Besides the requirement for lamin proteins to gain maturation, numerous proteins also demand protein farnesylation on certain levels. For example, the Ras proteins require the farnesyl lipid for anchoring the proteins to the plasma membrane and for proper protein functions. Mutations in Ras are involved in about 30% of all human cancers, thus prompts the development of many protein farnesyltransferase inhibitors (Cox and Der 2002, Downward 2003). However, treating primary human skin fibroblasts with FTIs resulted in high incidence of donut-shaped nuclei, which was also shown to be independent on the expression of progerin (Verstraeten, Peckham et al. 2011). This phenomenon continues to proceed with cell cycles and contributes to forming bi-nucleated cells and exhibit aneuploidy. Understanding the mechanisms of progerin-induced pathology in HGPS and searching for treatment of HGPS are still in highly demand.

6. Aim of the study

HGPS is a rare genetic disease that is caused by a single mutation in *LMNA* gene, which results in a toxic protein that leads to catastrophe in the cell nuclei of the patients. Firstly, given the characterization of HGPS cells, the aim of this study was to elucidate the molecular mechanism of cell morphology change and its association with cell senescence. Secondly, previous studies have shown the complex interactions between progerin and other nuclear and cytoplasmic components. Further detailed study of the pre-lamin A-/progerin-derived peptides and the nuclear envelope proteins were carried out to decipher the molecular mechanism of nuclear morphological change in progeroid cells.

While the disorganized microtubule network in HGPS cells has been previously described, little is known about the contribution of microtubule and its modification to cell senescence. Therefore, primary cultures of HGPS fibroblast were utilized to characterize the effects of microtubule and its posttranslational modification on important parameters of cell morphology and its correlation with progerin in cell senescence. Given the evidence of increased acetylation of microtubule in HGPS cells, this study focuses on the correlation of upregulated microtubule acetylation with progerin accumulation.

Further studies will aim to answer the question how toxic progerin peptides cause disorganization of nuclear membrane and interruption of nuclear integrity. Given the evidence that nuclear stress activates nucleophagy cascade, the putative targets of

autophagosome could be confirmed and subsequent studies on the essential role of autophagy in mediating the nuclear integrity in HGPS cells are needed.

7. Results

7.1.Phenotype analysis of HGPS cells

7.1.1.Morphology changes in HGPS cells

Cells depend on cytoskeletal polymers to establish their asymmetrical shapes, to transport intracellular constituents, and to drive their mobility. Because of the aberrant splicing event with truncated prelamin A in HGPS cells, progerin expression could only be observed in HGPS cells but not normal cells (Figure 5A). Immunocytochemistry staining of cytoskeletal tubulin showed that normal fibroblast cells present with spindle-like cell shape, while staining for progerin is negative (Figure 5B). In contrast, the appearance of flat cell shape was observed in HGPS cells together with dysmorphic nuclei, including altered nuclear shape, herniations, and wrinkles as evident by progerin staining (Figure 5B').

Further cell morphology analysis was performed by employing the Skeleton Intersection detection with ImageJ. The results showed that normal fibroblasts appear to have equally spread skeletal intersections in the cytoplasm (Figure 5C). However, HGPS cells tend to have rich skeletal intersections at the nuclear periphery region (Figure 5C'), suggesting a disorganized cytoskeletal structure in HGPS cells.

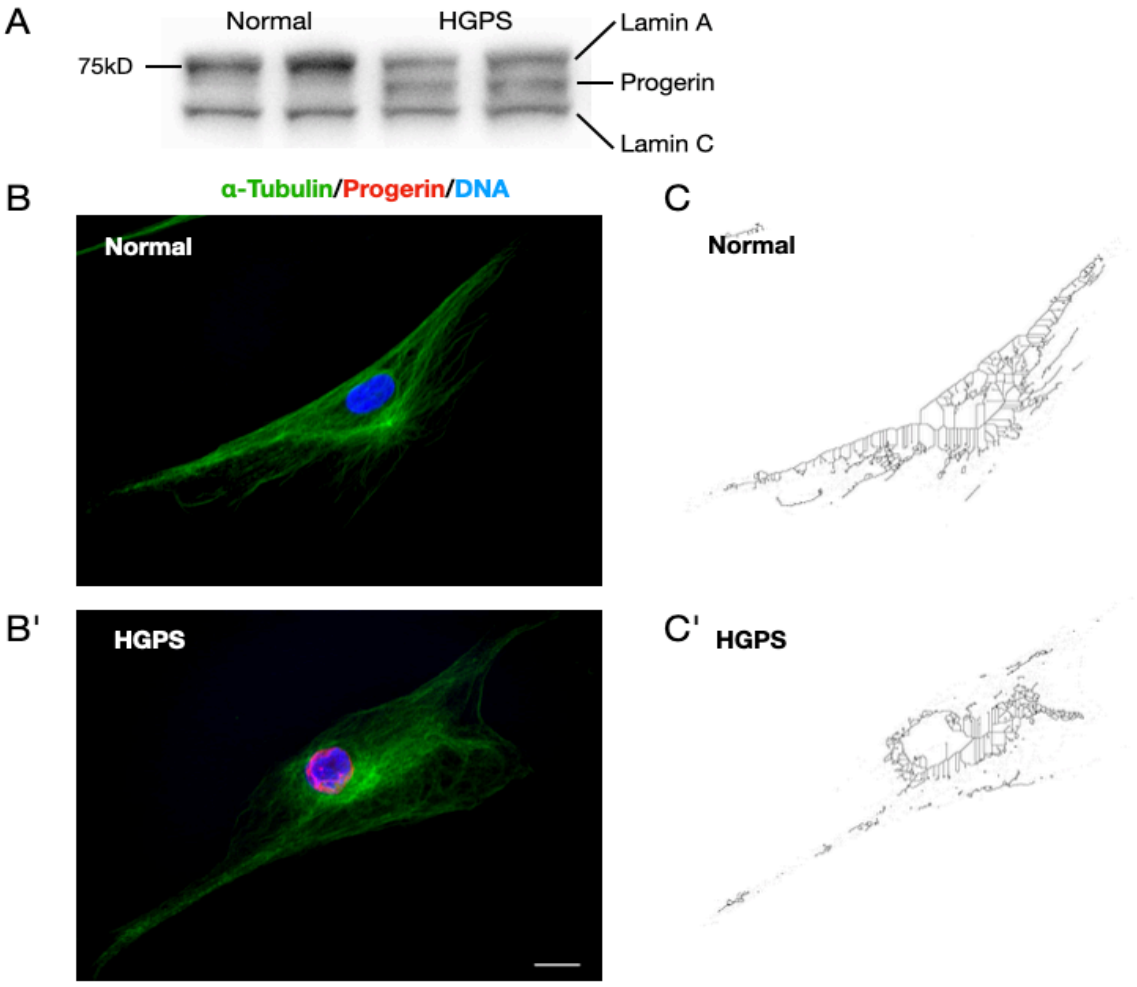

Figure 5. Cell morphology changes in HGPS fibroblast cells. (A) Western blot shows lamin A/C protein expression in normal and HGPS cells. In HGPS cells, expression of truncated prelamin A, termed as progerin, can be observed. (B, B') Immunofluorescent staining showed α-Tubulin in green, progerin in red, and DNA in blue. Staining for progerin in normal cells is negative. Altered nuclear shape for progerin staining in HGPS cells is shown. Scale bar 10μm. (C, C') Skeleton intersection analysis of the normal and HGPS fibroblasts. In normal cells, microtubules intersections spread equally in the cytoplasm. In HGPS cells, microtubule intersections are gathered in the nuclear periphery region.

7.1.2.Tubulin acetylation is increased in HGPS cells.

Tubulin can be subject to many PTMs, which affect MT dynamics, organization, and interactions with other cellular components. Given the observation of disorganized MT network in HGPS cells, we sought to evaluate the post-translational modification of MT in both normal and HGPS cells.

We first determined the subcellular distribution of acetylated tubulin. In normal cells, the acetylated tubulin is mostly spread in the cytoplasm and a concentrated microtubule organization center (MTOC) can be observed, which is distal to the cell nuclei (Figure 6A). The acetylation-free tubulin distributed throughout the cytoplasm showing asymmetrical spindle like pattern (Figure 6). However, in HGPS cells, the acetylated tubulin is mostly enriched in a large region proximal to the nuclear periphery (Figure 6). Besides, the acetylation-free tubulin was also found distributed in the same region as acetylated tubulin but less spread in the cytoplasm (Figure 6). These results suggest that the acetylation of tubulin alters the organization of the microtubule network.

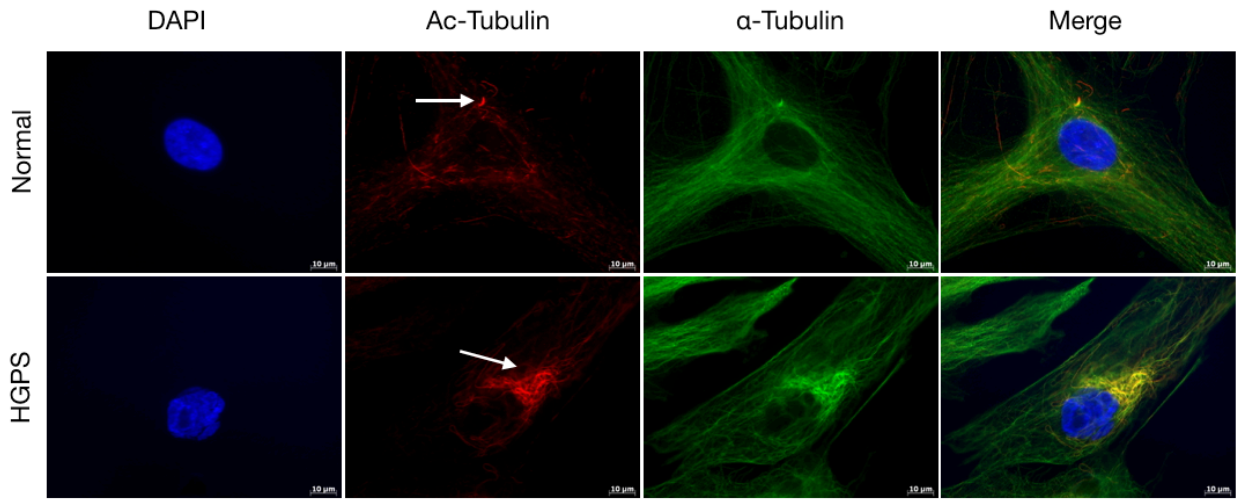

Figure 6. Tubulin acetylation alters the structural organization of microtubules. Immunocytochemistry stainings of DNA in blue, acetylated Tubulin in red and α-Tubulin in green are shown. Microtubule organization center (MTOC) is indicated by arrowheads. Scale bar: 10μm.

Further, cold treatment for depolymerizing acetylated tubulin was performed. After depolymerization, concentrated single MTOCs were revealed in normal cells, however, multiple MTOCs were maintained at the nuclear periphery region in HGPS cells (Figure 7A) with a significant proximal distance to the nuclei compared to the normal cells (Figure 7A, B). The result showed that acetylation of tubulin alters the distribution of MTOC in HGPS cells thus affecting the organization of microtubule networks.

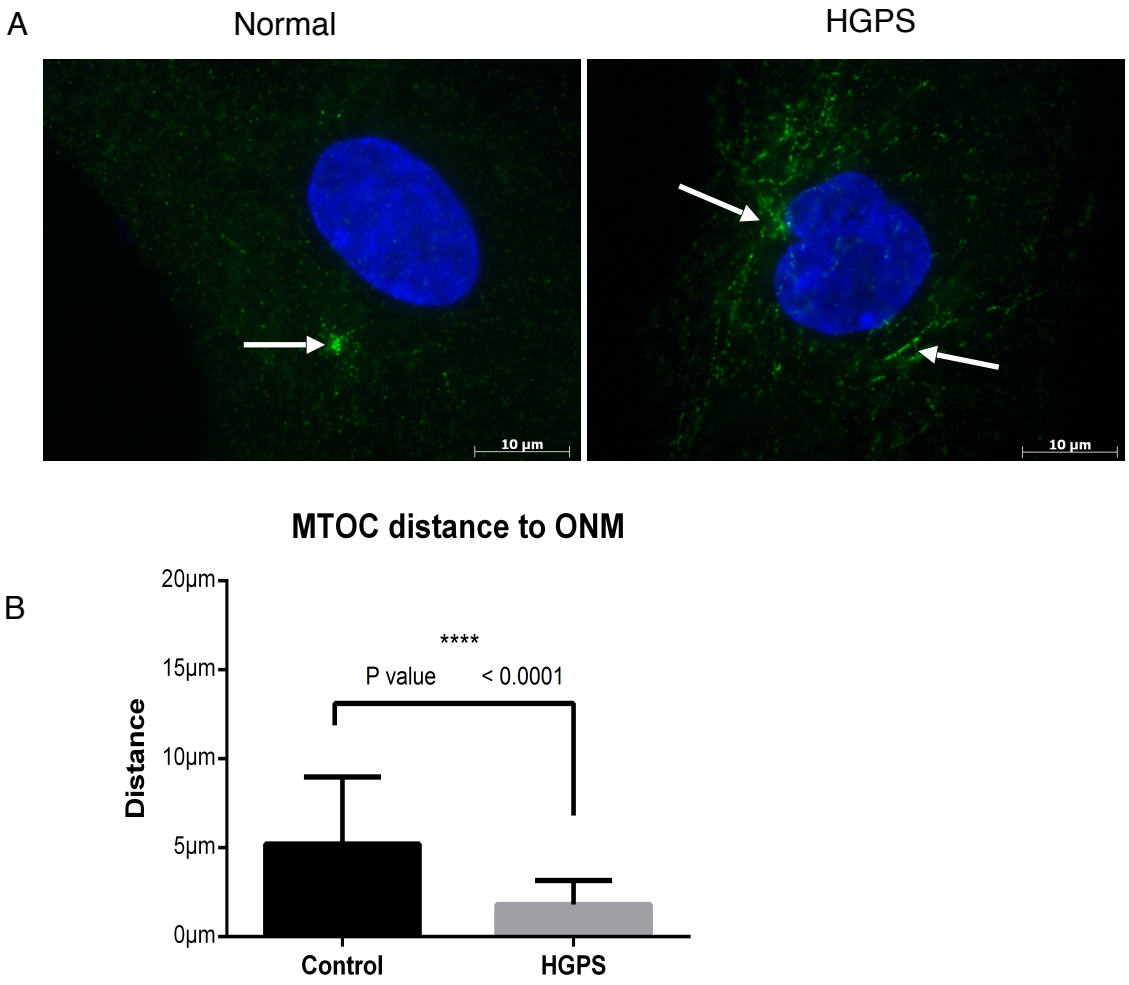

Figure 7. Abnormal distribution of the MTOC in HGPS cells. (A) Immunocytochemistry staining showed DNA in blue and acetylated Tubulin in green. MTOCs are indicated by arrowheads. Scale bar: 10μm. (B) Distance from MTOC to outer nuclear membrane is significantly closer in HGPS cells compared to control cells (>200 cells were collected, n=3).

Next, we determined the levels of acetylation of tubulin in both normal and HGPS cells. The western blot analysis showed that the level of acetylated tubulin is increased in HGPS cells compared to normal cells (Figure 8), while the level of acetylation-free tubulin remains unchanged (Figure 8), which is consistent with the observation of immunocytochemistry that acetylation of tubulin has no effect on the content of microtubules but alters the organization of microtubule network.

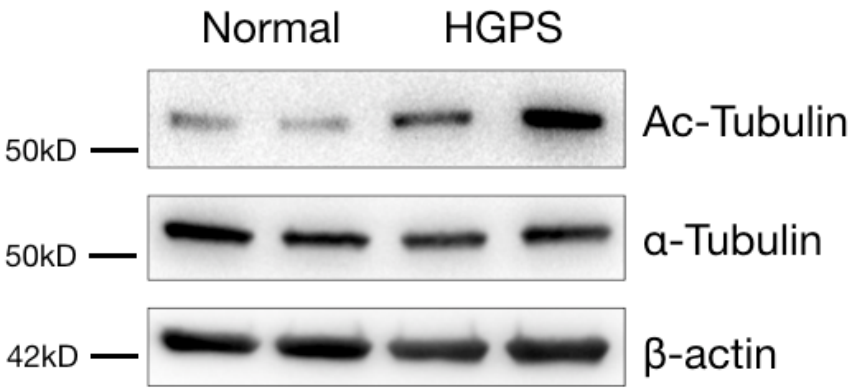

Figure 8. Tubulin acetylation increases in HGPS cells. Western blot analysis shows that the level of tubulin acetylation is increased in HGPS cells compared to normal cells. Level of acetylation-free tubulin does not change. α-Tubulin and β-actin are used as loading controls.

7.1.3. Tubulin hyperacetylation is correlated with progerin accumulation and contribute to cell senescence in HGPS cells.

Nuclear lamina functions as nucleoskeleton, which is connected via the LINC complex to the cytoskeleton. Progerin is permanently anchored to the inner nuclear membrane due to farnesylation at its carboxy-terminal end. Importantly, progerin is insoluble and progressively accumulates within cells. We sought to determine whether the

accumulation of progerin is associated with disorganization of the microtubule network in HGPS cells.

HGPS cells were stained with progerin and acetylated tubulin antibodies for fluorescent intensity determination (Figure 9A, B). The result showed that HGPS cells are heterogeneous in terms of progerin levels (Figure 9B, arrowheads). Interestingly, fluorescent intensity levels of the tubulin acetylation are more in cells with an accumulated amount of progerin than cells with a lesser amount of progerin (Figure 9B). Further, correlation analysis showed a positive correlation between the fluorescent intensity of progerin and acetylated tubulin (Figure 9C), suggesting that accumulation of progerin is positively correlated to increased microtubule acetylation. The results indicate that the accumulation of progerin may affect the organization of microtubule networks.

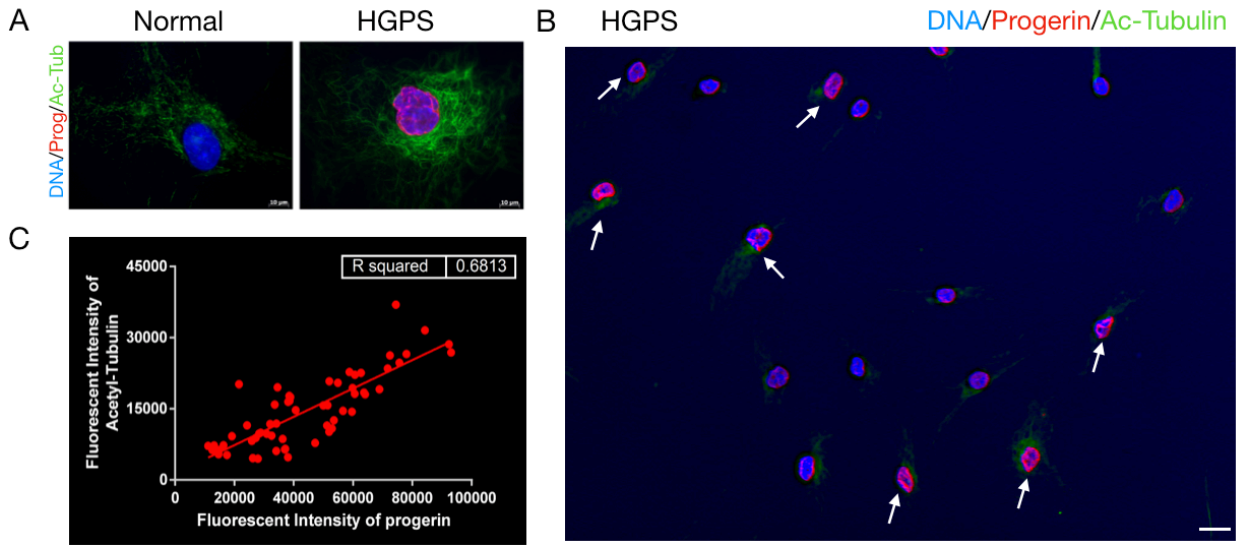

Figure 9. The correlation of progerin with tubulin acetylation. (A, B) Immunocytochemistry staining of normal and HGPS fibroblasts with DNA in blue, progerin in red, and acetylated tubulin in green are shown. Normal cells showed negative staining of progerin and scattered distribution of acetylated tubulin in the cytoplasm. HGPS cells showed altered nuclear shape by staining for progerin and rich acetylation of tubulin at the nuclear periphery. (B) Low magnification of HGPS cells stained with progerin and acetylated tubulin are collected for fluorescent intensity analysis. Heterogeneous of progerin levels in HGPS cells are indicated by arrowheads. (C) xx analysis showed positive correlation of fluorescent intensity between progerin and acetylated tubulin in HGPS cells.

Disorganization of microtubules affects not only the cell shape but also a wide variety of cellular events, including cell motility and cell division. Therefore, we examined the cell senescence level in both normal and HGPS cells to determine whether altered post-translational modification of microtubule is associated with cell senescence. β-galactosidase detection assay was performed to detect the levels of cell senescence. The results showed that HGPS cells have higher activity of β-galactosidase compared to normal cells (Figure 10). In normal cells, scattered distribution of the acetylated tubulin in the cytoplasm was observed (Figure 10). However, HGPS cells with increased activity of β-galactosidase appeared to have increased acetylation of tubulin, suggesting that cell senescence is associated with increased microtubule acetylation. Collectively, progerin is positively correlated with acetylation of the microtubule, which may also contribute to cell senescence.

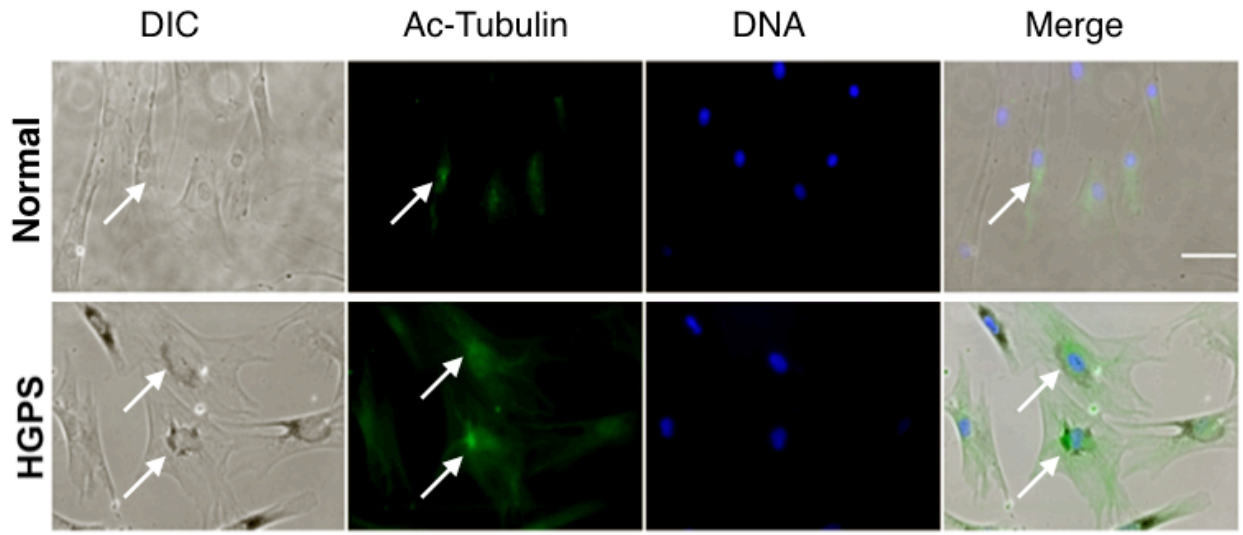

Figure 10. Microtubule hyperacetylation is associated with cell senescence. β-galactosidase activities detection in normal and HGPS cells and acetylated tubulin staining in green and DAPI in blue are shown. In normal cells, no β-galactosidase activity is detected, and scattered distribution of acetylated tubulin are shown (arrowheads). In HGPS cells, increases activities of β-galactosidase are detected and correspondingly, increased tubulin acetylation is observed (arrowheads). Scale bar: 20 μm.

7.2.Molecular mechanism of nuclear defects in HGPS cells

7.2.1.Intracellular Dynamics of the Prelamin A and Progerin Carboxy-Terminal Fusion Proteins

To study molecular mechanisms of the nuclear defects and cell aging in HGPS cells, we further analyzed the carboxy terminal of prelamin A and progerin in greater detail. We generated a series of EGFP constructs encoding various sizes of the carboxy-terminal (CT) domains of prelamin A and progerin (Figure 11)—including an NLS sequence and/or CaaX motif—to characterize the differences in the function of the CT domains of prelamin A and progerin. The sequences of the EGFP fusion proteins are indicated (Figure 11).

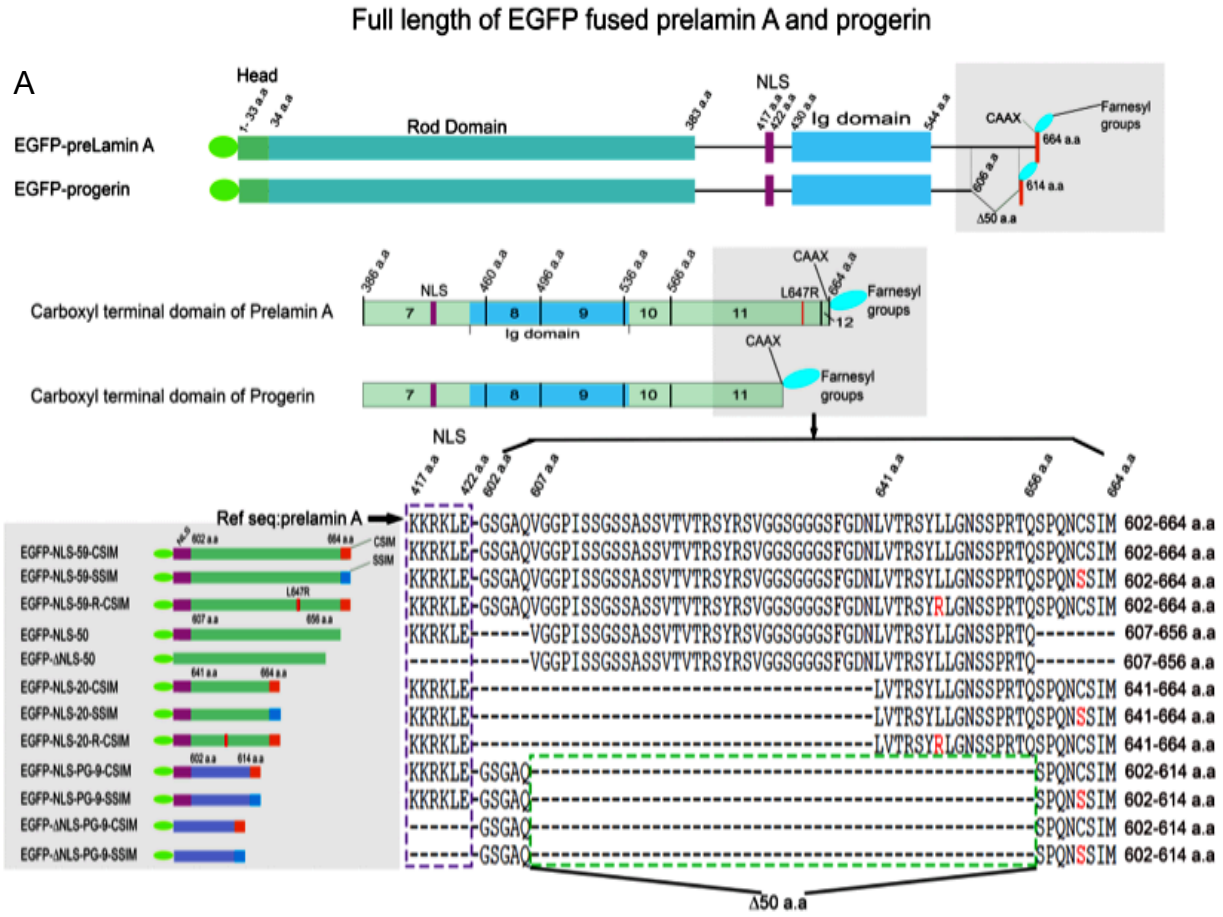

Figure 11. Schematic representation of the C-terminal fragments of prelamin A and progerin. (A) Schematics depicting the structures of the EGFP–prelamin A and EGFP–progerin proteins, and constructs derived from their C-terminal domains. The C-terminal domain of the indicated protein is enlarged, and the alignment of the construct sequences is shown. (1) Residues from 602 to 664 a.a. (amino acids) are marked as 59-CSIM/SSIM/R-CSIM, which represents the wild-type, C661S mutant, and L647R mutant C-terminal fragments of prelamin A, respectively. (2) The 50 a.a. construct encodes the 50 a.a. in-frame deletion of prelamin A from 607 to 656 a.a. (3) Residues from 641 to 664 a.a. of prelamin A are marked as 20-CSIM/SSIM/R-CSIM, which represent the short form of wild-type, C661S mutant, and L647R mutant C-terminal fragments of prelamin A, respectively. (4) The PG-9-CSIM/SSIM, residues from 602–614 a.a. of progerin, represents the C-terminal fragment of progerin and its corresponding C661S mutant form. A nuclear localization signal (NLS, KKRKLE) was linked to a part of the constructs as indicated.

Based on the properties of the protein sequence, we first predicted the features of each EGFP fusion protein, including pI value, static charge, and post-translational modifications such as farnesylation, carboxymethylation, Zmpste 24 cleavage, and nuclear membrane binding ability (Figure 12). Among these features, we proposed that (1) proteins containing the NLS sequence can be transported to the nucleus, (2) proteins containing 50 a.a. and CaaX motif can be processed as prelamin A, (3) proteins containing CaaX motif but lack the Zmpste 24 cleavage site can be farnesylated and retain the farnesylation group and bind to the nuclear membrane (Figure 12).

	Predicted features					
	pI	Charge	Farnesylation	Carboxy -methylation	Zmpste cleavage	NE binding
EGFP-NLS-59-CSIM	10.6	+	+	+	+	−
EGFP-NLS-59-SSIM	11.1	+	−	−	−	−
EGFP-NLS-59-R-CSIM	11.0	+	+	+	−	+
EGFP-NLS-50	11.1	+	−	−	−	−
EGFP-ΔNLS-50	10.1	+	−	−	−	−
EGFP-NLS-20-CSIM	10.5	+	+	+	−	+
EGFP-NLS-20-SSIM	11.1	+	−	−	−	−
EGFP-NLS-20-R-CSIM	11.1	+	+	+	−	+
EGFP-NLS-PG-9-CSIM	9.7	+	+	+	−	+
EGFP-NLS-PG-9-SSIM	10.3	+	−	−	−	−
EGFP-ΔNLS-PG-9-CSIM	5.7	−	+	+	−	+
EGFP-ΔNLS-PG-9-SSIM	5.5	−	−	−	−	−

Figure 12. Predicted features of EGFP fusion proteins. Based on the protein sequence properties, predicted features of all constructs were indicated: pI value, static charge, and post-translational properties, including farnesylation, carboxymethylation, Zmpste cleavage, and nuclear membrane binding ability.

Western blot analyses showed that all EGFP fusion proteins were expressed in transfected HeLa cells at the expected sizes (Figure 13). NLS-59-CSIM (602-664 a.a.), corresponding to the CT domain of prelamin A, showed a slightly smaller size than NLS-59-R-CSIM (containing the L647R mutation) and NLS-59-SSIM (containing the C661S mutation), indicating that this protein underwent post-translational processing (Figure 13). NLS-50 (607–656 a.a.), which corresponds to the 50 a.a. that are missing in the progerin protein, was of similar size as NLS-59-CSIM (Figure 13). Therefore, the NLS-59-CSIM protein was processed in a similar manner as full-length prelamin A, resulting in the production of a CT sequence similar to the corresponding mature lamin A CT domain (Sinensky, McLain T. et al. 1994). The NLS-59-R-CSIM and NLS-59-SSIM proteins, however, were not cleaved and therefore corresponded to the CT end of prelamin A.

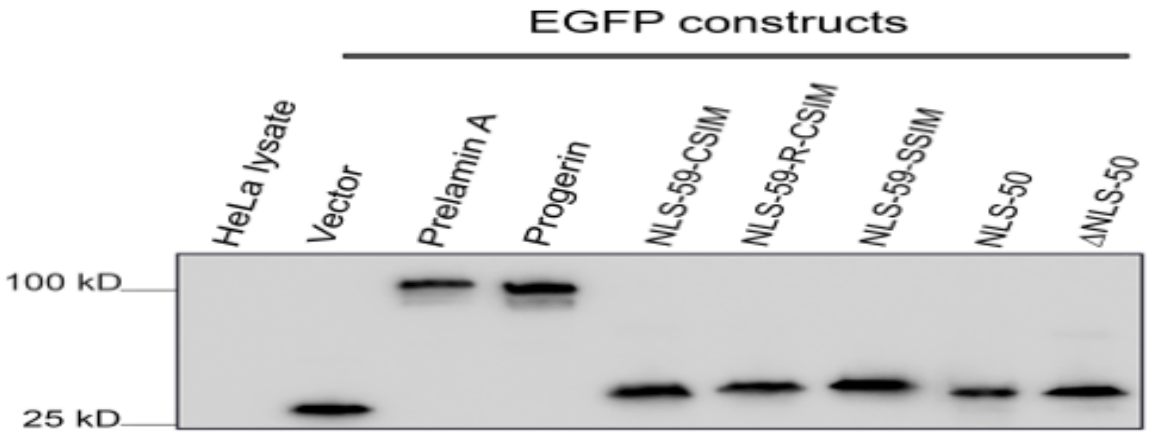

Figure 13. Western blot analysis of EGFP-fusion proteins. Full-length EGFP-prelamin A, progerin and 50 a.a. containing proteins were expressed in HeLa cells. Western blot analysis of EGFP-construct expressions showing corresponding sizes according to different post-translational modifications.

The Zmpste 24 enzyme requires the last 41 a.a. of the prelamin A CT for its efficient cleavage activity (Barrowman, Hamblet et al. 2012). The NLS-20-CSIM and NLS-20-R-CSIM proteins were in similar size but were slightly smaller than NLS-20-SSIM (Figure 14). Based on this result, both NLS-20-CSIM and NLS-20-R-CSIM were farnesylated but Zmpste 24 did not further process NLS-20-CSIM, due to the short a.a. sequence upstream of the Zmpste 24 cleavage site (Figure 14). The NLS-20-CSIM corresponds to the wild-type 20 a.a.-CaaX CT domain of prelamin A that maintained the last 15 amino acids and the farnesylated and carboxymethylated cysteine. The NLS-PG-9-CSIM, corresponding to the last 13 a.a. of the progerin CT domain, was slightly smaller in size than its counterpart, NLS-PG-9-SSIM, which cannot be farnesylated (Figure 14). Collectively, all EGFP fusion proteins were efficiently expressed in transfected HeLa cells, migrated at the expected molecular weights, and showed a certain degree of post-translational modifications (i.e., farnesylation and/or Zmpste 24 cleavage), according to the Western blot analyses.

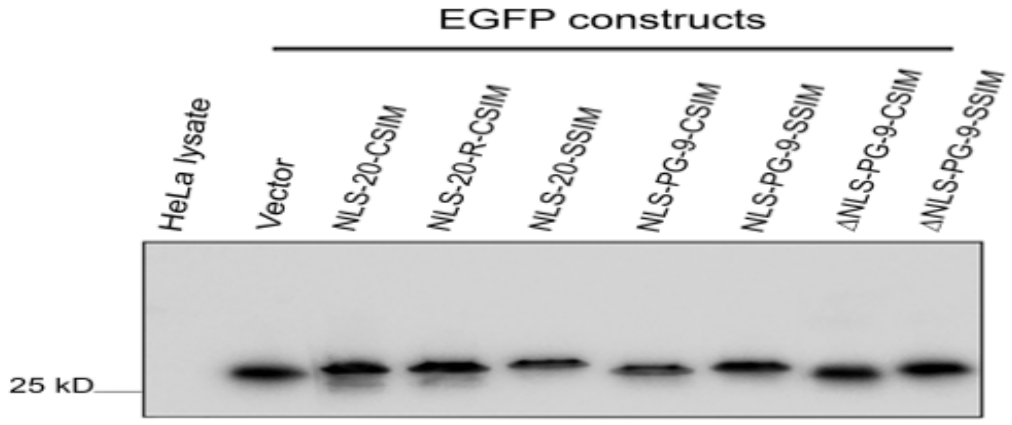

Figure 14. Western blot analysis of EGFP-fusion proteins. EGFP-constructs containing the last 20 a.a. of prelamin A and last 9 a.a. of progerin were expressed in HeLa cells., Western blot analysis of EGFP-construct expressions showing corresponding sizes according to different post-translational modifications.

7.2.2.The Farnesylated CT Domains of Prelamin A and Progerin Are Sufficient for Inducing NE Defects

We examined the subcellular localization of the various EGFP fusion proteins in transfected HeLa cells relative to lamin B1 using immunohistochemistry to identify the potential alterations in the subcellular targeting of the CT fragments of prelamin A and progerin.

In HeLa cells transfected with the EGFP–vector, the EGFP signal spread throughout the cytoplasm and the nucleus, and typical nuclear lamin B1 rim-like staining was observed (Figure 15). The EGFP–prelamin A fusion protein showed a nuclear rim signal overlapping lamin B1 staining at the NE (Figure 15). The EGFP–progerin signal colocalized with lamin B1 at the NE and NE invaginations, with most of the transfected cells showing an abnormal nuclear morphology (Figure 15). The EGFP–NLS-59-CSIM and EGFP–NLS-50 proteins were distributed in a diffused pattern in the nuclear compartment (Figure 15). This identical nuclear localization of EGFP–NLS-59-CSIM and EGFP–NLS-50 signified that NLS-59-CSIM underwent the same complete post-translational modifications as prelamin A and was no longer farnesylated. The EGFP–ΔNLS-50aa protein lacking the NLS exhibited a diffuse distribution throughout the cytoplasm and nucleus in transfected cells (Figure 15).

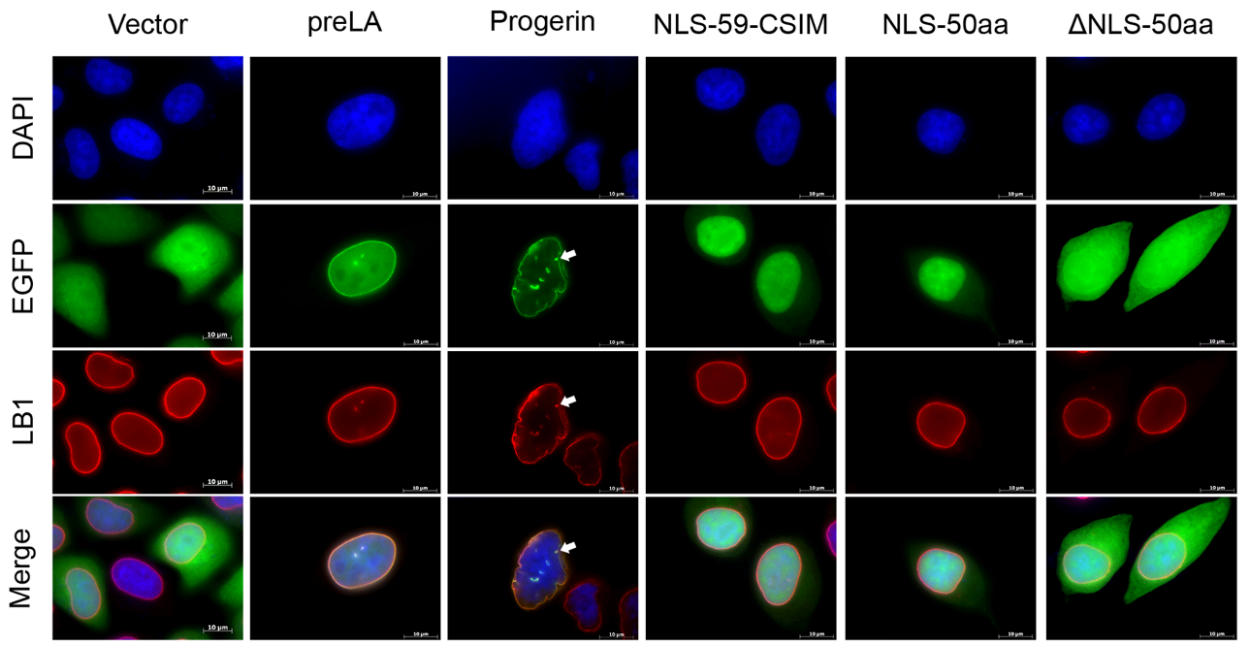

Figure 15. NLS directs the protein to the cell nucleus. Distribution of the subcellular localization of EGFP plasmids in transiently transfected HeLa cells is shown. Immunocytochemistry was performed on HeLa cells transfected with EGFP fusion proteins. Cells were stained with an anti-lamin B1 antibody. Chromatin was stained with DAPI. Representative images of lamin B1 staining in the indicated cells. Scale bar: 10μm.

EGFP–NLS-59-R-CSIM colocalized with lamin B1 at the NE (Figure 16). The abnormal nuclear shape and enlarged NE structures emanating from the NE were observed in the EGFP-positive cells (Figure 16A, B). Lamin B1 and EGFP–NLS-59-R-CSIM signals were superimposable at the NE evaginations (Figure 16A, B). The EGFP–NLS-PG-9-CSIM protein colocalized with lamin B1 at the NE and within NE evaginations, as observed in EGFP–NLS-59-R-CSIM-transfected cells (Figure 16A, B). The EGFP–ΔNLS-PG-9-CSIM protein, however, localized in the cytoplasm and at sites around the NE on the cytoplasmic face of the NE (Figure 16A). Based on these results, EGFP fusion proteins containing a terminal CSIM underwent farnesylation and fragments that remained farnesylated localized at the NE, except for NLS-20-CSIM, which was also present to a lesser extent at the cytoplasmic membrane (Figure 16).

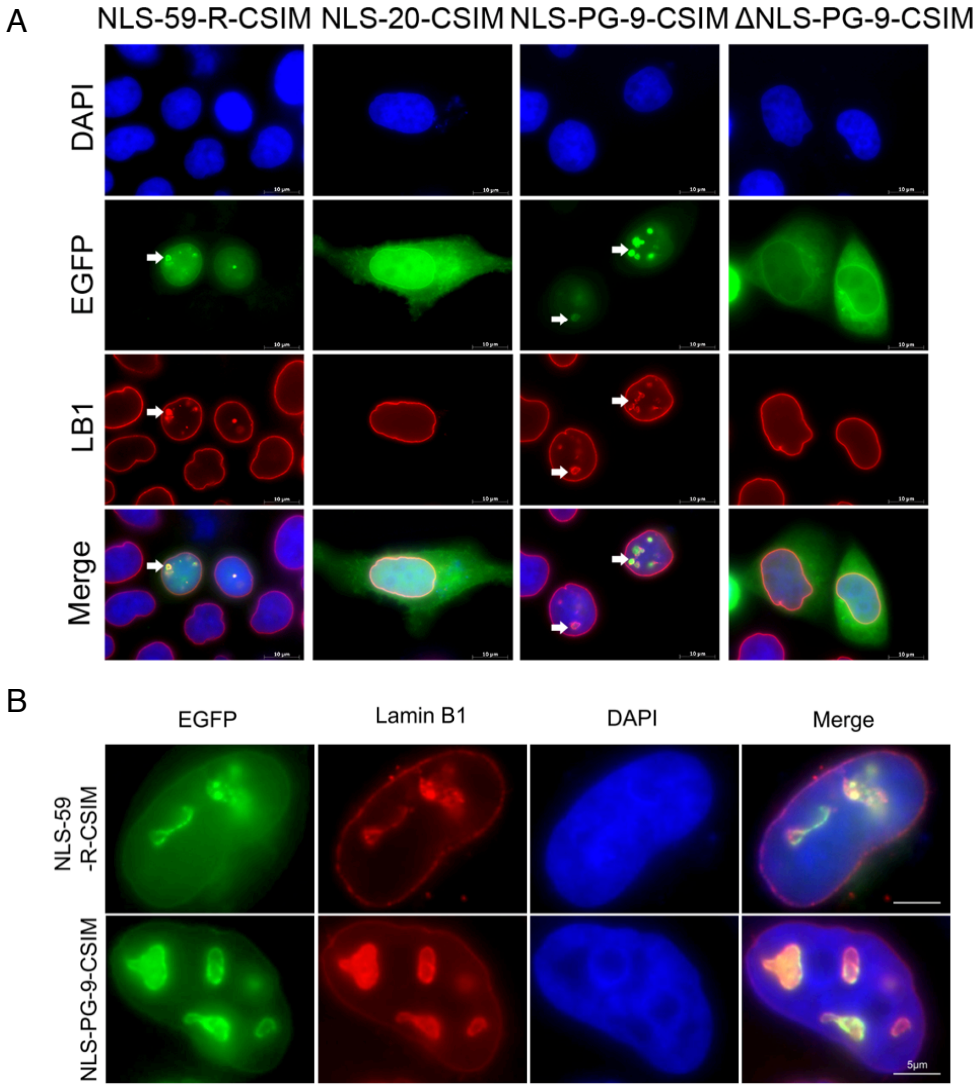

Figure 16. Determination of the cellular localization of EGFP plasmids in transiently transfected HeLa cells. Immunocytochemistry was performed on HeLa cells transfected with EGFP fusion proteins. Cells were stained with an anti-lamin B1 antibody. Chromatin was stained with DAPI. Representative images of lamin B1 staining in the indicated cells. (A) The farnesylated CaaX motif, along with the NLS, targets the EGFP–NLS-59-R-CSIM and EGFP–NLS-PG-9-CSIM proteins to the nuclear envelope (NE) and EGFP–NLS-20-CSIM protein to the NE and cytoplasm and membrane. Scale bar: 10 μm. (B) Abnormal nuclear envelope invaginations. Colocalization of EGFP-NLS-59-R-CSIM and EGFP-NLS-PG-9-CSIM with lamin B1 is shown. An enlarged view of EGFP signals emanating from the nuclear membrane shows abnormal nuclear invaginations. Scale bar: 5 μm.

The EGFP–NLS-20-CSIM protein was targeted at the NE, and a fraction of the protein was also detected at the plasma membrane as well as in the cytoplasmic compartments (Figure 16, 18A). Further immunodetection of GM130, a protein marker of the Golgi apparatus, showed that the EGFP–NLS-20-CSIM signal accumulated in the Golgi apparatus (Figure 17A) (Kondylis, Goulding et al. 2001). According to a previous report, the hypervariable region (HVR) of RAS proteins could undergo multiple post-translational modifications including CaaX farnesylation, carboxy-terminal methylation, and palmitoylation. The processed RAS proteins traffic through the classical secretory pathway via the Golgi to the plasma membrane, with the exception of K-Ras4B, which bypasses the Golgi (Hancock, Paterson et al. 1990, Hancock 2003). Based on this observation, we compared the protein sequences of NLS-20-CSIM with the HVRs of H-Ras, N-Ras, K-Ras4A, and K-Ras4B (Figure 17B). This sequence alignment indicated a certain degree of similarity between the NLS-20-CSIM and the HVRs of RAS proteins (Figure 17B). Thus, NLS-20-CSIM might traffic from the Golgi to the plasma membrane via the same route as RAS proteins.

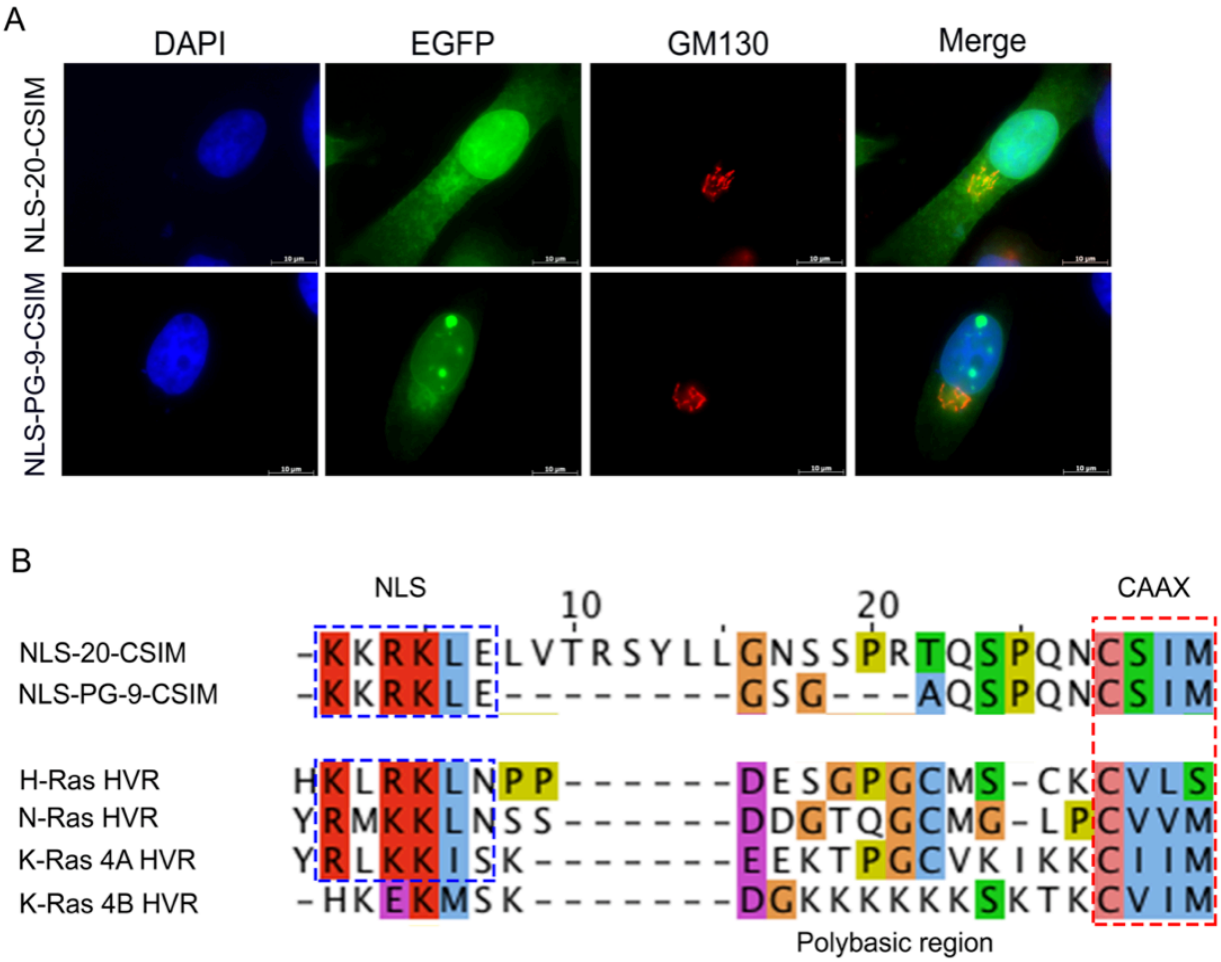

Figure 17. Trafficking of EGFP-NLS-20-CSIM. (A) GM130 was used to determine the cytoplasmic distribution of EGFP-NLS-20-CSIM signals. Representative images of cells expressing EGFP-NLS-20-CSIM showed the colocalization of cytoplasmic EGFP-NLS-20-CSIM with GM130. Chromatin was stained with DAPI. Scale bar, 10 μm. (B) An analysis of the similarity of the sequence of the NLS-20-CSIM proteins and hypervariable regions of RAS proteins, including H-Ras, N-Ras, K-Ras4A, and K-Ras4B. The NLS-20-CSIM protein showed a certain degree of similarity to the HVR of RAS proteins. Cellular distributions of RAS proteins are indicated by the rectangle. Scale bar, 10 μm.

Next, we generated mutants of these proteins by modifying the cysteine at position 661 to a serine residue (C661S), thus changing the CSIM to SSIM that is no longer farnesylated. Our results confirm that the farnesylation of the cysteine residue within the CSIM is required for the membrane interaction and NE localization (Figure 18A). These EGFP fusion proteins ending with an SSIM and containing an NLS sequence were not detected at the NE but localized throughout the nucleoplasm, and accompanied by a regular lamin B1 rim staining (Figure 18A). Moreover, EGFP–ΔNLS-PG-9-SSIM did not accumulate around the NE on the cytoplasmic face, indicating that the EGFP–ΔNLS-PG-9-CSIM fragment was farnesylated and localized to the outer NE. Further analysis of EGFP–ΔNLS-PG-9-CSIM distribution in relation to GM130, a Golgi marker (Kondylis, Goulding et al. 2001) showed that populations of this short farnesylated progerin peptide localized in Golgi apparatus (Figure 18B).

Taken together, the farnesyl modification is responsible for targeting the EGFP fusion proteins to the NE and causing abnormalities of NE and nuclear shape, as shown by the full-length progerin protein in transfected HeLa cells.

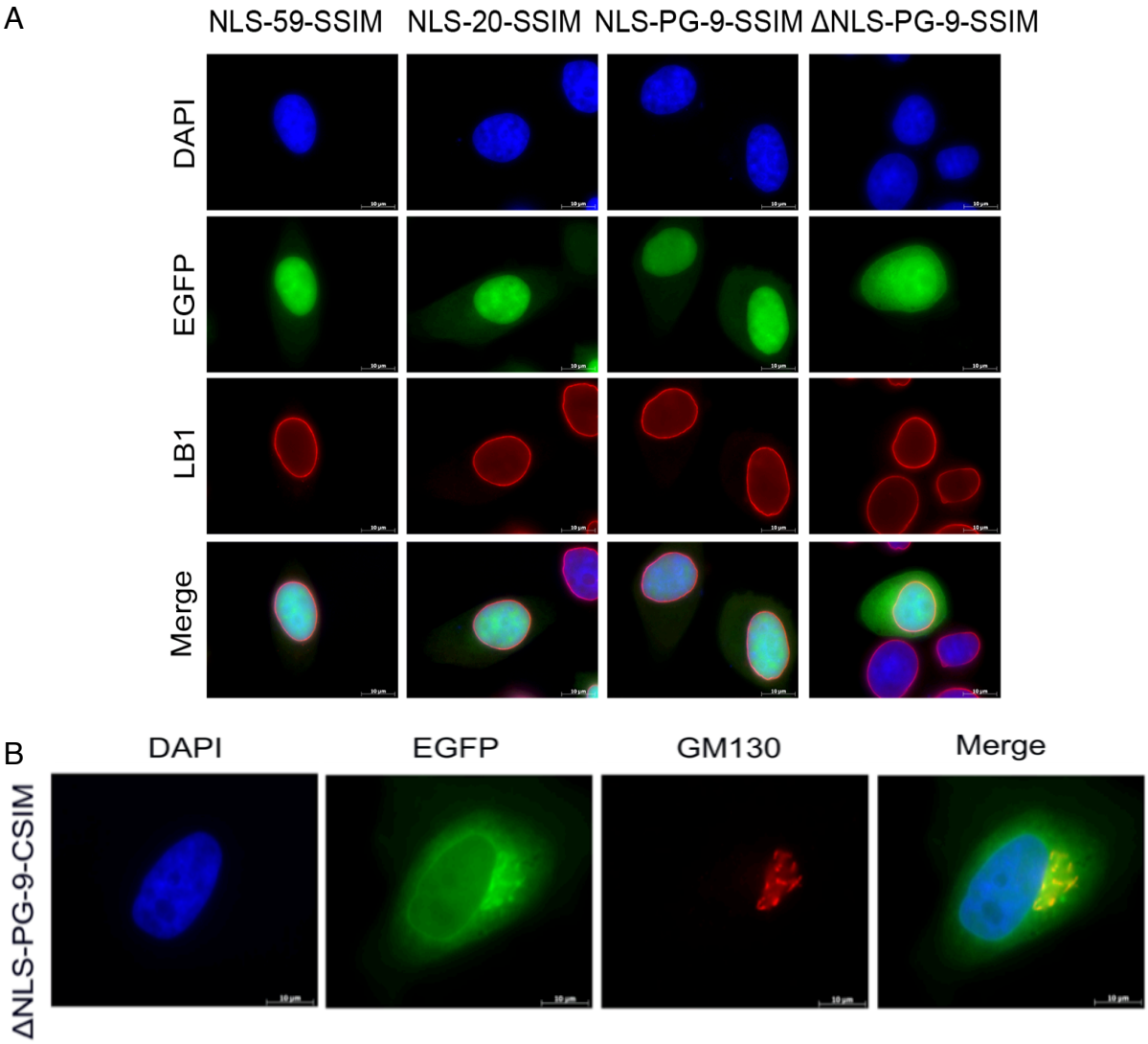

Figure 18. Distribution of EGFP-fusion proteins containing C661S mutation and further determination of ΔNLS-PG-9-CSIM. Immunocytochemistry was performed on HeLa cells transfected with EGFP fusion proteins. (A) Cells were stained with an anti-lamin B1 antibody. Chromatin was stained with DAPI. Representative images of lamin B1 staining in the indicated cells. (B) GM130 staining in ΔNLS-PG-9-CSIM transfected cells. ΔNLS-PG-9-CSIM targeted at the ONM and colocalized with GM130. Scale bar: 10 μm.

7.2.3.NE Proteins Are Mislocalized by the Farnesylated CT of Prelamin A and Progerin

Because the EGFP–NLS-59-R-CSIM and EGFP–NLS-PG-9-CSIM proteins induced NE deformations and evagination, we sought to evaluate their impacts on nuclear lamin B1, lamin C, and NE proteins—including emerin, nuclear pore complexes (NPC), and SUN1—in transfected HeLa cells.

Cells transfected with the empty EGFP vector exhibited a typical NE rim signal for lamin B1, lamin C, emerin, NPC-414, and SUN1 proteins (Figure 19A). In EGFP–NLS-59-R-CSIM-transfected cells, lamin B1, lamin C, emerin, and NPC-414 were all colocalized with the EGFP signal at the NE and the NE evaginations (Figure 19B, arrowheads). Meanwhile, SUN1 was present at the NE, but not in NE evaginations (Figure 19B). Notably, 54.33 ± 3.81% of lamin B1, 100% of lamin C, 74.78 ± 3.27% of emerin, and 94.86 ± 2.69 of NPC-414 signals overlapped with EGFP–NLS-59-R-CSIM at the NE invaginations (Figure 19C). In contrast, SUN1 signal was barely detectable at the NE tubular structures (Figure 19C).

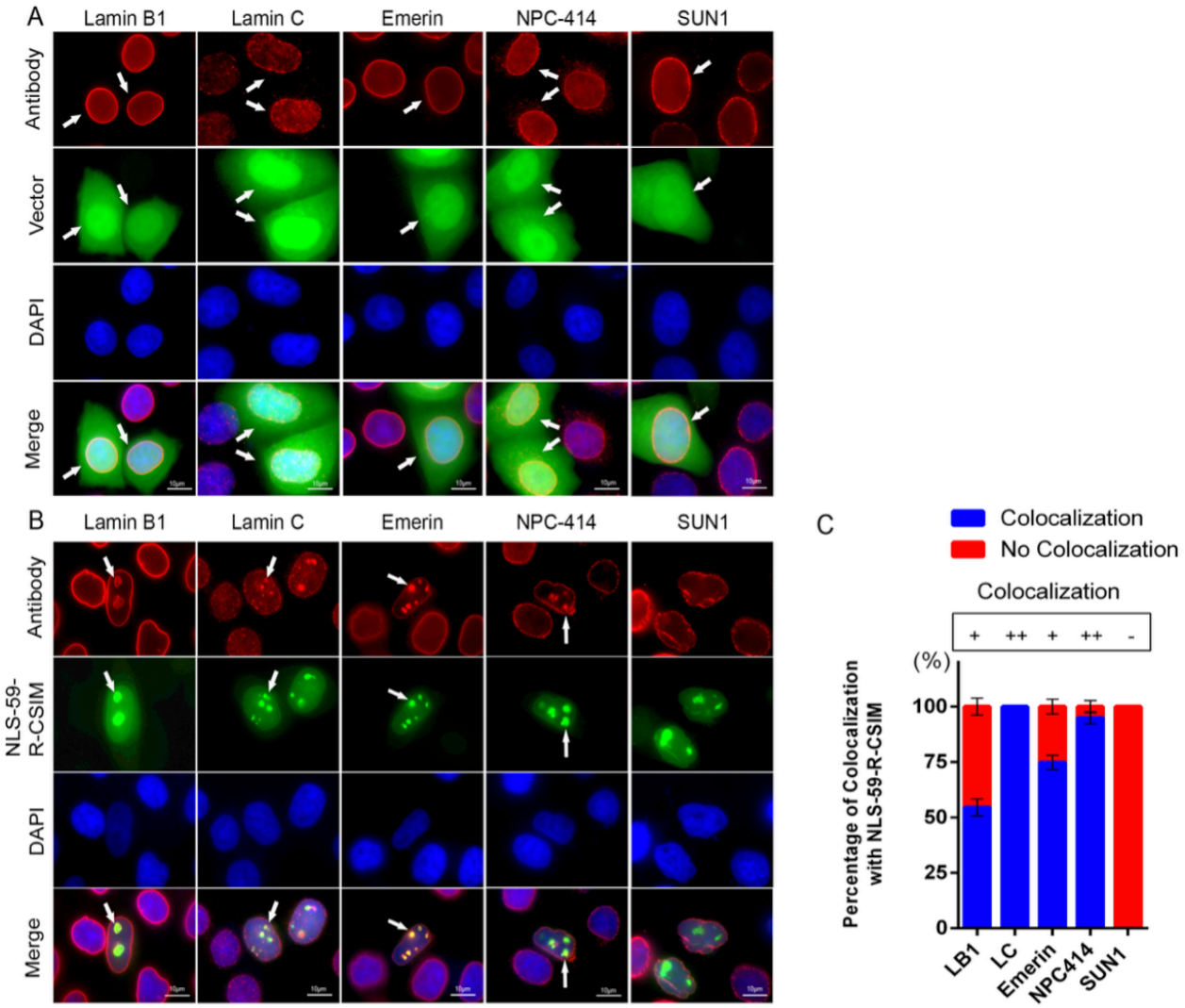

Figure 19. Disorganized distributions of NE proteins in NLS-59-R-CSIM transfected cells. (A) Immunocytochemistry was performed on EGFP vector, (B) EGFP–NLS-59-R-CSIM-transfected cells. Cells were stained with anti-lamin B1, lamin C, emerin, NPC-414, and SUN1 antibodies. Chromatin was stained with DAPI. Representative images showed colocalization of lamin B1, lamin C, emerin, and NPC-414 with EGFP signals at the NE as indicated with arrowheads. Scale bar, 10 μm. (C) Percentages of cells displaying colocalization of the NE protein and EGFP signal in the images shown. More than 300 EGFP-positive cells for each construct were counted, n = 3.

A similar distribution pattern was also observed for EGFP–NLS-PG-9-CSIM and lamin B1, lamin C, emerin, and NPC-414 at the NE and NE protrusions (Figure 20A,

arrowheads), whereas SUN1 was also absent from the NE evaginations in cells transfected with this construct. Colocalization frequencies indicated that EGFP–NLS-PG-9-CSIM overlapped with 55.72 ± 1.38% of lamin B1, 100% of lamin C, 70.51 ± 3.64% of emerin, and 95.17 ± 1.39% of NPC-414 signals at the NE evaginations, and SUN1 was absent from these NE protrusions (Figure 20B).

Furthermore, cells expressing high levels of both EGFP fusion protein fragments exhibited more nuclear abnormalities (Appended Fig. S 1–2). Therefore, the degree of NE disorganization directly depends on the expression level of these protein fragments in transfected HeLa cells. Based on these results, the farnesylated CT fragments of prelamin A and progerin induced NE deformation by interfering with the distribution of lamin B1, lamin C, as well as the inner NE proteins, emerin and NPC.

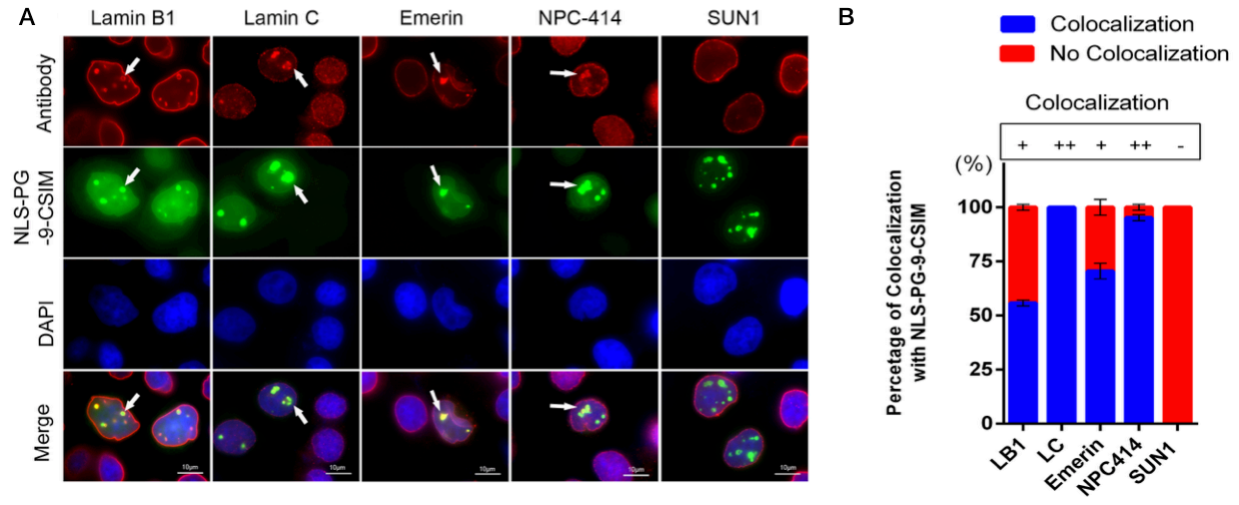

Figure 20. Disorganized distributions of NE proteins in NLS-PG-9-CSIM transfected cells. (A) Immunocytochemistry was performed on EGFP–NLS-PG-9-CSIM-transfected cells. Cells were stained with anti-lamin B1, lamin C, emerin, NPC-414, and SUN1 antibodies. Chromatin was stained with DAPI. Representative images showed colocalization of lamin B1, lamin C, emerin, and NPC-414 with EGFP signals at the NE and NE invaginations as indicated by arrowheads. Scale bar, 10 μm. (C) Percentages of cells displaying colocalization of the NE protein and EGFP signal in the images shown. More than 300 EGFP-positive cells for each construct were counted, n = 3.

7.2.4.NE Deformation Induces Heterochromatin Disorganization and Reduces Cell Proliferation

Because lamin B1 and emerin are intimately linked to heterochromatin organization, we evaluated the distribution of the heterochromatin protein HP1β (Eissenberg, James et al. 1990). In cells transfected with the EGFP vector alone, HP1β was exclusively located within the nucleoplasm (Figure 21). However, in both EGFP–NLS-59-R-CSIM- and EGFP–NLS-PG-9-CSIM-expressing cells, the HP1β signal was also detected in some cytoplasmic areas emanating from the NE (Figure 21, arrowheads). Moreover, the HP1β signal in these blebs colocalized with DAPI staining, indicating these foci contain

DNA (Figure 21). Therefore, both EGFP-farnesylated CT fragments could induce the loss of chromatin from the nuclear compartment.

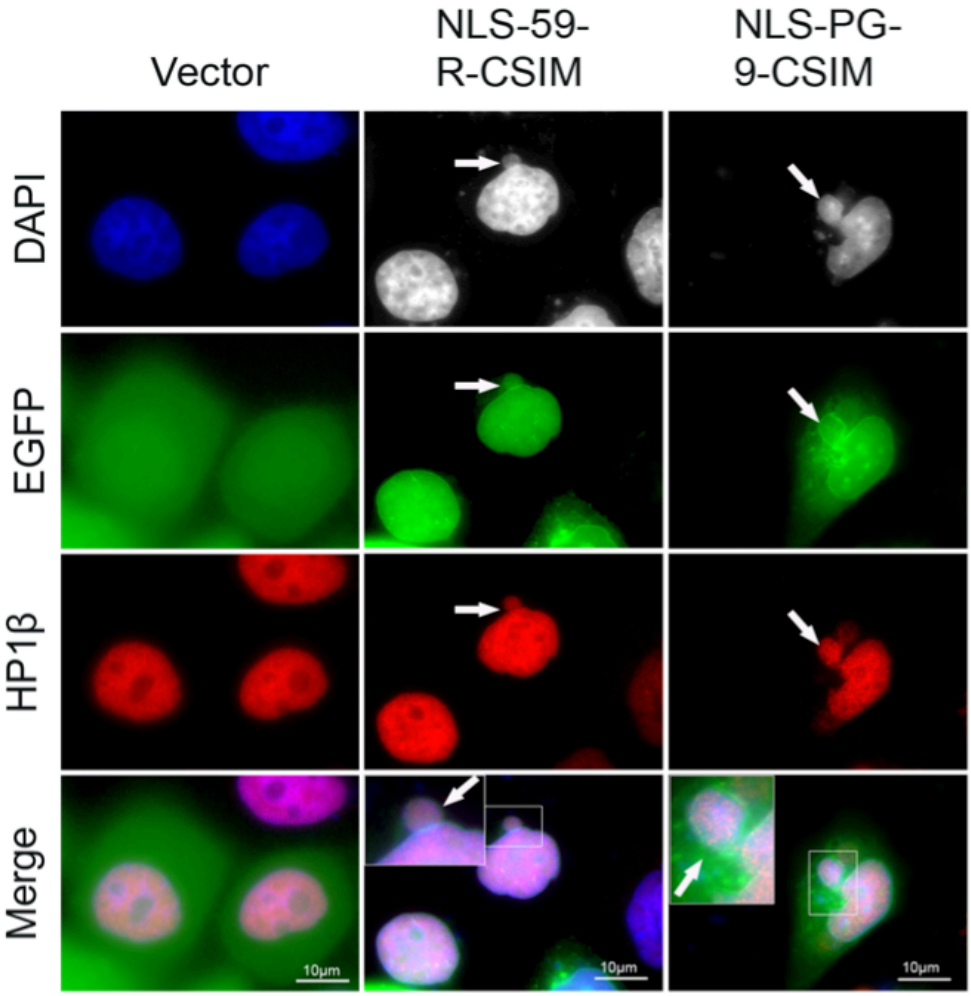

Figure 21. Determination of the heterochromatin organization. (A) Representative images of heterochromatin staining by anti-HP1β antibody in EGFP vector-, EGFP–NLS-59-R-CSIM-, and EGFP–NLS-PG-9-CSIM-transfected cells. Cytoplasmic HP1β staining shows the disorganized heterochromatin signals in EGFP–NLS-59-R-CSIM- and EGFP–NLS-PG-9-CSIM-transfected cells, as indicated by the arrowheads. Higher magnification images show the colocalization of DAPI and heterochromatin staining in the cytoplasm. Scale bar, 10 μm.

We postulated that these chromatin aggregates in the cytoplasm might be due to altered mitotic events. Therefore we examined the distribution of Ki67, a proliferation marker and a protein detected on actively replicating chromosomes (Scholzen and Gerdes 2000). Cells expressing the empty EGFP vector exhibited numerous large Ki67-positive speckles in the nucleus, indicating that the nuclei were replicating and, therefore, these cells were proliferating (Figure 22A).

In contrast, the Ki67 signal was barely detectable in cells transfected with EGFP–NLS-59-R-CSIM and EGFP–NLS-PG-9-CSIM (Figure 22A, circled region), indicating that these cells were not replicating. Based on these findings, cells transfected with these CT-farnesylated fragments were not mitotically active. For the statistical analysis of three independent experiments, 919 EGFP–NLS-59-R-CSIM-positive cells and 934 EGFP–NLS-PG-9-CSIM-positive cells were counted, and the number of Ki67-positive cells among these populations was determined (Figure 22B). Only 27.5 ± 2.5% of EGFP–NLS-59-R-CSIM cells and 26.3 ± 3.5% NLS-PG-9-CSIMcells were Ki67-positive and therefore remained mitotically active ($p < 0.001$, Figure 13C). These numbers were significantly reduced compared to EGFP vector-expressing cells (Figure 22B).

Thus, these two farnesylated CT fragments significantly delayed the growth of transfected cells, possibly by interfering with the chromatin distribution during mitosis, as indicated by the presence of DNA and HP1β in the nuclear and cytoplasmic blebs of transfected cells.

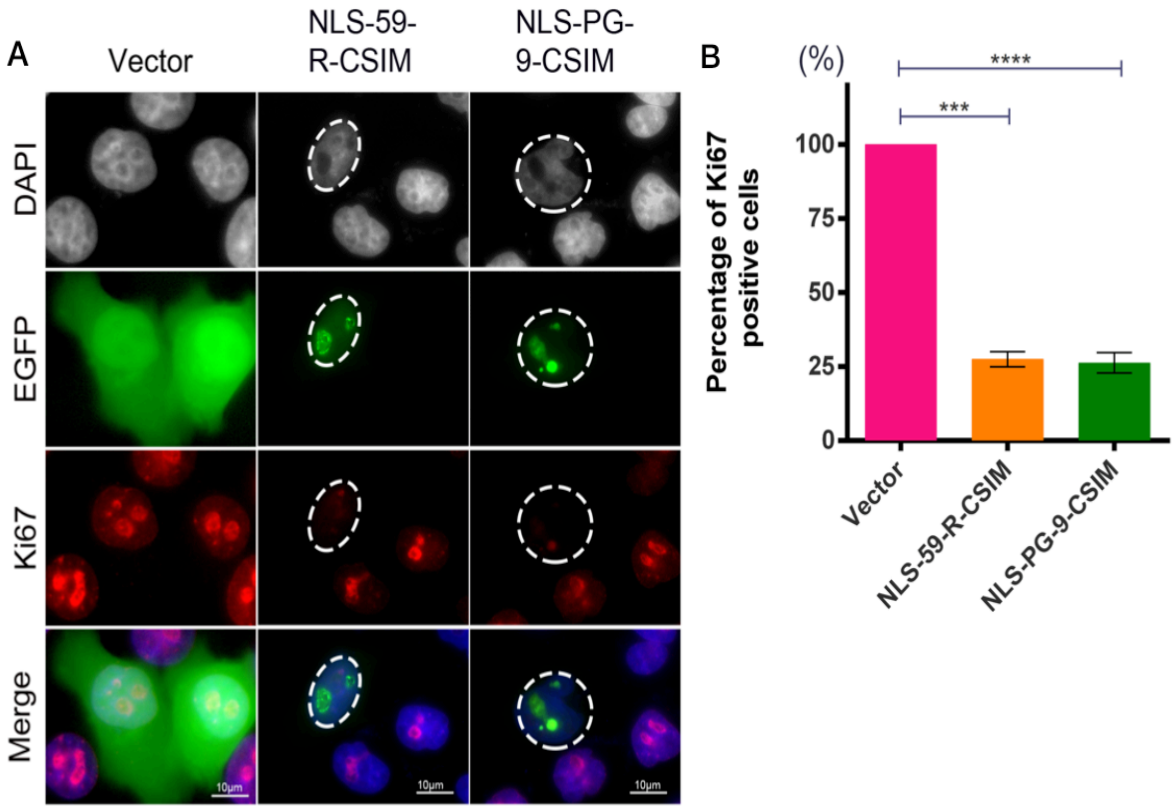

Figure 22. Determination of cell proliferation activity. (A) Ki67 was used to detect the actively replicating chromosomal DNA. Representative images of Ki67 staining and signals for EGFP fusion proteins are shown. Ki67 signals are barely detectable in EGFP–NLS-59-R-CSIM- and NLS-PG-9-CSIM-expressing cells, as indicated with circles. (B) Percentages of cells expressing both EGFP and Ki67. Nine hundred sixty cells expressing the EGFP vector, 919 cells expressing EGFP–NLS-59-R-CSIM, and 934 cells expressing EGFP–NLS-PG-9-CSIM were counted (n = 3). Scale bar, 10 μm.

7.2.5.The Autophagy–Lysosome Machinery Is Involved in the Formation of NE Evaginations

The observed NE defects and genomic instability in EGFP–NLS-59-R-CSIM- and EGFP–NLS-PG-9-CSIM-expressing cells indicated that several nuclear components were disrupted. The turnover of nuclear components is mediated by autophagy (Park, Hayashi et al. 2009, Dou, Xu et al. 2015). We determined the distribution of LC3B, a marker of autophagosomes (Drake, Kang et al. 2010), to determine whether components of the autophagy machinery were recruited to sites of NE blebs.

First, we analyzed the distribution of LC3B in primary fibroblasts derived from normal individuals and patients with HGPS. In control fibroblast cells, the punctate form of the LC3B signal was spread throughout the cytoplasm (Figure 23 and Figure S3A). In HGPS fibroblast cells, the cytoplasmic LC3B signal was reduced, but a fraction of LC3B localized at the nuclear compartment, indicating that autophagosomes were located in the vicinity of the deformed NE (Figure 23, arrowheads). In HeLa cells transfected with empty vector, LC3B foci were detected in the cytoplasm (Figure 23 and Figure S3A). In HeLa cells transfected with EGFP–NLS-59-R-CSIM, and EGFP–NLS-PG-9-CSIM, the EGFP signal colocalized with LC3B-positive vesicles at the nuclear compartment (Figure 23). EGFP–LC3B-positive foci were not observed at the NE of non-transfected cells.

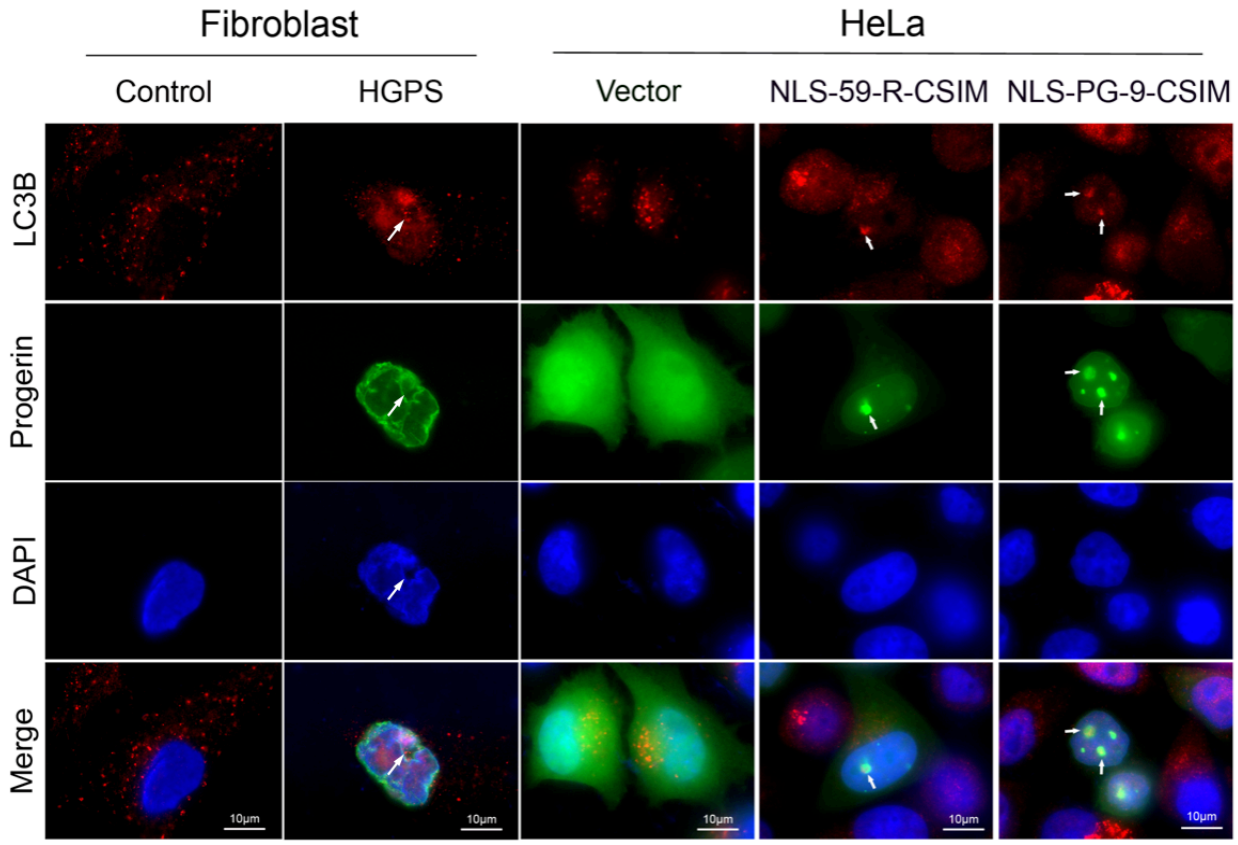

Figure 23. Detection of autophagosome distributions. LC3B was used as markers to detect autophagosomes. Chromatin was stained with DAPI. Representative images of LC3B staining in normal and HGPS fibroblasts and EGFP vector-, EGFP–NLS-59-R-CSIM-, and EGFP–NLS-PG-9-CSIM-transfected cells. Redistribution and colocalization patterns of LC3B in the NE and NE invaginations are shown in HGPS fibroblasts and EGFP–NLS-59-R-CSIM- and EGFP–NLS-PG-9-CSIM-transfected cells, as indicated with arrowheads. Scale bar, 10 μm.

Next, we examined the localization of LAMP-2, a lysosomal membrane marker (Hunziker and Geuze 1996). In control fibroblasts, the vacuolar signal of LAMP-2 spread throughout the cytoplasm (Figure 24 and Figure S3B). In HGPS fibroblast cells, in addition to the cytoplasmic signal, a granular staining pattern of LAMP-2 was also observed surrounding the nucleus (Figure 24 and Figure S3B). A fraction of LAMP-2 colocalized with progerin at the periphery of the NE fold in HGPS cells (Figure 24, arrowheads).

In HeLa cells transfected with the vector alone, the LAMP-2 signal was distributed in the cytoplasm, as observed in normal fibroblasts (Figure 24). In EGFP–NLS-59-R-CSIM- and EGFP–NLS-PG-9-CSIM-expressing cells, LAMP-2 and EGFP colocalized at the NE periphery and NE evaginations, as observed in HGPS fibroblast (Figure 24). Therefore, LC3B and LAMP-2 were recruited to the NE in cells expressing EGFP–CT farnesylated fragments of prelamin A or progerin.

Based on these observations, components of the autophagy-lysosome system are recruited to the nuclear periphery of HGPS cells and HeLa cells expressing the farnesylated C-terminal ends of prelamin A or progerin. The expression of these short farnesylated proteins induced NE evaginations and LC3B recruitment. LAMP-2 was also detected in the vicinity of the NE evaginations in HeLa cells transfected with these constructs. Thus, the accumulation of farnesylated proteins in the nuclear compartment activates nuclear autophagy to possibly maintain the integrity of the nucleus.

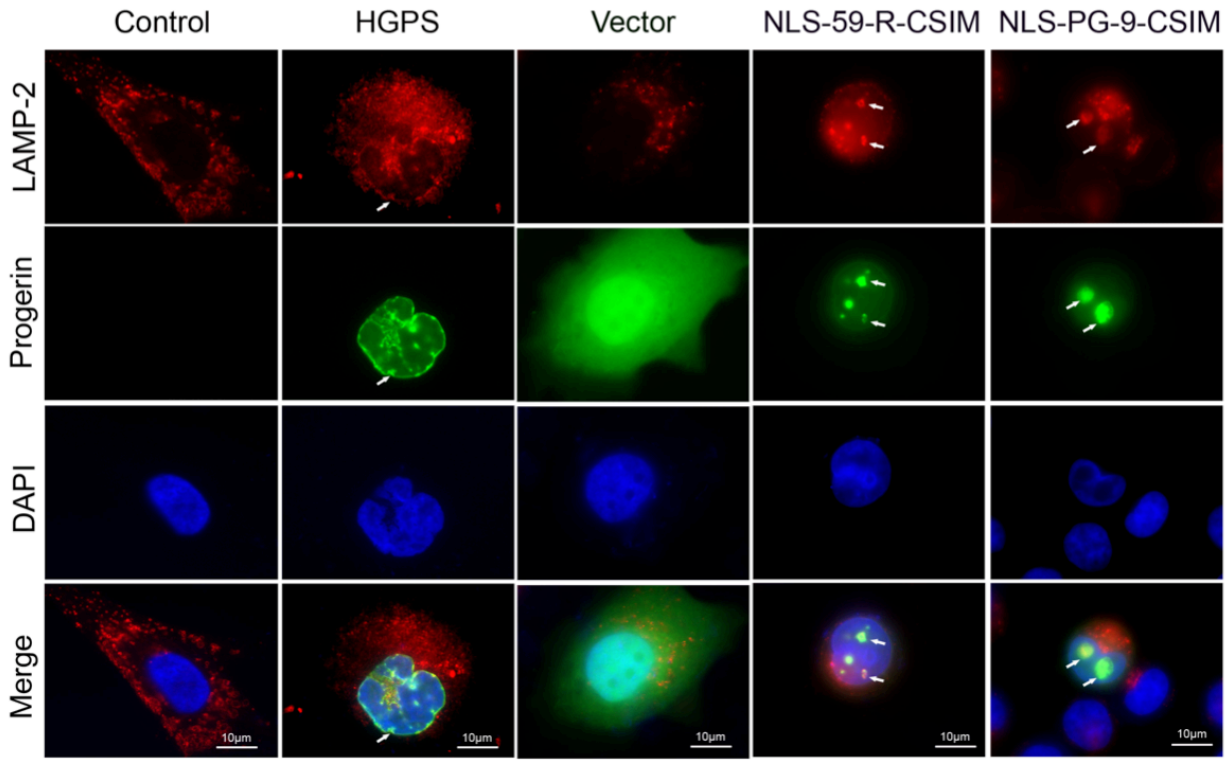

Figure 24. Detection of lysosome distributions. LAMP2 was used as a marker to detect lysosomes. Chromatin was stained with DAPI. Representative images of LAMP2 staining in normal and HGPS fibroblasts and EGFP vector-, EGFP–NLS-59-R-CSIM-, and EGFP–NLS-PG-9-CSIM-transfected cells. Redistribution and colocalization patterns of LAMP2 in the NE and NE invaginations are shown in HGPS fibroblasts and EGFP–NLS-59-R-CSIM- and EGFP–NLS-PG-9-CSIM-transfected cells, as indicated with arrowheads. Scale bar, 10 μm.

7.2.6.NE Defects Are Associated with Lower Autophagy Activity and Increased Cell Death

HGPS cells display reduced autophagy activity (Cao, Graziotto et al. 2011, Gabriel, Roedl et al. 2015). Because components of autophagosomes were recruited to the NE invagination in HGPS cells and HeLa cells expressing EGFP–CT farnesylated fragments, we evaluated autophagy activity in these cells. We applied a monodansylcadaverine (MDC)/cytotoxicity dual staining assay in living cells that enables the simultaneous detection of autophagy and cell death. MDC is a fluorescent probe that detects autophagic vacuoles in living cells and propidium iodide (PI) is a marker of cell death (Niemann, Takatsuki et al. 2000). A bright vacuolar signal of autophagosomes (MDC) distributed throughout the cytoplasm was observed in control cells, and no PI-positive cells were detected, indicating the absence of cell death (Figure 25A, C). In contrast, HGPS fibroblasts exhibited an average decrease in the MDC signal by 60% compared to control fibroblasts, signifying a reduction in the number of autophagosomes (Figure 25A, B). In addition, an increased percentage of dead cells of 4.22 ± 1.27% was observed in HGPS cells compared to control fibroblasts (Figure 25C). Hence, in PI-positive HGPS, the MDC signal was barely detectable (Figure 25A).

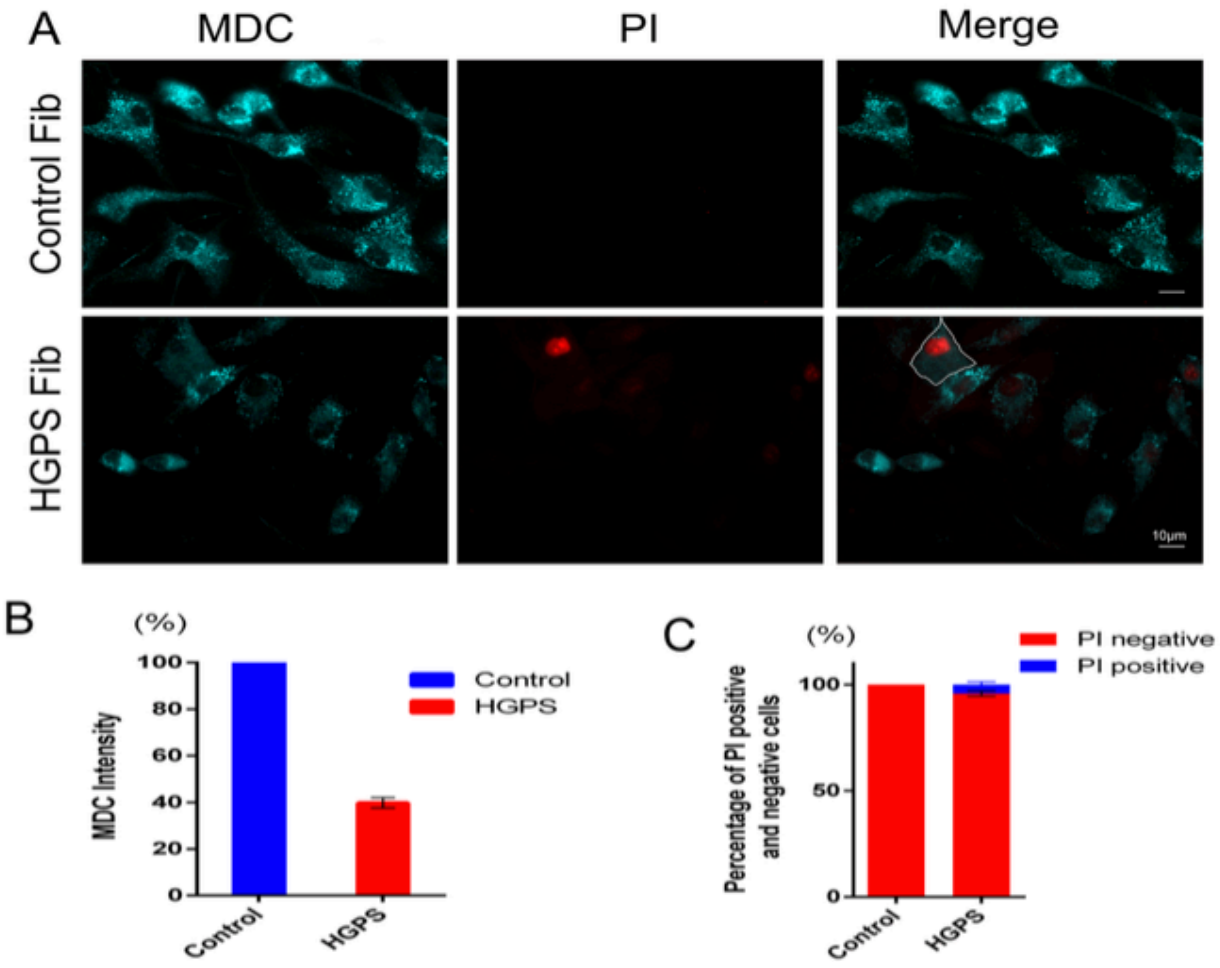

Figure 25. Determination of autophagy activity. (A) Monodansylcadaverine (MDC) and propidium iodide (PI) staining were performed to detect the numbers of autophagosomes and dead cells in normal and HGPS fibroblasts. Representative images of cells are shown. HGPS cells exhibit a heterogeneous brightness of MDC fluorescence intensity. A PI-positive cell with no detectable MDC signal is outlined. (B) The fluorescence intensity of MDC was measured in control and HGPS fibroblasts. Two hundred fifty-three control cells and 244 HGPS cells were counted. The average MDC fluorescence intensity was used for the statistical analysis. (C) The percentages of PI-positive cells were calculated by counting 317 control cells and 309 HGPS fibroblasts. All statistical analyses were performed using Student's t-test. Two-tailed p-values were calculated and $p < 0.05$ was considered significant. Scale bar, 10 μm.

All HeLa cells transfected with the empty EGFP vector showed a strong MDC signal and no PI-positive signals, indicating the absence of dead cells (Figure 26). In EGFP–NLS-59-R-CSIM- and EGFP–NLS-PG-9-CSIM-expressing HeLa cells, the cytoplasmic signal for MDC was dramatically reduced (Figure 26, circled region). However, superimposable bright signals for EGFP, MDC, and PI were detected at the NE evaginations in transfected HeLa cells (Figure 26). The presence of the PI signal within these NE blebs indicates that the NE permeability was compromised, and cells were undergoing apoptosis.

Based on these findings, the accumulation of farnesylated proteins at the NE induces NE alterations and the disorganization of the numerous nuclear components, including NE proteins (emerin and SUN1), lamins, chromatin, and other nuclear factors. These changes evidently induce the formation of NE evaginations, the recruitment of autophagy components, and the activation of nucleophagy in an attempt to prevent further nuclear alterations. However, the dramatic disruption of the NE integrity ultimately leads to apoptosis.

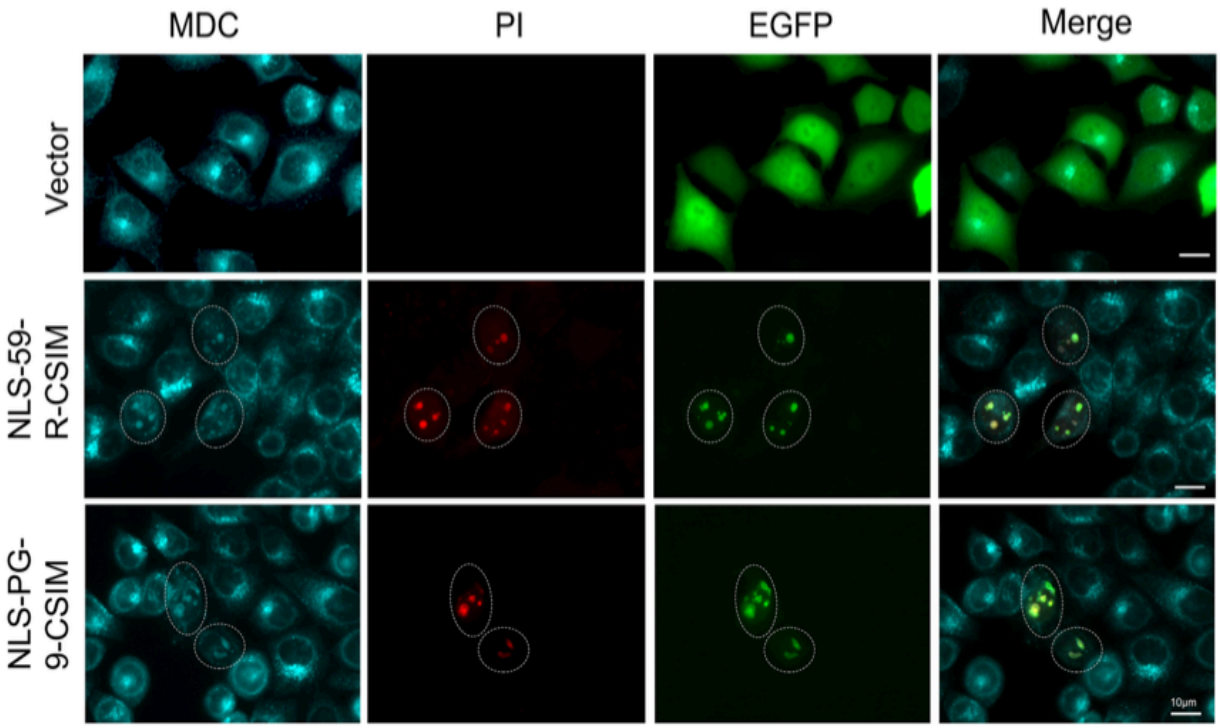

Figure 26. Determination of autophagy activity in transfected HeLa cells. MDC and PI staining in EGFP vector-, EGFP–NLS-59-R-CSIM-, and EGFP–NLS-PG-9-CSIM-transfected cells are shown. EGFP–NLS-59-R-CSIM- and EGFP–NLS-PG-9-CSIM-transfected cells showing colocalization of MDC with the EGFP signal at the NE invaginations (indicated in circle). Scale bar, 10 μm.

8. Discussion

At least 15 inherited diseases called laminopathies are linked to LMNA mutations that cause the characteristic abnormal nuclear morphology (worman 2012, Gruenbaum and Foisner 2015). Currently, progerin accumulation at the NE is known to produce dysmorphic nuclei in patients with HGPS (Burtner and Kennedy 2010). Likewise, a loss of Zmpste 24 activity in progeroid mice causes the accumulation of farnesylated prelamin A at the NE, which also induces NE abnormalities (Pendas, Zhou et al. 2002). Further investigations are required to determine the mechanisms by which farnesylated progerin and prelamin A interact with NE proteins and other components to induce nuclear structural abnormalities. The findings from this study provide new evidence that the farnesylated carboxy-terminal moieties of prelamin A and progerin play critical roles in NE association and deformation. Hence, the results highlight an important role of the autophagy-lysosome system in the maintenance of the integrity of the NE and nuclear structure.

8.1. Subcellular Trafficking of the Farnesylated Progerin Carboxyl-Terminal Fragment

The structure and function of the progerin CT domain were dissected to determine the mechanism by which modifications to the progerin carboxy-terminus cause NE defects in HGPS cells. We created a series of plasmids that encode the progerin CT domain and the wild-type preLA CT domain, as outlined in Figure 11. We analyzed the distribution of the EGFP fusion proteins with or without a nuclear localization signal (NLS) and a functional CaaX motif to provide novel insights into progerin processing

and intracellular trafficking in transfected HeLa cells. Progerin farnesylated CT fragments with an NLS motif induced NE deformation in transfected HeLa cells and fibroblasts from patients with HGPS, similar to the full-length progerin protein (Paradisi, McClintock et al. 2005). The farnesylated CT–preLA and –progerin fragments were mainly localized at the NE. Nuclear accumulation of these prenylated fusion proteins induced NE deformation, including blebs and NE elongations or protrusions of various sizes and numbers. These NE protrusions were not observed in cells transfected with the full-length progerin cDNA or in HGPS fibroblasts, which showed NE invaginations and small blebs, as previously reported (Gabriel, Roedl et al. 2015). These NE protrusions were not observed in HeLa cells expressing non-farnesylated CT–preLA or –progerin fusion proteins, which were localized throughout the nucleoplasm. Hence, EGFP–NLS-59-CSIM and EGFP–NLS-50 proteins corresponding to the 50-amino acid fragment that is missing in the progerin protein showed a diffuse distribution in the nucleus, indicating that this protein fragment does not associate with any particular subnuclear compartment. Meanwhile, the EGFP–NLS-59-R-CSIM protein corresponding to the farnesylated 50-amino acid fragment was localized at the NE, indicating that the CaaX modification promoted the membrane interaction, as previously reported (Holtz, Tanaka et al. 1989, Rusinol and Sinensky 2006). Consistent with these observations, the farnesylated progerin CT peptide without the NLS (EGFP–ΔNLS-PG-9-CSIM) was localized at the ONM that is continuous with the ER compartment. Cells expressing high levels of EGFP–ΔNLS-PG-9-CSIM showed accumulation of this fragment in the Golgi apparatus. Based on this observation, the short farnesylated

progerin CT peptide was attached to the ER membrane and transported to the Golgi compartment.

The subcellular distribution of the short NLS CT–preLA peptide (EGFP–NLS-20-CSIM) showed NE localization and accumulation in the Golgi apparatus and the plasma membrane, whereas the NLS CT–progerin peptide (EGFP–NLS-PG-9-CSIM) was restricted at the NE. We compared the amino acid sequence of these two short peptides and performed protein sequence alignments using Predict Protein software (Rost, Yachdav et al. 2004) to understand the differences in the localization of these peptides. In contrast to NLS-PG-9-CSIM, NLS-20-CSIM showed some degree of similarity with the hypervariable region (HVR) of the RAS proteins (H-RAS, N-RAS, K-RAS4A, and K-RAS4B), which are also known to contain a CaaX motif (Hancock, Paterson et al. 1990). K-RAS is targeted from the ER to Golgi and the plasma membrane immediately after post-translational modification (Hancock, Paterson et al. 1990). K-RAS contains a polybasic sequence that is comparable to the NLS sequence and is located upstream of its CaaX motif. Furthermore, the distance between the two motifs (NLS and CaaX) are critical for plasma membrane targeting, as EGFP–NLS-59-R-CSIM exhibited only nuclear localization at the NE (Kim, Han et al. 2017). According to these findings, the NLS-20-CSIM protein residing in the ER after prenylation by the specific enzymes was targeted to the nucleus or transported to the Golgi and the plasma membrane, as previously reported for K-RAS protein (Hancock 2003). Moreover, high levels of farnesylated proteins tend to accumulate at the Golgi.

8.2. Farnesylated CT–Progerin and –preLA Peptides Dislodge SUN1 from NE Protrusions

Previous studies, including studies from our group, have shown that progerin colocalizes with SUN1 in interphase HGPS fibroblasts (Chen, Chi et al. 2012, Chen, Wang et al. 2014, Eisch, Lu et al. 2016). Progerin accumulated at the NE and co-distributed with SUN1 at the NE invaginations or blebs but did not induce NE elongations in interphase HGPS fibroblasts or transfected HeLa cells. The spatiotemporal distribution of SUN1 during mitosis is substantially altered in the presence of progerin. SUN1 recruitment to the nuclear periphery is delayed in anaphase, and SUN1 predominately co-distributes with progerin at the ER membrane structures in mitotic HGPS cells (Eisch, Lu et al. 2016). According to a study by Chen et al., SUN1 not only binds lamin A but also binds strongly to farnesylated progerin and preLA, indicating that the farnesyl moiety was partially responsible for the stronger association with SUN1 (Chen, Wang et al. 2014). SUN1 is a component of the multifunctional nuclear membrane protein assembly, the linker of nucleoskeleton and cytoskeleton (LINC) complex, which consists of the INM-spanning protein SUN and the ONM-spanning protein nesprin (Crisp, Liu et al. 2006). The crystal structure of the LINC complex indicates that this assembly involves three KASH peptides interacting with a SUN trimer (Sosa, Rothballer et al. 2012). Additionally, a disulfide bond covalently links the SUN and KASH domains, thereby bridging the INM and the ONM and creating a force-resistant device that permits mechanical signal transmission across the NE (Lombardi, Jaalouk et al. 2011, Sosa, Rothballer et al. 2012). Moreover, it has been suggested that SUN trimers within the perinuclear space could form higher-order

clusters by lateral association of their SUN domains (Jahed, Fadavi et al. 2018). In the context of HGPS fibroblasts, because SUN1 is increased at the NE compared to normal fibroblasts, SUN1 clustering might be favored, thereby increasing the stiffness of the NE. Moreover, this LINC complex directly connects the cytoskeleton (e.g., actin filaments or microtubule motors) and the nucleoskeleton (e.g., lamins or chromatin) and plays a major role in shaping and positioning the nucleus and in cell migration (Starr and Fridolfsson 2010, Lombardi, Jaalouk et al. 2011). HGPS cells with the most dysmorphic nuclei resulting from high levels of progerin accumulation exhibit reduced migration potency (Paradisi, McClintock et al. 2005). This observation suggests that increased LINC connections at the NE would disrupt the nucleoskeleton and cytoskeleton networks inhibiting cell migration. By contrast, a recent study indicates that reduced levels of SUN1 and other LINC-associated components in cancer cells cause a decrease in cellular rigidity and, consequently, increase cell migration (Matsumoto, Hieda et al. 2015).

The impact of the CT–progerin (EGFP–NLS-PG-9-CSIM) and CT–preLA (EGFP–NLS-59-R-CSIM) peptides on the distribution of SUN1 were further inverstigated. At normal areas of the NE, the farnesylated protein fragments were colocalized with lamin A/C, lamin B1, and the INM proteins emerin and SUN1, as well as with the nuclear pores (NPCs). By contrast, within the large NE protrusions, the EGFP signal was colocalized with all of the abovementioned nuclear constituents, with the exception of SUN1. The NE protrusions were depleted of SUN1 but contained the INM protein emerin and the NPCs, indicating that these NE elongations are composed of the double-membrane bilayers of the INM and the ONM. SUN1 may have been excluded

from sites of NE elongation due to the membrane flexibility required to allow NE outgrowth. Indeed, as part of the LINC complex, SUN1 forms immobile and rigid connections among the NE, the nuclear lamina, and the cytoskeleton (Lu, Gotzmann et al. 2008). The LINC complex requires a degree of disassembly to permit membrane flexibility and allow NE outgrowth, whereas SUN1 clustering might permit local NE flexibility to allow NE evaginations, as indicated in the results. SUN1 loosens its connection to the nuclear lamina during mitosis (Patel, Bottrill et al. 2014). However, during the nuclear breakdown, the LINC complex remains stable (Patel, Bottrill et al. 2014). Whether SUN1 or the LINC complex can disassemble in interphase nuclei remains to be investigated. Therefore, based on this finding, macro protein complexes containing SUN1 might restrict NE outgrowth, which otherwise would cause NE rupture, whereas SUN1 depletion would facilitate NE elongation. Further studies are needed to address this question in more detail and validate this hypothesis.

8.3.Autophagy Is Involved in the Formation of NE Protrusions

In this study, a fraction of heterochromatin, as indicated by the DAPI and the HP1β signals, was present in a cytoplasmic area close to the nucleus in EGFP–NLS-59-R-CSIM- and EGFP–NLS-PG-9-CSIM-expressing cells. Thus, nuclear accumulation of those farnesylated protein fragments not only compromised the NE structure but also induced chromatin disorganization, which consequently caused genomic instability. Moreover, the transfected cells showed reduced Ki67 signals, indicating that they lost function of proliferation. To understand why transfected cells with such atypical dysmorphic nuclei persisted in these cultures, we investigated whether these cells

attempted to eliminate their damaged NE via autophagy to support their survival. Autophagy is a catabolic membrane trafficking process that degrades a variety of cellular constituent. The presence of key autophagy components within the nucleus, including microtubule-associated protein 1/light chain 3 (LC3B), has suggested a role for autophagy in the turnover of nuclear components (Drake, Kang et al. 2010). Autophagy has recently been shown to target nuclei in mammalian cells (Chen, Huang et al. 2014, Dou, Xu et al. 2015, Luo, Zhao et al. 2016).

We performed an immunohistochemical analysis of LC3B in HGPS fibroblasts and transfected HeLa cells to determine whether these elongated NE structures were autophagic vacuoles. LC3B is a commonly used marker of autophagy because it associates with the inner and outer membranes of autophagosomes (Kabeya, Mizushima et al. 2000).

LC3B immunostaining showed a predominant localization of the signal in the cytoplasm of normal fibroblasts, whereas in HGPS fibroblasts, the signal was concentrated at the nuclear compartment. HeLa cells transfected with EGFP–NLS-59-R-CSIM and EGFP–NLS-PG-9-CSIM showed extensive colocalization of LC3B with the EGFP signal at sites of NE elongations. The involvement of lysosomes was also determined to further characterize the autophagic nature of these NE protrusions. The results showed that LAMP-2, a lysosomal membrane protein, was present in the vicinity of the EGFP signal in HeLa cells transfected with EGFP–NLS-59-R-CSIM and EGFP–NLS-PG-9-CSIM. In HGPS cells, the LAMP-2 signal was also detected at the periphery of the NE. Collectively, these findings indicate that autophagosome/autolysosomes were present at

the nuclear periphery in HGPS cells. However, transfected HeLa cells that had accumulated high amounts of farnesylated CT–progerin or –preLA fragments formed large NE protrusions that were labeled with markers of autophagosomes/ autolysosomes. Thus, cells formed these structures in an attempt to eliminate these toxic farnesylated EGFP-fusion proteins. Moreover, these elongated NE autophagosomes also contained lamina components (lamin A/C and lamin B), the INM protein emerin, chromatin, and chromatin-interacting proteins (HP1β), as well as NPCs. However, SUN1 was not detected in these NE autophagosome-like structures, suggesting that SUN1 might either be degraded by another mechanism and/or be excluded from these structures because of its inherent function in maintaining the shape and rigidity of the NE through its role in the LINC complex formation (Crisp, Liu et al. 2006).

Remarkably, elongated NE autophagosomes were not observed in HGPS fibroblasts expressing high levels of progerin. The lack of these giant protrusions in HGPS cells might be related to the tight association of progerin with the nuclear lamina and particularly with SUN1, as reported previously (Chen, Wang et al. 2014). Strong progerin interactions with the lamina meshwork and the INM might reduce progerin mobility at the NE in interphase nuclei and consequently reduce its rate of degradation via autophagy. Thus, progerin degradation might occur at the end of mitosis when a large amount of progerin remains trapped with SUN1 in the cytoplasm, although further investigations are needed to validate this assumption (Chen, Wang et al. 2014, Eisch, Lu et al. 2016). Nevertheless, based on accumulating evidence, progerin is degraded via autophagy, and the activation of the autophagy pathway in HGPS cells by various

drugs, including rapamycin and sulforaphane, significantly enhances progerin clearance and ameliorates the HGPS cellular phenotype (Cao, Graziotto et al. 2011, Cenni, Capanni et al. 2011, Choi, Muchir et al. 2012, Gabriel, Roedl et al. 2015, Pellegrini , Columbaro et al. 2015, Gabriel, Gordon et al. 2016). Studies aiming to improve our understanding of nucleophagy-dependent degradation of progerin in HGPS cells are needed to develop novel therapeutics to further modulate nuclear autophagy in patients with HGPS and possibly other conditions.

The results also provide a plausible answer to the question of what becomes of the farnesylated 15-amino acid fragment cleaved from the preLA after normal processing. In a previous study by Sinenski et al., the cleaved CT farnesylated preLA peptide was suggested to play a role as a signal peptide (Sinensky 2000). Numerous studies have investigated the processing of preLA, however, little is known about the outcome of the cleaved C-terminal 15-amino acid farnesylated moiety (Sinensky, McLain T. et al. 1994, Davies, Fong et al. 2011, Michaelis and Hrycyna 2013). The results showed that the CT farnesylated progerin fragment (NLS-PG-9-CSIM) associated with the NE and was targeted for degradation via nucleophagy. Analogously to the progerin–CT peptide, the cleaved CT–preLA peptide most likely follows a similar degradation route. Therefore, this CT–preLA peptide probably has no additional functions other than targeting preLA to the NE, where it is modified to produce mature lamin A. Based on our findings, a better understanding of the mechanisms regulating the degradation of farnesylated lamins (progerin, prelamin A, and lamin B) is needed, and future studies should illuminate mechanisms to enhance the clearance of these proteins and restore the phenotype of progeria cells.

9. Material and Method

9.1.Material

9.1.1.Reagents

Reagents	Manufacturer
1 kb DNA ladder	Life Technology
Acrylamide (38%, 2% Bisacrylamide)	Roth
Agarose, ultrapure	Life Technology
Ammoniumperoxodisulfate (APS)	BioRad
Ampicillin	Roth
Autophagy/Cytotoxicity Dual Staining Kit	Cayman Chemical
Bacteria-Agar	Roth
Bacteria-Trypton	Roth
Bacteria-Yeast Extract	Roth
DEPC treated water	Life Technology
Dithiothreitol (DTT)	Roth
DMEM (1x) GlutaMax 1 g/l D-glucose+pyruvate	Life Technology
DMEM (1x) GlutaMax 4.5 g/l D-glucose+pyruvate	Life Technology
Dulbecco's phosphate-buffered saline (DPBS)	Life Technology
Dulbecco's phosphate-buffered saline (DPBS)	Sigma-Aldrich
ECL-Western blot Detection System	BioRad
Ethanol	VWR
Ethidium bromide	Sigma-Aldrich
Ethylendiamintetraacidic acid (EDTA)	Merck
Fetal bovine serum	Sigma-Aldrich
Fetal bovine serum	Life Technology

Formaldehyde	Merck
Fugene HD	Promega
Fungizone antimycotic (250μg/ml)	Life Technology
Gentamycin (10mg/ml)	Life Technology
Glutamine 200 mM	Life Technology
Glycerol, 99 %	Sigma-Aldrich
Glycine	Sigma-Aldrich
Isoproponal	Roth
Kanamycin	Sigma-Aldrich
Laemmli Buffer	BioRad
Lipofectamine 2000	Life Technology
Maxi Plasmid Extraction Kit	Qiagen
Methanol	AppliChem
Midi Plasmid Extraction Kit	Promega
Milk powder	Nestle
Mini Plasmid Extraction Kit	Qiagen
N, N, N´,N´-Tetramethylethylendiamine (TEMED)	BioRad
Omniscript RT Kit	Qiagen
OptiMem	Life Technology
Penicillin-Streptomycin (5,000U/mL)	Life Technology
Phusion Hot Star II	Roche
Poly-D-Lysine	Sigma-Aldrich
Poly-L-Lysine	Sigma-Aldrich
Ponceau S	Sigma-Aldrich
Precision Plus Protein Dual Color Standard	BioRad
Protease Inhibitor Mix	Roche
QIAshredder Kit	Qiagen

RNeasy Mini Kit	Qiagen
SDS	Sigma-Aldrich
Senescence detection Kit	BioVision
Triton X-100	Sigma-Aldrich
Trizma Base	Sigma-Aldrich
Trypsin 0.25%EDTA	Life Technology
Tween 20	AppliChem
Tween 20	Sigma-Aldrich
Vectashield mounting medium	Vector Inc.
β-Mercaptoethanol, pure	BioRad

9.1.2.Technical Equipment

Technical Equipment

Device	**Manufacturer**
Axio Imager D3	Zeiss
Axiovert 40CFL	Zeiss
Centrifuge	Eppendorf
ChemiDoc MP Imaging System	BioRad
iCycler	BioRad
Mini Trans-Blot Cell	BioRad
Mini-PROTERN® Tetra Vertical Gel Cell	BioRad
Nanodrop Spectrometer ND-1000	Thermofisher
Powerpac Universal Power Supply	BioRad
Rocking platform	VMR
Shaking Incubator	Sartorius

Technical Equipment

Device	Manufacturer
Trans-Blot Turbo Transfer System	BioRad
Ultracentrifuge	Thermofisher

9.1.3.Buffers for Western-blot Analysis

Sample Laemmli Buffer

Laemmli Buffer 2X	950 µl
2-Mercaptoethanol	50 µl
Proteinase Inhibitor Cocktail	10 µl
PMSF	5 µl

10X SDS Gel Running Buffer

1.92 M Glycine	144g
248 mM Tris-Base	30g
1%SDS	10g
H2O	5µl

Western blot Transfer Buffer

200 mM Tris-Base	2.42 g
150 mM Glycine	11.3g
20% Methanol	200ml
0.1%SDS	1g

Western blot Transfer Buffer	
H2O	add to 1 L

Acrylamide (30% T, 2.67% C)	
Acrylamide (292.g/100ml)	87.60g
N'N'-bis-methylene-acrylamide	2.40g
dH2O	add to 300 ml

1.5 M Tris-HCl, pH 8.8 (150ml)	
Tris-Base (18.15 g/ 100 ml)	27.23 g
dH2O	80ml
Adjust to pH 8.8 with 6 N HCl	
dH2O	add to 150 ml

0.5 M Tris-HCl, pH 6.8	
Tris-Base (18.15 g/ 100 ml)	6 g
dH2O	60ml
Adjust to pH 6.87 with 6 N HCl	
dH2O	add to 100 ml

10% (w/v) SDS (100ml)	
SDS	10.00 g
dH2O	90ml
Dissolve with gentle stirring	
dH2O	add to 100 ml

10% (w/v) APS (fresh)	
Ammonium persulfate	0.10 g
dH2O	1 ml

TBS 10X (TBS stock)	
Trizma HCl	24.23 g
NaCl	80.06 g
dH2O	800 ml
Adjust pH to 7.6 with HCl	
dH2O	add to 1 L

TBST	
TBS 10X	100 ml
dH2O	900 ml
Tween 20	1 ml

Medium Stripping Buffer	
Glycine	15 g
SDS	1 g
Tween 20	1 ml
Adjust pH to 2.2	
dH2O	add to 1 L

9.1.4.Antibodies

Primary antibody

Antibody	Species	IF	WB	Supplier	Catalog No.
Acetylated Tubulin	Mouse	1:1000	1:1000	Sigma-Aldrich	T7451
Calnexin	Mouse	1:500	-	Abcam	ab31290
EGFP	Mouse	-	1:1000	Clonetech	632569
Emerin	Mouse	1:500	-	Leica Biosystem	NCL 4G5
GAPDH	Mouse	-	1:1000	Sigma-Aldrich	G8795
GM130	Mouse	1:100	-	BD	610823
HP1	Rabbit	1:400	-	Sigma-Aldrich	H2039
Ki67	Goat	1:400	-	BD	610968
Lamin A	Rabbit	-	1:10000	Santa Cruz	H-110 sc-20681
Lamin B1	Goat	1:50	-	Santa Cruz	M-20, sc-6217
Lamin C	Mouse	1:500	-	Abcam	ab125679
LAMP-2	Mouse	1:400	-	Santa Cruz	sc-18822
LC3B	Rabbit	1:400	-	Cell Signaling	#2775
NPC 414	Mouse	1:2000	-	Biolegend	MMS-120P

Primary antibody

Progerin	Rabbit	no dilution	-	monoclonal antibody	(ref. 30)
Progerin	Mouse	1:600	-	Enzo	ALX-804-662, 13A4
SUN1	Rabbit	1:600	1:1000	Sigma-Aldrich	HAP-008346
α-Tubulin	Mouse	1:4000	1:4000	Sigma-Aldrich	T5196
β-actin	Mouse	-	1:10000	Sigma-Aldrich	A1978

Secondary antibody

Antibody	Species	Dilution	Supplier	Catalog No.
α-mouse-Alexa Fluor® 488	Donkey	1:1000	Invitrogen	A21202
α-rabbit-Alexa Fluor® 488	Donkey	1:1000	Invitrogen	A21206
α-mouse-Alexa Fluor® 555	Donkey	1:1000	Invitrogen	A31570
α-rabbit-Alexa Fluor® 555	Donkey	1:1000	Invitrogen	A31572
α-goat-Alexa Fluor® 555	Donkey	1:1000	Invitrogen	A21432
α-mouse-HRP	Goat	1:5000	ImmunoResearch Jackson	115-035-003
α-goat-HRP	Donkey	1:5000	ImmunoResearch Jackson	705-035-003
α-rabbit-HRP	Goat	1:5000	ImmunoResearch Jackson	111-005-003

9.2.Method

9.2.1.Plasmid Constructs

The full-length prelamin A and progerin cDNA were inserted into the pEGFP-c1 vector (Clontech, Fremont, CA, USA). Protein residues 602–664 a.a. from the C-terminus of prelamin A linked to a classical nuclear localization signal (NLS, KKRKLLE) were designed as NLS-59-CSIM. The NLS-59-R-CSIM containing the L647R mutation and NLS-59-SSIM containing the C661S mutation were designed as corresponding mutant isoforms. The in-frame deletion of 50 a.a. from residues 607–656 of prelamin A were designed as NLS-50 and ΔNLS-50; these constructs either contained or lacked the NLS, respectively. Residues 641–664 a.a. of prelamin A linked to NLS were designed as NLS-20-CSIM. The NLS-20-R-CSIM and NLS-20-SSIM corresponded to L647R and C661S mutant of NLS-20-CSIM. The C-terminal residues 602–614 of progerin were linked to the NLS to create NLS-PG-9-CSIM. The corresponding mutant isoform was NLS-PG-9-SSIM. The PG-9-CISM and PG-9-SSIM isoforms were designed to determine the cellular distribution of progerin C-terminal fragments lacking the NLS. All constructs were subcloned into the EcoR I and Kpn I sites of the pEGFP-c1 vector (Clontech). The DNA sequence of each construct was confirmed by direct sequencing (GenScript.com).

9.2.2.Cell Culture and Transfection

HeLa cells were cultured in DMEM (Sigma-Aldrich, Saint Louis, MO, USA) containing 10% FBS (Invitrogen, Thermo Fisher Scientific, Karlsruhe, Germany) at 37 ºC in a 5%

CO_2 atmosphere. An initial density of 1.5 X 10^5 cells was seeded on glass coverslips incubated at 37 ºC for 24 h and then transfected with 2 µg of the designated plasmids using FuGene HD Transfection Reagent (Promega, Madison, WI, USA), according to the manufacturer's instructions. Twenty-four or 48 h after transfection, cells were fixed with 4% paraformaldehyde (PFA) at room temperature for 15 min and washed with PBS at room temperature. Thereafter, cells were permeabilized with PBS supplemented with 0.2% Triton X-100 for 3 min, blocked with PBS containing 10% fetal bovine serum and 0.2% Tween 20 for 30 min, and then processed for immunohistochemistry.

9.2.3. HGPS and Normal Fibroblast Cultures

Fibroblasts from patients with HGPS were obtained from The Progeria Research Foundation Cell and Tissue Bank (http://www.progeriaresearch.org). The following fibroblasts were used: HGADFN003, HGADFN127, HGADFN155, and HGADFN164. Control fibroblasts were obtained from the Coriell Institute for Medical Research (Camden, NJ, USA). The following cell lines were used: GM01651C, GM03349C, and GM08398A.

9.2.4.Immunohistochemistry

After fixation, cells were subjected to indirect immunofluorescence staining with the following primary antibodies: goat-anti-lamin B1 (Santa Cruz Biotechnology, Heidelberg, Germany, M-20, sc-6217, 1:50), rabbit-anti-lamin C (Abcam, Cambridge, UK, ab125679, 1:500), mouse-anti-emerin (Leica Biosystems, NCL-Emerin, 4G5, 1:500), mouse-anti-NPC 414 (BioLegend, MMS-120P, Mab414, 1:2000), rabbit-anti-SUN1 (Sigma-Aldrich,

HPA008346, 1:600), rabbit-anti-LC3B (Cell Signaling Technology #2775, 1:400), mouse-anti-LAMP-2 (Santa Cruz Biotechnology, sc-18822, 1:400), rabbit-anti-HP1 (Sigma-Aldrich, H2039,1:400), goat-anti-Ki67 (BD, 610968, 1:400), mouse-anti-EGFP (Clontech, 1:1000), rabbit-anti-progerin (Monoclonal antibody, 0.1 µg/mL), mouse-anti-progerin (Enzo, ALX-804-662, 13A4, 1:600), mouse-anti-Calnexin (Abcam, ab31290, 1:500), and mouse-anti-GM130 (BD, 610823, 1:100). The secondary antibodies used in the present study were affinity-purified Alexa Fluor® 555 or 488 conjugated anti-goat/rabbit/mouse antibodies (Life Technologies, Carlsbad, CA, USA, A21432 anti-goat-555, A21206 anti-rabbit-488, A21202 anti-mouse-488, A31570 anti-mouse-555, and A31572 anti-rabbit-555, 1:1000). Cells were incubated with indicated primary antibodies for 1 to 2 h and washed with PBS containing 0.2% Tween 20 three times for 5 min each. Next, cells were incubated with the corresponding secondary antibodies for 1 h and washed with PBS three times for 5 min each. All samples were counterstained with DAPI in Vectashield mounting medium (Vector Inc., VEC-H-1200). Images were acquired using an Axio Imager D2 fluorescence microscope (Objective X63 oil objective, Carl Zeiss, Oberkochen, Germany) and a Zeiss AxioCam MRm or a Zeiss LSM 510 META confocal laser-scanning microscope (Carl Zeiss).

9.2.5.Western Blot Analysis

Cell pellets were lysed in Laemmli Sample Buffer containing 5% -mercaptoethanol (Bio-Rad), 1X protease inhibitor cocktail (Calbiochem, Darmstadt, Germany), and 10 mM PMSF. Protein samples were heated three times 2 min at 95 C and vigorously vortexed between incubations to completely dissolve the extracts. Total protein concentrations

were determined by dot plotting. The samples were electrophoretically resolved on 4–20% Mini-Protean® TGXTM gel (Bio-Rad, Berkeley, CA, USA) and subsequently transferred onto nitrocellulose membranes (Amersham, NJ, USA) for antibody detection. The blot was incubated with a monoclonal mouse-anti-EGFP antibody (Clonetech, Fremont, CA, USA, 632569, 1:2000) overnight at 4 C to determine the expression of EGFP fusion proteins. After three washes with PBS-T buffer containing 0.2% Tween 20 for 5 min each, the membrane was incubated with the corresponding horseradish peroxidase-conjugated secondary antibody (Jackson Immuno-Research Laboratories, West Grove, PA, USA). Protein bands were visualized using the enhanced Clarity Western ECL substrate (Bio-Rad). Chemiluminescent signals were captured using a ChemiDOC MP system (Bio-Rad).

9.2.6.Monodansylcadaverine (MDC) Staining Assay

The autophagic vacuoles and dead fibroblasts and transfected HeLa cells were determined using an Autophagy/Cytotoxicity Dual Staining Kit (Cayman Chemical Company, Ann Arbor, MI, USA). Cells were plated on glass coverslips and then probed with 1:1000 dilution of MDC in staining buffer (Cell-Based Assay Buffer Tablet dissolved in water). After 10 min incubation at 37 ºC, cells were washed twice with assay buffer in the dark. Fluorescence microscopy was performed immediately after MDC staining. Autophagic vacuoles were detected using the filter set for DAPI detection. Propidium iodide (PI) staining was detected using the Cy3 Red filter set.

9.2.7.Statistical Analysis

For calculations of the percentage of Ki67 positive, 960 cells transfected with the EGFP vector alone, 919 EGFP-NLS-59-R-CSIM expressing cells, and 934 EGFP-NLS-PG-9-CSIM expressing cells were counted. Three independent immunohistochemistry experiments and counts were performed.

The measurement of MDC fluorescence intensity was performed using ImageJ software. Cells of interest were selected using free-form selection tools. The analysis was set to Area, Integrated Density, and Mean Gray Value. The total fluorescence of the cell was measured and a neighboring region without fluorescence was selected and measured as background reading. The corrected total cell fluorescence (CTCF) was calculated using the formula: CTCF = integrated density (area of selected cell X mean fluorescence of background readings). The CTCF of 253 control cells and 244 HGPS fibroblasts was measured.

For cell death evaluations, the percentages of PI-positive control and HGPS fibroblast cells were evaluated. A total number of 317 cells for control and 309 cells for HGPS fibroblasts were counted. Three independent experiments and counts were performed. All statistical analyses were performed using Student's t-test. Two-tailed p-values were calculated and $p < 0.05$ was considered significant.

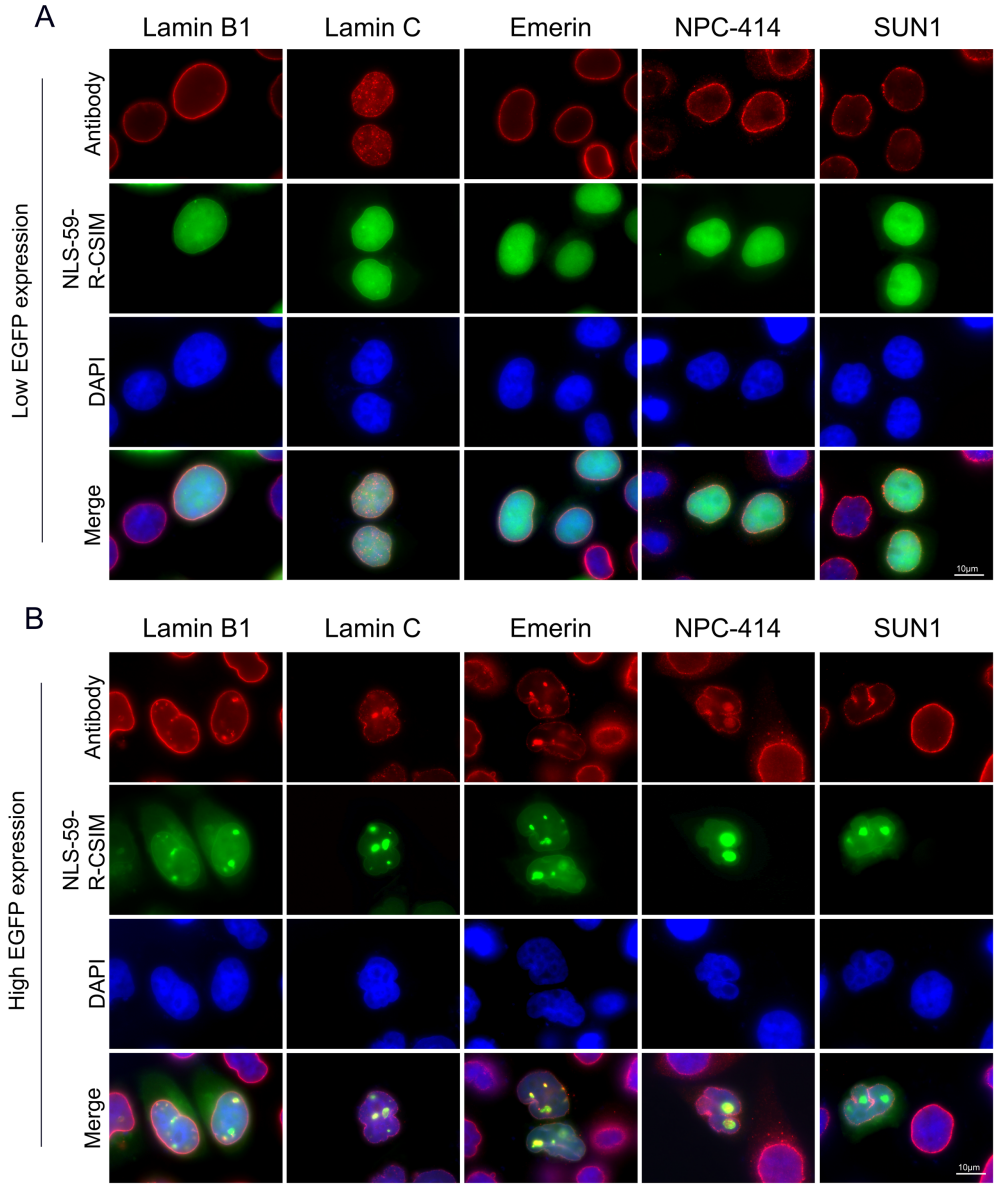

Figure S1. Concentration-dependent NE protein disorganization in EGFP-NLS-59-R-CSIM-expressing cells. Immunocytochemistry was performed on EGFP-NLS-59-R-CSIM-transfected HeLa cells. Cells were stained with lamin B1, lamin C, emerin, NPC-414, and SUN1 antibodies. Chromatin was stained with DAPI. Representative images of cells labeled for each protein are shown. Panel A shows cells with normal nuclear shapes and low EGFP signals. Panel B shows the co-localization of lamin B1, lamin C, emerin, and NPC-414 with EGFP signals at the NE, as EGFP-NLS-59-R-CSIM accumulates at the NE. SUN1 is absent from the NE invaginations. Scale bar, 10 μm.

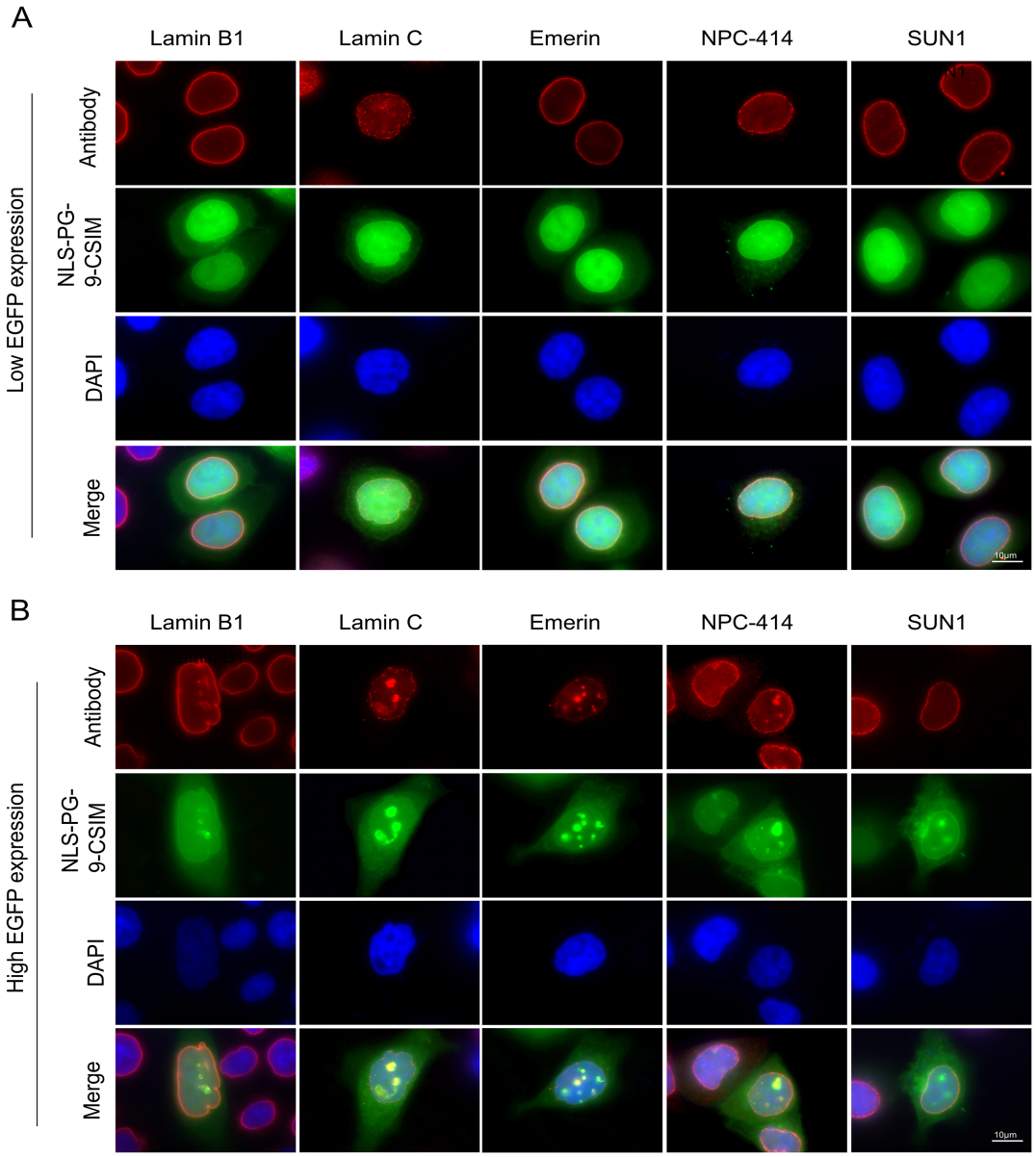

Figure S2. Concentration-dependent NE protein disorganization in EGFP-NLS-PG-9-CSIM-expressing cells. Immunocytochemistry was performed on EGFP-NLS-PG-9-CSIM-transfected HeLa cells. Cells were stained with lamin B1, lamin C, emerin, NPC-414, and SUN1 antibodies. Chromatin was stained with DAPI. Representative images of staining for each protein are shown. Panel A shows cells with normal nuclear shapes and low EGFP signals. Panel B shows the co-localization of lamin B1, lamin C, emerin, and NPC-414 with EGFP signals at the NE; EGFP-NLS-PG-9-CSIM accumulates at the NE. SUN1 is absent from the NE invaginations. Scale bar, 10 μm.

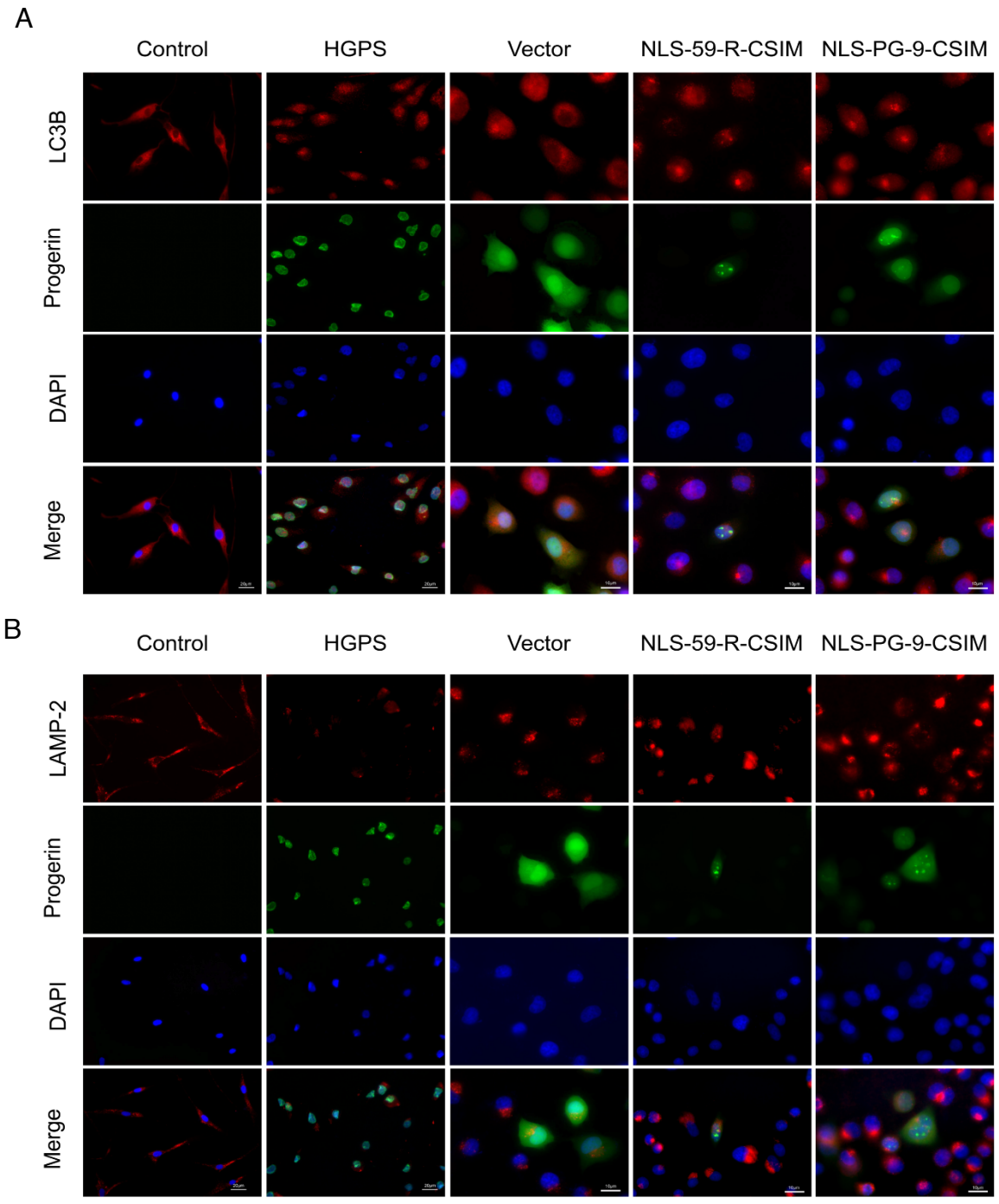

Figure S3. Autophagosome and lysosome distributions. (**A**) Immunocytochemistry was performed on primary fibroblasts from control subjects and patients with HGPS, as well as HeLa cells transfected with the empty vector, EGFP-NLS-59-R-CSIM or EGFP-NLS-PG-9-CSIM plasmids. Cells were stained with anti-LC3B and anti-progerin antibodies. Chromatin was stained with DAPI. Representative images of staining for each protein are shown. (**B**) Immunocytochemistry was performed on similar cells as indicated in (A) and probed with anti-LAMP2 and anti-progerin antibodies. Chromatin was stained with DAPI. Representative images of stained cells are shown. Scale bar, 10 μm.

Curriculum Vitae

Xiang Lu

Am Waldrand 10

81377, Munich

Date of Birth: 26.07.1987

Scientific Education

Oct. 2013-May 2019	PhD candidate (Dr. rer. nat. candidate) Medical Graduate Center Technical University of Munich
Sep. 2010-Jul. 2013	M.Sc. of Science Kunming Institute of Zoology Chinese Academy of Sciences
Sep. 2006-Jul. 2010	Bachelor of Science School of Life Science Yunnan University

Publication List

1. Xiang Lu, Karima Djabali, Autophagic removal of farnesylated carboxy-terminal lamin peptides, Cells, 04/2018;

2. Veronika Eisch, Xiang Lu, et.al.: Progerin impairs chromosome maintenance by depleting CENP-F from metaphase kinetochores in Hutchinson-Gilford progeria fibroblasts. Oncotarget 03/2016

Reference

Akhtar, A. and S. M. Gasser (2007). "The nuclear envelope and transcriptional control." Nat Rev Genet 8(7): 507-517.

Allen, N. P., L. Huang, A. Burlingame and M. Rexach (2001). "Proteomic analysis of nucleoporin interacting proteins." J Biol Chem 276(31): 29268-29274.

Anisimov, V. N., M. A. Zabezhinski, I. G. Popovich, T. S. Piskunova, A. V. Semenchenko, M. L. Tyndyk, M. N. Yurova, S. V. Rosenfeld and M. V. Blagosklonny (2011). "Rapamycin increases lifespan and inhibits spontaneous tumorigenesis in inbred female mice." Cell Cycle 10(24): 4230-4236.

Barrowman, J., C. Hamblet, C. M. George and S. Michaelis (2008). "Analysis of prelamin A biogenesis reveals the nucleus to be a CaaX processing compartment." Molecular and Cellular Biology 19: 5398-5408.

Barrowman, J., C. Hamblet, M. S. Kane and S. Michaelis (2012). "Requirements for efficient proteolytic cleavage of prelamin A by ZMPSTE24." PLoS One 7: e32120.

Beck, L. A., T. J. Hosick and M. Sinensky (1990). "Isoprenylation is required for the processing of the lamin A precursor." J Cell Biol 110(5): 1489-1499.

Behrends, C., M. E. Sowa, S. P. Gygi and J. W. Harper (2010). "Network organization of the human autophagy system." Nature 466(7302): 68-76.

Benson, E. K., S. W. Lee and S. A. Aaronson (2010). "Role of progerin-induced telomere dysfunction in HGPS premature cellular senescence." J Cell Sci 123(Pt 15): 2605-2612.

Berger, Z., B. Ravikumar, F. M. Menzies, L. G. Oroz, B. R. Underwood, M. N. Pangalos, I. Schmitt, U. Wullner, B. O. Evert, C. J. O'Kane and D. C. Rubinsztein (2006).

"Rapamycin alleviates toxicity of different aggregate-prone proteins." Hum Mol Genet 15(3): 433-442.

Best, B. P. (2009). "Nuclear DNA damage as a direct cause of aging." Rejuvenation research 12(3): 199-208.

Bilokapic, S. and T. U. Schwartz (2012). "3D ultrastructure of the nuclear pore complex." Curr Opin Cell Biol 24(1): 86-91.

Burkle, A. (2001). "PARP-1: a regulator of genomic stability linked with mammalian longevity." Chembiochem 2(10): 725-728.

Burtner, C. R. and B. K. Kennedy (2010). Progeria syndromes and ageing: what is the connection? 11: 567-578.

Butin-Israeli, V., S. A. Adam, N. Jain, G. L. Otte, D. Neems, L. Wiesmuller, S. L. Berger and R. D. Goldman (2015). "Role of lamin b1 in chromatin instability." Mol Cell Biol 35(5): 884-898.

Cai, M., Y. Huang, R. Ghirlando, K. L. Wilson, R. Craigie and G. M. Clore (2001). "Solution structure of the constant region of nuclear envelope protein LAP2 reveals two LEM-domain structures: one binds BAF and the other binds DNA." EMBO J 20(16): 4399-4407.

Campisi, J. (2005). "Suppressing cancer: the importance of being senescent." Science 309(5736): 886-887.

Cao, K., J. J. Graziotto, C. D. Blair, J. R. Mazzulli, M. R. Erdos, D. Krainc and F. S. Collins (2011). "Rapamycin Reverses Cellular Phenotypes and Enhances Mutant Protein Clearance in Hutchinson-Gilford Progeria Syndrome Cells." Science Translational Medicine 3: 89ra58.

Reference

Capell, B. C., M. R. Erdos, J. P. Madigan, J. J. Fiordalisi, R. Varga, K. N. Conneely, L. B. Gordon, C. J. Der, A. D. Cox and F. S. Collins (2005). "Inhibiting farnesylation of progerin prevents the characteristic nuclear blebbing of Hutchinson-Gilford progeria syndrome." Proceedings of the National Academy of Sciences 102: 12879-12884.

Casey, P. J. and M. C. Seabra (1996). "Protein prenyltransferases." Journal of Biological Chemistry 271: 5289-5292.

Cenni, V., C. Capanni, M. Columbaro, M. Ortolani, M. R. D'Apice, G. Novelli, M. Fini, S. Marmiroli, E. Scarano, N. M. Maraldi, S. Squarzoni, S. Prencipe and Lattanzi. G. (2011). "Autophagic degradation of farnesylated prelamin A as a therapeutic approach to lamin-linked progeria." European Biophysics Journal 55: 200-2005.

Chen, C. Y., Y. H. Chi, R. A. Mutalif, M. F. Starost, T. G. Myers, S. A. Anderson, C. L. Stewart and K. T. Jeang (2012). "Accumulation of the inner nuclear envelope protein Sun1 is pathogenic in progeric and dystrophic laminopathies." Cell 149(3): 565-577.

Chen, C. Y., Y. H. Chi, R. A. Mutalif, M. F. Starost, T. G. Myers, S. A. Anderson, C. L. Stewart and K. T. Jeang (2012). "Accumulation of the inner nuclear envelope protein sun1 is pathogenic in progeric and dystrophic laminopathies." Cell 149: 565-577.

Chen, K., C. Huang, J. Yuan, H. Cheng and R. Zhou (2014). "Long-term artificial selection reveals a role of TCTP in autophagy in mammalian cells." Molecular Biology Evolution 31: 2194-2211.

Chen, Z. J., W. P. Wang, Y. C. Chen, J. Y. Wang, W. H. Lin, L. A. Tai, G. G. Liou, C. S. Yang and Y. H. Chi (2014). "Dysregulated interactions between lamin A and SUN1 induce abnormalities in the nuclear envelope and endoplasmic reticulum in progeric laminopathies." Journal of Cell Science 127: 1792-17804.

Chen, Z. J., W. P. Wang, Y. C. Chen, J. Y. Wang, W. H. Lin, L. A. Tai, G. G. Liou, C. S. Yang and Y. H. Chi (2014). "Dysregulated interactions between lamin A and SUN1 induce abnormalities in the nuclear envelope and endoplasmic reticulum in progeric laminopathies." J Cell Sci 127(Pt 8): 1792-1804.

Choi, J. C., A. Muchir, W. Wu, S. Iwata, S. Homma, J. P. Morrow and H. J. Worman (2012). "Temsirolimus activates autophagy and ameliorates cardiomyopathy caused by lamin a/c gene mutation." Science Translational Medicine 4: 144ra102.

Colman, R. J., R. M. Anderson, S. C. Johnson, E. K. Kastman, K. J. Kosmatka, T. M. Beasley, D. B. Allison, C. Cruzen, H. A. Simmons, J. W. Kemnitz and R. Weindruch (2009). "Caloric restriction delays disease onset and mortality in rhesus monkeys." Science 325(5937): 201-204.

Cox, A. D. and C. J. Der (2002). "Ras family signaling: therapeutic targeting." Cancer Biol Ther 1(6): 599-606.

Crisp, M., Q. Liu, K. Roux, J. B. Rattner, C. Shanahan, B. Burke, P. D. Stahl and D. Hodzic (2006). "Coupling of the nucleus and cytoplasm: role of the LINC complex." Journal of Cell Biology 172: 43-51.

Cronshaw, J. M. and M. J. Matunis (2004). "The nuclear pore complex: disease associations and functional correlations." Trends Endocrinol Metab 15(1): 34-39.

Cuervo, A. M. (2004). "Autophagy: in sickness and in health." Trends Cell Biol 14(2): 70-77.

Cullinan, S. B., J. D. Gordan, J. Jin, J. W. Harper and J. A. Diehl (2004). "The Keap1-BTB protein is an adaptor that bridges Nrf2 to a Cul3-based E3 ligase: oxidative stress sensing by a Cul3-Keap1 ligase." Mol Cell Biol 24(19): 8477-8486.

Davies, B. S., L. G. Fong, S. H. Yang, C. Coffinier and S. G. Young (2011). "The posttranslational processing of prelamin A and disease." Nucleus 10: 153-174.

De Sandre-Giovannoli, A., R. Bernard, P. Cau, C. Navarro, J. Amiel, I. Boccaccio, S. Lyonnet, C. L. Stewart, A. Munnich, M. Le Merrer and N. Levy (2003). "Lamin a truncation in Hutchinson-Gilford progeria." Science 300(5628): 2055.

Dechat, T., K. Pfleghaar, K. Sengupta, T. Shimi, D. K. Shumaker, L. Solimando and R. D. Goldman (2008). "Nuclear lamins: major factors in the structural organization and function of the nucleus and chromatin." Genes Dev 22(7): 832-853.

Dechat, T., K. Pfleghaar, K. Sengupta, T. Shimi, D. K. Shumaker, L. Solimando and R. D. Goldman (2008). "Nuclear lamins: major factors in the structural organization and function of the nucleus and chromatin." Genes and Development 22: 832-853.

Decker, M. L., E. Chavez, I. Vulto and P. M. Lansdorp (2009). "Telomere length in Hutchinson-Gilford progeria syndrome." Mech Ageing Dev 130(6): 377-383.

Demmerle, J., A. J. Koch and J. M. Holaska (2012). "The nuclear envelope protein emerin binds directly to histone deacetylase 3 (HDAC3) and activates HDAC3 activity." J Biol Chem 287(26): 22080-22088.

Dorner, D., J. Gotzmann and R. Foisner (2007). "Nucleoplasmic lamins and their interaction partners, LAP2alpha, Rb, and BAF, in transcriptional regulation." FEBS J 274(6): 1362-1373.

Dou, Z., C. Xu, G. Donahue, T. Shimi, J. A. Pan, J. Zhu, A. Ivanov, B. C. Capell, A. M. Drake, P. P. Shah, J. M. Catanzaro, M. D. Ricketts, T. Lamark, S. A. Adam, R. Marmorstein, W. X. Zong, T. Johansen, R. D. Goldman, P. D. Adams and S. L. Berger

(2015). "Autophagy mediates degradation of nuclear lamina." Nature (London) 527: 105-109.

Dou, Z., C. Xu, G. Donahue, T. Shimi, J. A. Pan, J. Zhu, A. Ivanov, B. C. Capell, A. M. Drake, P. P. Shah, J. M. Catanzaro, M. D. Ricketts, T. Lamark, S. A. Adam, R. Marmorstein, W. X. Zong, T. Johansen, R. D. Goldman, P. D. Adams and S. L. Berger (2015). "Autophagy mediates degradation of nuclear lamina." Nature 527(7576): 105-109.

Downward, J. (2003). "Targeting RAS signalling pathways in cancer therapy." Nat Rev Cancer 3(1): 11-22.

Drake, K. R., M. Kang and A. K. Kenworthy (2010). "Nucleocytoplasmic distribution and dynamics of the autophagosome marker EGFP-LC3." PLoS One 5: e9806

Dreesen, O., A. Chojnowski, P. F. Ong, T. Y. Zhao, J. E. Common, D. Lunny, E. B. Lane, S. J. Lee, L. A. Vardy, C. L. Stewart and A. Colman (2013). "Lamin B1 fluctuations have differential effects on cellular proliferation and senescence." J Cell Biol 200(5): 605-617.

Eisch, V., X. Lu, D. Gabriel and K. Djabali (2016). "Progerin impairs chromosome maintenance by depleting CENP-F from metaphase kinetochores in Hutchinson-Gilford progeria fibroblasts." Oncotarget 7(17): 24700-24718.

Eisch, V., X. Lu, D. Gabriel and K. Djabali (2016). "Progerin impairs chromosome maintenance by depleting CENP-F from metaphase kinetochores in Hutchinson-Gilford progeria fibroblasts." Oncotarget.

Eissenberg, J. C., T. C. James, D. M. Foster-Hartnett, T. Hartnett, V. Ngan and S. C. Elgin (1990). "Mutation in a heterochromatin-specific chromosomal protein is associated

with suppression of position-effect variegation in Drosophila melanogaster." Proceedings of the National Academy of Sciences 87: 9923-9927.

Faggioli, F., T. Wang, J. Vijg and C. Montagna (2012). "Chromosome-specific accumulation of aneuploidy in the aging mouse brain." Hum Mol Genet 21(24): 5246-5253.

Finlan, L. E., D. Sproul, I. Thomson, S. Boyle, E. Kerr, P. Perry, B. Ylstra, J. R. Chubb and W. A. Bickmore (2008). "Recruitment to the nuclear periphery can alter expression of genes in human cells." PLoS Genet 4(3): e1000039.

Fiserova, J. and M. W. Goldberg (2010). "Relationships at the nuclear envelope: lamins and nuclear pore complexes in animals and plants." Biochem Soc Trans 38(3): 829-831.

Fisher, D., N. Chaudhary and G. Blobel (1986). "cDNA sequencing of nuclear lamins A and C reveals primary and secondary structure homology to intermediate filaments proteins." Proceedings of the National Academy of Sciences 83: 6450-6454.

Forman, M. S., J. Q. Trojanowski and V. M. Lee (2004). "Neurodegenerative diseases: a decade of discoveries paves the way for therapeutic breakthroughs." Nat Med 10(10): 1055-1063.

Forsberg, L. A., C. Rasi, H. R. Razzaghian, G. Pakalapati, L. Waite, K. S. Thilbeault, A. Ronowicz, N. E. Wineinger, H. K. Tiwari, D. Boomsma, M. P. Westerman, J. R. Harris, R. Lyle, M. Essand, F. Eriksson, T. L. Assimes, C. Iribarren, E. Strachan, T. P. O'Hanlon, L. G. Rider, F. W. Miller, V. Giedraitis, L. Lannfelt, M. Ingelsson, A. Piotrowski, N. L. Pedersen, D. Absher and J. P. Dumanski (2012). "Age-related somatic structural changes in the nuclear genome of human blood cells." Am J Hum Genet 90(2): 217-228.

Fu, H. W. and P. J. Casey (1999). "Enzymology and biology of CaaX protein prenylation." Recent Progress in Hormone Research 54: 315-342.

Furukawa, M. and Y. Xiong (2005). "BTB protein Keap1 targets antioxidant transcription factor Nrf2 for ubiquitination by the Cullin 3-Roc1 ligase." Mol Cell Biol 25(1): 162-171.

Gabriel, D., L. B. Gordon and K. Djabali (2016). "Temsirolimus Partially Rescues the Hutchinson-Gilford Progeria Cellular Phenotype." PLoS One 11(12): e0168988.

Gabriel, D., D. Roedl, L. B. Gordon and K. Djabali (2015). "Sulforaphane enhances progerin clearance in Hutchinson-Gilford progeria fibroblasts." Aging Cell 14: 78-91.

Gerace, L. and G. Blobel (1980). "The nuclear envelope lamina is reversibly depolymerized during mitosis." Cell 19: 277-287.

Gerace, L., A. Blum and G. Blobel (1978). "Immunocytochemical localization of the major polypeptides of the nuclear pore complex-lamina fraction. Interphase and mitotic distribution." Journal of Cell Biology 79: 546-566.

Goldman, R. D., D. K. Shumaker, M. R. Erdos, M. Eriksson, A. E. Goldman, L. B. Gordon, Y. Gruenbaum, S. Khuon, M. Mendez, R. Varga and F. S. Collins (2004). "Accumulation of mutant lamin A causes progressive changes in nuclear architecture in Hutchinson-Gilford progeria syndrome." Proceedings of the National Academy of Sciences 101: 8963-8968.

Gordon, L. B., M. E. Kleinman, D. T. Miller, D. S. Neuberg, A. Giobbie-Hurder, M. Gerhard-Herman, L. B. Smoot, C. M. Gordon, R. Cleveland, B. D. Snyder, B. Fligor, W. R. Bishop, P. Statkevich, A. Regen, A. Sonis, S. Riley, C. Ploski, A. Correia, N. Quinn, N. J. Ullrich, A. Nazarian, M. G. Liang, S. Y. Huh, A. Schwartzman and M. W. Kieran

(2012). "Clinical trial of a farnesyltransferase inhibitor in children with Hutchinson-Gilford progeria syndrome." Proc Natl Acad Sci U S A 109(41): 16666-16671.

Gregg, S. Q., V. Gutierrez, A. R. Robinson, T. Woodell, A. Nakao, M. A. Ross, G. K. Michalopoulos, L. Rigatti, C. E. Rothermel, I. Kamileri, G. A. Garinis, D. B. Stolz and L. J. Niedernhofer (2012). "A mouse model of accelerated liver aging caused by a defect in DNA repair." Hepatology 55(2): 609-621.

Greider, C. W. and E. H. Blackburn (1985). "Identification of a specific telomere terminal transferase activity in Tetrahymena extracts." Cell 43(2 Pt 1): 405-413.

Grossman, E., O. Medalia and M. Zwerger (2012). "Functional architecture of the nuclear pore complex." Annu Rev Biophys 41: 557-584.

Gruenbaum, Y. and R. Foisner (2015). "Lamins: Nuclear Intermediate Filament Proteins with Fundamental Functions in Nuclear Mechanics and Genome Regulation." Annual Review of Biochemistry 84: 131-164.

Gruenbaum, Y., A. Margalit, R. D. Goldman, D. K. Shumaker and K. L. Wilson (2005). "The nuclear lamina comes of age." Nat Rev Mol Cell Biol 6(1): 21-31.

Guo, Y., Y. Kim, T. Shimi, R. D. Goldman and Y. Zheng (2014). "Concentration-dependent lamin assembly and its roles in the localization of other nuclear proteins." Mol Biol Cell 25(8): 1287-1297.

Hancock, J. F. (2003). "Ras proteins: different signals from different locations." Nature Reviews Molecular cell Biology 4: 373-384.

Hancock, J. F., H. Paterson and C. J. Marshall (1990). "A polybasic domain or palmitoylation is required in addition to the CAAX motif to localize p21ras to the plasma membrane." Cell 5: 133-139.

Hara, T., K. Nakamura, M. Matsui, A. Yamamoto, Y. Nakahara, R. Suzuki-Migishima, M. Yokoyama, K. Mishima, I. Saito, H. Okano and N. Mizushima (2006). "Suppression of basal autophagy in neural cells causes neurodegenerative disease in mice." Nature 441(7095): 885-889.

Haraguchi, T., J. M. Holaska, M. Yamane, T. Koujin, N. Hashiguchi, C. Mori, K. L. Wilson and Y. Hiraoka (2004). "Emerin binding to Btf, a death-promoting transcriptional repressor, is disrupted by a missense mutation that causes Emery-Dreifuss muscular dystrophy." Eur J Biochem 271(5): 1035-1045.

Hayflick, L. (1965). "The Limited in Vitro Lifetime of Human Diploid Cell Strains." Exp Cell Res 37: 614-636.

Heessen, S. and M. Fornerod (2007). "The inner nuclear envelope as a transcription factor resting place." EMBO Rep 8(10): 914-919.

Hetzer, M. W. (2010). "The nuclear envelope." Cold Spring Harb Perspect Biol 2(3): a000539.

Hoeijmakers, J. H. (2009). "DNA damage, aging, and cancer." N Engl J Med 361(15): 1475-1485.

Holaska, J. M. (2008). "Emerin and the nuclear lamina in muscle and cardiac disease." Circ Res 103(1): 16-23.

Holaska, J. M., K. K. Lee, A. K. Kowalski and K. L. Wilson (2003). "Transcriptional repressor germ cell-less (GCL) and barrier to autointegration factor (BAF) compete for binding to emerin in vitro." J Biol Chem 278(9): 6969-6975.

Holtz, D., R. A. Tanaka, J. Hartwig and F. McKeon (1989). "The CaaX motif of lamin A functions in conjunction with the nuclear localization signal to target assembly to the nuclear envelope." Cell 59: 969-977.

Hunziker, W. and H. J. Geuze (1996). "Intracellular trafficking of lysosomal membrane proteins." BioEssays 18: 379-389.

Hutchison, C. J. (2002). "Lamins: building blocks or regulators of gene expression?" Nat Rev Mol Cell Biol 3(11): 848-858.

Itoh, K., N. Wakabayashi, Y. Katoh, T. Ishii, K. Igarashi, J. D. Engel and M. Yamamoto (1999). "Keap1 represses nuclear activation of antioxidant responsive elements by Nrf2 through binding to the amino-terminal Neh2 domain." Genes Dev 13(1): 76-86.

Jahed, Z., D. Fadavi, U. T. Vu, E. Asgari, G. W. G. Luxton and M. R. K. Mofrad (2018). "Molecular Insights into the Mechanisms of SUN1 Oligomerization in the Nuclear Envelope." Biophysical Journal 114(5): 1190-1203.

Kabeya, Y., N. Mizushima, T. Ueno, A. Yamamoto, T. Kirisako, T. Noda, E. Kominami, Y. Ohsumi and T. Yoshimori (2000). "LC3, a mammalian homologue of yeast Apg8p, is localized in autophagosome membranes after processing." EMBO Journal 19: 5720-5728.

Kabeya, Y., N. Mizushima, T. Ueno, A. Yamamoto, T. Kirisako, T. Noda, E. Kominami, Y. Ohsumi and T. Yoshimori (2000). "LC3, a mammalian homologue of yeast Apg8p, is localized in autophagosome membranes after processing." EMBO J 19(21): 5720-5728.

Karantza-Wadsworth, V., S. Patel, O. Kravchuk, G. Chen, R. Mathew, S. Jin and E. White (2007). "Autophagy mitigates metabolic stress and genome damage in mammary tumorigenesis." Genes Dev 21(13): 1621-1635.

Kenyon, C. J. (2010). "The genetics of ageing." Nature 464(7288): 504-512.

Kim, Y. H., M. E. Han and S. O. Oh (2017). "The molecular mechanism for nuclear transport and its application." Anatomy and Cell Biology 50: 77-85.

Klionsky, D. J. (2005). "The molecular machinery of autophagy: unanswered questions." J Cell Sci 118(Pt 1): 7-18.

Kobayashi, A., M. I. Kang, H. Okawa, M. Ohtsuji, Y. Zenke, T. Chiba, K. Igarashi and M. Yamamoto (2004). "Oxidative stress sensor Keap1 functions as an adaptor for Cul3-based E3 ligase to regulate proteasomal degradation of Nrf2." Mol Cell Biol 24(16): 7130-7139.

Komatsu, M., H. Kurokawa, S. Waguri, K. Taguchi, A. Kobayashi, Y. Ichimura, Y. S. Sou, I. Ueno, A. Sakamoto, K. I. Tong, M. Kim, Y. Nishito, S. Iemura, T. Natsume, T. Ueno, E. Kominami, H. Motohashi, K. Tanaka and M. Yamamoto (2010). "The selective autophagy substrate p62 activates the stress responsive transcription factor Nrf2 through inactivation of Keap1." Nat Cell Biol 12(3): 213-223.

Komatsu, M., S. Waguri, T. Chiba, S. Murata, J. Iwata, I. Tanida, T. Ueno, M. Koike, Y. Uchiyama, E. Kominami and K. Tanaka (2006). "Loss of autophagy in the central nervous system causes neurodegeneration in mice." Nature 441(7095): 880-884.

Kondylis, V., S. E. Goulding, J. C. Dunne and C. Rabouille (2001). "Biogenesis of Golgi stacks in imaginal discs of Drosophila melanogaster." Molecular Biology of the Cell 12: 2308-2327.

Kujoth, G. C., A. Hiona, T. D. Pugh, S. Someya, K. Panzer, S. E. Wohlgemuth, T. Hofer, A. Y. Seo, R. Sullivan, W. A. Jobling, J. D. Morrow, H. Van Remmen, J. M. Sedivy, T. Yamasoba, M. Tanokura, R. Weindruch, C. Leeuwenburgh and T. A. Prolla (2005).

"Mitochondrial DNA mutations, oxidative stress, and apoptosis in mammalian aging." Science 309(5733): 481-484.

Kurihara, Y., T. Kanki, Y. Aoki, Y. Hirota, T. Saigusa, T. Uchiumi and D. Kang (2012). "Mitophagy plays an essential role in reducing mitochondrial production of reactive oxygen species and mutation of mitochondrial DNA by maintaining mitochondrial quantity and quality in yeast." J Biol Chem 287(5): 3265-3272.

Laguri, C., B. Gilquin, N. Wolff, R. Romi-Lebrun, K. Courchay, I. Callebaut, H. J. Worman and S. Zinn-Justin (2001). "Structural characterization of the LEM motif common to three human inner nuclear membrane proteins." Structure 9(6): 503-511.

Lamming, D. W., L. Ye, P. Katajisto, M. D. Goncalves, M. Saitoh, D. M. Stevens, J. G. Davis, A. B. Salmon, A. Richardson, R. S. Ahima, D. A. Guertin, D. M. Sabatini and J. A. Baur (2012). "Rapamycin-induced insulin resistance is mediated by mTORC2 loss and uncoupled from longevity." Science 335(6076): 1638-1643.

Levine, B. and D. J. Klionsky (2004). "Development by self-digestion: molecular mechanisms and biological functions of autophagy." Dev Cell 6(4): 463-477.

Levine, B. and G. Kroemer (2008). "Autophagy in the pathogenesis of disease." Cell 132(1): 27-42.

Lin, F. and H. J. Worman (1993). "Structural organization of the human gene encoding nuclear lamin A and nuclear lamin C." J Biol Chem 268(22): 16321-16326.

Lombardi, M. L., D. E. Jaalouk, C. M. Shanahan, B. Burke, K. J. Roux and J. Lammerding (2011). "The interaction between nesprins and sun proteins at the nuclear envelope is critical for force transmission between the nucleus and cytoskeleton." Journal of Cell Biochemistry 286(30): 26743-26753.

Lu, W., J. Gotzmann, L. Sironi, V. M. Jaeger, M. Schneider, Y. Lüke, M. Uhlén, C. A. Szigyarto, A. Brachner, J. Ellenberg, R. Foisner, A. A. Noegel and I. Karakesisoglou (2008). "Sun1 forms immobile macromolecular assemblies at the nuclear envelope." Biochimica et Biophysica Acta 1783: 2415-2426.

Luo, M., X. Zhao, Y. Song, H. Cheng and R. Zhou (2016). "Nuclear autophagy: An evolutionarily conserved mechanism of nuclear degradation in the cytoplasm." Autophagy 12: 1973-1983.

Maeshima, K., H. Iino, S. Hihara, T. Funakoshi, A. Watanabe, M. Nishimura, R. Nakatomi, K. Yahata, F. Imamoto, T. Hashikawa, H. Yokota and N. Imamoto (2010). "Nuclear pore formation but not nuclear growth is governed by cyclin-dependent kinases (Cdks) during interphase." Nat Struct Mol Biol 17(9): 1065-1071.

Maeshima, K., K. Yahata, Y. Sasaki, R. Nakatomi, T. Tachibana, T. Hashikawa, F. Imamoto and N. Imamoto (2006). "Cell-cycle-dependent dynamics of nuclear pores: pore-free islands and lamins." J Cell Sci 119(Pt 21): 4442-4451.

Markiewicz, E., K. Tilgner, N. Barker, M. van de Wetering, H. Clevers, M. Dorobek, I. Hausmanowa-Petrusewicz, F. C. Ramaekers, J. L. Broers, W. M. Blankesteijn, G. Salpingidou, R. G. Wilson, J. A. Ellis and C. J. Hutchison (2006). "The inner nuclear membrane protein emerin regulates beta-catenin activity by restricting its accumulation in the nucleus." EMBO J 25(14): 3275-3285.

Mathew, R., C. M. Karp, B. Beaudoin, N. Vuong, G. Chen, H. Y. Chen, K. Bray, A. Reddy, G. Bhanot, C. Gelinas, R. S. Dipaola, V. Karantza-Wadsworth and E. White (2009). "Autophagy suppresses tumorigenesis through elimination of p62." Cell 137(6): 1062-1075.

Matsumoto, A., M. Hieda, Y. Yokoyama, Y. Nishioka, K. Yoshidome, M. Tsujimoto and N. Matsuura (2015). "Global loss of a nuclear lamina component, lamin A/C, and LINC complex components SUN1, SUN2, and nesprin-2 in breast cancer." Cancer Medecin 4(10): 1547-1557.

Mattout, A., T. Dechat, S. A. Adam, R. D. Goldman and Y. Gruenbaum (2006). "Nuclear lamins, diseases and aging." Curr Opin Cell Biol 18(3): 335-341.

McClintock, D., L. D. Gordon and K. Djabali (2006). "Hutchinson-Gilford progeria mutant lamin A primarily targets human vascular cells as detected by an anti-Lamin A G608G antibody." Proceedings of the National Academy of Sciences 103: 2154-2159.

Merideth, M. A., L. B. Gordon, S. Clauss, V. Sachdev, A. C. Smith, M. B. Perry, C. C. Brewer, C. Zalewski, H. J. Kim, B. Solomon, B. P. Brooks, L. H. Gerber, M. L. Turner, D. L. Domingo, T. C. Hart, J. Graf, J. C. Reynolds, A. Gropman, J. A. Yanovski, M. Gerhard-Herman, F. S. Collins, E. G. Nabel, R. O. Cannon, 3rd, W. A. Gahl and W. J. Introne (2008). "Phenotype and course of Hutchinson-Gilford progeria syndrome." N Engl J Med 358(6): 592-604.

Michaelis, S. and C. A. Hrycyna (2013). "Biochemistry. A protease for the ages." Science 339: 1529-1530.

Mizushima, N. and D. J. Klionsky (2007). "Protein turnover via autophagy: implications for metabolism." Annu Rev Nutr 27: 19-40.

Mizushima, N., B. Levine, A. M. Cuervo and D. J. Klionsky (2008). "Autophagy fights disease through cellular self-digestion." Nature 451(7182): 1069-1075.

Morley, A. (1998). "Somatic mutation and aging." Annals of the New York Academy of Sciences 854(1): 20-22.

Moskalev, A. A., M. V. Shaposhnikov, E. N. Plyusnina, A. Zhavoronkov, A. Budovsky, H. Yanai and V. E. Fraifeld (2013). "The role of DNA damage and repair in aging through the prism of Koch-like criteria." Ageing Res Rev 12(2): 661-684.

Murga, M., S. Bunting, M. F. Montana, R. Soria, F. Mulero, M. Canamero, Y. Lee, P. J. McKinnon, A. Nussenzweig and O. Fernandez-Capetillo (2009). "A mouse model of ATR-Seckel shows embryonic replicative stress and accelerated aging." Nat Genet 41(8): 891-898.

Niemann, A., A. Takatsuki and H. P. Elsasser (2000). "The lysosomotropic agent monodansylcadaverine also acts as a solvent polarity probe." Journal of Histochemistry and Cytochemstry 48: 251-258.

Ouellette, M. M., L. D. McDaniel, W. E. Wright, J. W. Shay and R. A. Schultz (2000). "The establishment of telomerase-immortalized cell lines representing human chromosome instability syndromes." Hum Mol Genet 9(3): 403-411.

Paradisi, M., D. McClintock, R. L. Boguslavsky, C. Pedicelli, H. J. Worman and K. Djabali (2005). "Dermal fibroblasts in Hutchinson-Gilford progeria syndrome with the lamin A G608G mutation have dysmorphic nuclei and are hypersensitive to heat stres." BioMed Central Cell Biology 6: 27.

Park, Y. E., Y. K. Hayashi, G. Bonne, T. Arimura, S. Noguchi, I. Nonaka and I. Nishino (2009). " Autophagic degradation of nuclear components in mammalian cells." Autophagy 5: 795-804.

Patel, J. T., A. Bottrill, S. L. Prosser, S. Jayaraman, K. Straatman, A. M. Fry and S. Shackleton (2014). "Mitotic phosphorylation of SUN1 loosens its connection with the nuclear lamina while the LINC complex remains intact." Nucleus 5(5): 462-473.

Pellegrini , C., M. Columbaro, C. Capanni, M. R. D'Apice, C. Cavallo, M. Murdocca, G. Lattanzi and S. Squarzoni (2015). "All-trans retinoic acid and rapamycin normalize Hutchinson Gilford progeria fibroblast phenotype." Oncotarget 6: 29914-29928.

Pendas, A. M., Z. Zhou, J. Cadinanos, J. M. Freije, J. Wang, K. Hultenby, A. Astudillo, A. Wernerson, F. Rodriguez, K. Tryggvason and C. Lopez-Otin (2002). "Defective prelamin A processing and muscular and adipocyte alterations in Zmpste24 metalloproteinase-deficient mice." Nature Genetics 31: 94-99.

Pickles, S., P. Vigie and R. J. Youle (2018). "Mitophagy and Quality Control Mechanisms in Mitochondrial Maintenance." Curr Biol 28(4): R170-R185.

Ravikumar, B., Z. Berger, C. Vacher, C. J. O'Kane and D. C. Rubinsztein (2006). "Rapamycin pre-treatment protects against apoptosis." Hum Mol Genet 15(7): 1209-1216.

Ravikumar, B., R. Duden and D. C. Rubinsztein (2002). "Aggregate-prone proteins with polyglutamine and polyalanine expansions are degraded by autophagy." Hum Mol Genet 11(9): 1107-1117.

Ravikumar, B., C. Vacher, Z. Berger, J. E. Davies, S. Luo, L. G. Oroz, F. Scaravilli, D. F. Easton, R. Duden, C. J. O'Kane and D. C. Rubinsztein (2004). "Inhibition of mTOR induces autophagy and reduces toxicity of polyglutamine expansions in fly and mouse models of Huntington disease." Nat Genet 36(6): 585-595.

Reddy, K. L., J. M. Zullo, E. Bertolino and H. Singh (2008). "Transcriptional repression mediated by repositioning of genes to the nuclear lamina." Nature 452(7184): 243-247.

Richter, C., J. W. Park and B. N. Ames (1988). "Normal oxidative damage to mitochondrial and nuclear DNA is extensive." Proc Natl Acad Sci U S A 85(17): 6465-6467.

Roberts, P., S. Moshitch-Moshkovitz, E. Kvam, E. O'Toole, M. Winey and D. S. Goldfarb (2003). "Piecemeal microautophagy of nucleus in Saccharomyces cerevisiae." Mol Biol Cell 14(1): 129-141.

Rost, B., G. Yachdav and J. Liu (2004). "The PredictProtein server." Nucleic Acids Research 32: W321-W326.

Rubinsztein, D. C., P. Codogno and B. Levine (2012). "Autophagy modulation as a potential therapeutic target for diverse diseases." Nat Rev Drug Discov 11(9): 709-730.

Rubinsztein, D. C., J. E. Gestwicki, L. O. Murphy and D. J. Klionsky (2007). "Potential therapeutic applications of autophagy." Nat Rev Drug Discov 6(4): 304-312.

Rusinol, A. E. and M. S. Sinensky (2006). "Farnesylated lamins, progeroid syndromes and farnesyl transferase inhibitors." Journal of Cell Science 119: 3265-3272.

Sagne, C., C. Agulhon, P. Ravassard, M. Darmon, M. Hamon, S. El Mestikawy, B. Gasnier and B. Giros (2001). "Identification and characterization of a lysosomal transporter for small neutral amino acids." Proc Natl Acad Sci U S A 98(13): 7206-7211.

Scholzen, T. and J. Gerdes (2000). "The ki-67 protein: From the known and the unknown." Journal of cellular physiology 182: 311-322.

Shah, P. P., G. Donahue, G. L. Otte, B. C. Capell, D. M. Nelson, K. Cao, V. Aggarwala, H. A. Cruickshanks, T. S. Rai, T. McBryan, B. D. Gregory, P. D. Adams and S. L. Berger (2013). "Lamin B1 depletion in senescent cells triggers large-scale changes in gene expression and the chromatin landscape." Genes Dev 27(16): 1787-1799.

Shigenaga, M. K., T. M. Hagen and B. N. Ames (1994). "Oxidative damage and mitochondrial decay in aging." Proc Natl Acad Sci U S A 91(23): 10771-10778.

Shimi, T., V. Butin-Israeli, S. A. Adam, R. B. Hamanaka, A. E. Goldman, C. A. Lucas, D. K. Shumaker, S. T. Kosak, N. S. Chandel and R. D. Goldman (2011). "The role of nuclear lamin B1 in cell proliferation and senescence." Genes Dev 25(24): 2579-2593.

Shintani, T. and D. J. Klionsky (2004). "Autophagy in health and disease: a double-edged sword." Science 306(5698): 990-995.

Sinensky, M. (2000). "Recent advances in the study of prenylated proteins." Biochimica et Biophysica Acta 1484: 93-106.

Sinensky, M., McLain T. and K. Fantle (1994). "Expression of prelamin A but not mature lamin A confers sensitivity of DNA biosynthesis to lovastatin on F9 teratocarcinoma cells." Journal of Cell Science 107: 2215-2218.

Sosa, B. A., A. Rothballer, U. Kutay and T. U. Schwartz (2012). "LINC complexes form by binding of three KASH peptides to domain interfaces of trimeric SUN proteins." Cell 149(5): 1035-1047.

Starr, D. A. and H. N. Fridolfsson (2010). "Interactions between nuclei and the cytoskeleton are mediated by SUN-KASH nuclear-envelope bridges." Annual review in cell developmental biology 26: 421-444.

Stuurman, N., S. Heins and U. Aebi (1998). "Nuclear lamins: their structure, assembly, and association." Journal of Structural Biology 122: 42-66.

Sun, Z., D. Feng, B. Fang, S. E. Mullican, S. H. You, H. W. Lim, L. J. Everett, C. S. Nabel, Y. Li, V. Selvakumaran, K. J. Won and M. A. Lazar (2013). "Deacetylase-

independent function of HDAC3 in transcription and metabolism requires nuclear receptor corepressor." Mol Cell 52(6): 769-782.

Suriapranata, I., U. D. Epple, D. Bernreuther, M. Bredschneider, K. Sovarasteanu and M. Thumm (2000). "The breakdown of autophagic vesicles inside the vacuole depends on Aut4p." J Cell Sci 113 (Pt 22): 4025-4033.

Tapley, E. C. and D. A. Starr (2013). "Connecting the nucleus to the cytoskeleton by SUN-KASH bridges across the nuclear envelope." Curr Opin Cell Biol 25(1): 57-62.

Terry, L. J. and S. R. Wente (2009). "Flexible gates: dynamic topologies and functions for FG nucleoporins in nucleocytoplasmic transport." Eukaryot Cell 8(12): 1814-1827.

Trifunovic, A., A. Wredenberg, M. Falkenberg, J. N. Spelbrink, A. T. Rovio, C. E. Bruder, Y. M. Bohlooly, S. Gidlof, A. Oldfors, R. Wibom, J. Tornell, H. T. Jacobs and N. G. Larsson (2004). "Premature ageing in mice expressing defective mitochondrial DNA polymerase." Nature 429(6990): 417-423.

Vermulst, M., J. Wanagat, G. C. Kujoth, J. H. Bielas, P. S. Rabinovitch, T. A. Prolla and L. A. Loeb (2008). "DNA deletions and clonal mutations drive premature aging in mitochondrial mutator mice." Nat Genet 40(4): 392-394.

Verstraeten, V. L., L. A. Peckham, M. Olive, B. C. Capell, F. S. Collins, E. G. Nabel, S. G. Young, L. G. Fong and J. Lammerding (2011). "Protein farnesylation inhibitors cause donut-shaped cell nuclei attributable to a centrosome separation defect." Proc Natl Acad Sci U S A 108(12): 4997-5002.

Vlcek, S. and R. Foisner (2007). "A-type lamin networks in light of laminopathic diseases." Biochim Biophys Acta 1773(5): 661-674.

Vorburger, K., G. T. Kitten and E. A. Nigg (1989). "Modification of nuclear lamin proteins by a mevalonic acid derivative occurs in reticulocyte lysates and requires the cysteine residue of the C-terminal CXXM motif." EMBO Journal 8: 4007-4013.

Wakabayashi, N., K. Itoh, J. Wakabayashi, H. Motohashi, S. Noda, S. Takahashi, S. Imakado, T. Kotsuji, F. Otsuka, D. R. Roop, T. Harada, J. D. Engel and M. Yamamoto (2003). "Keap1-null mutation leads to postnatal lethality due to constitutive Nrf2 activation." Nat Genet 35(3): 238-245.

Webb, J. L., B. Ravikumar, J. Atkins, J. N. Skepper and D. C. Rubinsztein (2003). "Alpha-Synuclein is degraded by both autophagy and the proteasome." J Biol Chem 278(27): 25009-25013.

worman, H. J. (2012). "Nuclear lamins and laminopathies." Journal of Pathology 226: 316-325.

Wu, D., A. R. Flannery, H. Cai, E. Ko and K. Cao (2014). "Nuclear localization signal deletion mutants of lamin A and progerin reveal insights into lamin A processing and emerin targeting." Nucleus 5(1): 66-74.

Wydner, K. L., J. A. McNeil, F. Lin, H. J. Worman and J. B. Lawrence (1996). "Chromosomal assignment of human nuclear envelope protein genes LMNA, LMNB1, and LBR by fluorescence in situ hybridization." Genomics 32(3): 474-478.

Yang, S. H., M. O. Bergo, J. I. Toth, X. Qiao, Y. Hu, S. Sandoval, M. Meta, P. Bendale, M. H. Gelb, S. G. Young and L. G. Fong (2005). "Blocking protein farnesyltransferase improves nuclear blebbing in mouse fibroblasts with a targeted Hutchinson-Gilford progeria syndrome mutation." Proceedings of the National Academy of Sciences 102: 10291-10296.

Yang, Z., J. Huang, J. Geng, U. Nair and D. J. Klionsky (2006). "Atg22 recycles amino acids to link the degradative and recycling functions of autophagy." Mol Biol Cell 17(12): 5094-5104.

Acknowledgement

Firstly, I would like to express my sincere gratitude to my advisor Prof. Karima Djabali for the continuous support of my Ph.D. study and related research, for her patience, motivation, and immense knowledge. Her guidance helped me in all the time of research and writing this thesis. I am so grateful to have her as my advisor and mentor for my Ph.D. study.

Besides my advisor, I sincerely thank my second advisor Prof. Thomas Brück for his encouragement, insightful comments, and valuable help throughout my Ph.D. study. I would also like to thank Prof. Markus Ollert for being a very supportive mentor during my Ph.D. study. Without their precious support, it would not be possible for me to conduct this research.

Many thanks to my fellow lab mates Dr. Daniela Rödl, Dr. Leithe Budel, Veronika Eisch, Dr. Diana Gabriel, Chang Liu for the enormous help, stimulating discussions, and all the good and difficult times we spent together inside and outside the lab.

Dany was like a big sister to me, thanks to her for helping me getting adapted fast to the life and work in Germany.

Leithe, you are a good lab mate and great movie buddy, “May the force be with you, bro”.

Veronika, working with you is doubtlessly productive, thanks for all your help.

Acknowledgement

Diana, thanks for the valuable advices on my studies and experiments.

Chang, thanks for your help and support in my studies and experiments.

My thanks also go to Jenifer Röhrl and Rouven Arnold. I love the burger day and Karaoke night, you guys ROCK. We are gonna have more fun!

Oh my friends, Dr. Qiuyan Dong from University of Münster, Drs. Zhu Liu, Long Cheng, Weiwei Xie, Xiuxiu Wu, Di Xu, Zhen Yao from Technical University of Munich, Yanxin Fan, and Ms. Yuanyuan Qu from Ludwig Maximilian University of Munich (LMU), thank you so much for your great companion and all the good times we spent together in Garching, Munich, and countless happy hours in the past years. May our future paths cross again!!!

My warmest thanks to my loving family: my parents and sister for your unconditionally love and support in all my studies and life in general.

May all of you have a long, prosper, and happy life!!!

Last but not the least, my special thanks to the most special women in my life, Yue Li, for always having faith in me, for always having my back, and for always being by my side. I will be there for you, too. No one else ever knows me better than you do. I love you!

This thesis is dedicated to Yue Li.

July 2018

In München